Universidad de Huelva

Departamento de Ingeniería Química, Química Física y Ciencias de los Materiales

An energetical approach to study the structural degradation of traditional and biogenic lubricating greases

Memoria para optar al grado de doctora
presentada por:

Nazli Acar

Fecha de lectura: 21 de junio de 2022

Bajo la dirección de los doctores:

José María Franco Gómez

Erik Kuhn

Huelva, 2022

UNIVERSITY OF HUELVA

Department of Chemical Engineering, Physical Chemistry and Materials Science

AN ENERGETICAL APPROACH TO STUDY THE STRUCTURAL DEGRADATION OF TRADITIONAL AND BIOGENIC LUBRICATING GREASES

Ph.D. Thesis

Doctoral Program in Industrial and Environmental Science and Technology

NAZLI ACAR

2022

Supervisors:

Prof. Dr. José María Franco Gómez

Prof. Dr. Erik Kuhn

AN ENERGETICAL APPROACH TO STUDY THE STRUCTURAL DEGRADATION OF TRADITIONAL AND BIOGENIC LUBRICATING GREASES

Research memory presented by Nazlı Acar to apply for a Doctoral degree at the University of Huelva.

Nazlı Acar

The present dissertation has been performed at the Department of Chemical Engineering, Physical Chemistry and Materials Science of the University of Huelva, in cooperation with the Hamburg University of Applied Sciences (HAW-Hamburg) at the Department of Mechanical Engineering and Production Management (Hamburg, Germany), under the supervision of Dr. José María Franco Gómez and Dr. Erik Kuhn, who approve its defense:

Dr. José María Franco Gómez

Dr. Erik Kuhn

Huelva, April 2022

Acknowledgements

The completion of this Doctoral Thesis would not have been possible without those people that, in the professional and personal fields, provided me with their support and help. My most heartfelt thanks.

First and foremost, I would like to thank my supervisors, Prof. Dr. José María Franco Gómez and Prof. Dr. Erik Kuhn. To Prof. Dr. José María Franco Gómez, for his invaluable advice, constructive feedback, and excellent guidance. I have benefited greatly from your wealth of knowledge and meticulous editing. To Prof. Dr. Erik Kuhn, for his marvelous supervision, excellent guidance and encouragement. His immense knowledge and plentiful experience have encouraged me in all the time of my academic research and daily life. Thank you both, for your assistance and dedicated involvement in every step throughout the process. Their levels of patience, knowledge, and ingenuity are something I will always keep aspiring to. I could not have imagined having a better advisor and mentor for my PhD study.

To the members of the *Tribology Research Center (TREC)* from the *Hamburg University of Applied Sciences (HAW Hamburg),* Dipl.-Ing. Thomas Rieling and Dipl.-Ing. Niels Eiben, for their kind help, support, and a cherished time spent together in the laboratory. I am pleased to say thank you both, who were always ready to help with any questions that I had.

To Dr. Concepción Valencia Barragán and Dr. Miguel Angel Delgado from the *University of Huelva*, for their great help and unconditional support. Thank you for the warm welcome and making me feel at home every time I come to Huelva, a marvelous place. Also, I extend my thanks to Dr. Esperanza Cortés Triviño and Dr. Adrián Tenorio Alfonso from the *University of Huelva*, for their kind support and helping me unconditionally during my PhD study.

Thank to Dr. David E. P. Gonçalves, Prof. Dr. Jorge H. O. Seabra and Ms. Beatriz Graça for their support and helping in performing the rolling bearing tests.

Also, many thanks to *German Ministry of Education and Research* (grant number FKZ13FH018IX4) for allowing the execution of these projects that have enabled the development of this Doctoral Thesis, and financial support. Also, I would like to thank the *Fuchs Europe Schmierstoffe GmbH* (Mannheim, Germany), *Fuchs Lubritech GmbH* (Kaiserslautern, Germany) and *Research Centre in Chemical Product and Process Technology*

(Pro²TecS, University of Huelva, Huelva, Spain) for kindly providing model samples for this Doctoral Thesis.

Finally, and for that reason more importantly, none of this could have happened without my family. To my husband, my life, my soulmate and my confidante, Yavuz Acar, because my best memories are full of you and for being my guiding light in all the bad times. I would like to thank you wholeheartedly for staying with me with the unconditional love and support throughout the entire thesis process and every day. And, of course, thank you for being the world´s best Dad to our daughter. To my daughter, my everything, Mila Duru Acar, for being in my life, sharing the best and amazing experiences, and making me unbelievably happy every day. My accomplishments and success are all for you. To my parents, Ayşe and Atilla Ünal, and to my brother, Yalın Ünal, the best family I have ever known, whose constant love, endless support, and inexhaustible effort keep me motivated and make me feel proud of being part of your life. Thank you all for the strength you gave me throughout the entire thesis process and my life in general. And to my parents-in-law, Aysu and Selahattin Acar, and sister-in-law, Rabia Acar Akdağ, for encouraging and supporting me whenever I needed them.

Thanks to all.

Contents

Chapter 1

Introduction

1.1. Summary

In a tribological contact, the friction processes lead to irreversible effects associated with wear, which are the result of frictional energy input to a tribological system. In general, various types of lubricants are applied to machine elements in order to reduce friction and wear. In the last decades, environmental damages caused by chemicals and/or end-use products, such as lubricants based on petrochemically refined mineral oils, have driven the demand of natural components in a wide variety of manufactured products. In this sense, some lubricant industries have promoted the development of their products with the replacement of non-renewable raw materials by natural resources in order to avoid direct and indirect environmental pollution caused by their products. With this purpose, first, vegetable oils instead of mineral oils, and then, completely biogenic lubricating greases, which are obtained using vegetable oils, as well as by substituting traditionally used thickener agents with biogenic thickeners, have been introduced into a variety of industrial and consumer applications. In this sense, the target of this work is to investigate the tribological and rheological response of new completely biogenic lubricating greases, two reference semi-biogenic lubricating greases, and some traditional lubricating grease samples, emphasizing the energetic aspects of the friction and wear processes.

With this aim, completely biogenic lubricating grease samples, which were formulated with different biogenic oils, e.g., high-oleic sunflower oil (HOSO), glycerol, castor oil, and a combination of HOSO and castor oil, and different biodegradable thickener agents, e.g., beeswax, corncob grits, natural cellulose, and lignin, have been tribologically examined with a nanotribometer and a tribometer using a material combination of a steel ball on a steel disc and compared with traditional lithium-12-hydroxystearate/HOSO and lithium-calcium soap/synthetic ester greases. In this way, it was gained a deeper understanding of the influence of the composition of these model greases on the friction and wear processes in a tribological contact. In addition, using the energy-based wear model, the friction and wear processes could be interpreted as a cause-effect sequence.

In addition, rolling bearing tests were performed to investigate the tribological behaviour of some selected biogenic greases during real machine element contact and to assess their lubrication performance. These real application tests allowed for the quantification of the friction torque of the full bearing at different operating conditions and the wear produced through lubricant analysis procedures, i.e., ferrometry and ferrography.

Moreover, the model greases were rheologically investigated by means of rotational transient flow measurements at different temperatures to monitor the evolution of the shear stress with time at a constant shear rate, and to characterize the internal friction behaviour by quantifying the energy density. Furthermore, correlations between the activation energy and structural degradation of some traditional lubricating grease samples under different shear situations were studied by means of rotational transient flow and oscillation amplitude sweep tests. This experimental work provided useful information for a better understanding of the shear-induced structural degradation process in greases which can facilitate the improvement of the service life of lubricating greases.

Overall, a number of new biogenic lubricating greases completely based on renewable raw materials, two reference semi-biogenic lubricating greases, and some traditional lubricating grease samples were investigated for a better understanding of grease lubrication mechanisms in tribological contacts. All results were also analyzed from an energetic point of view which can help to qualify these biogenic lubricating greases as real alternatives to conventional lubricating greases.

1.2. Resumen

En un contacto tribológico, los procesos de fricción conducen a efectos irreversibles asociados al desgaste, que son el resultado de un aporte de energía de fricción al un sistema tribológico. En general, se aplican diversos tipos de lubricantes a los elementos mecánicos de cualquier maquinaria para reducir la fricción y el desgaste. En las últimas décadas, los daños medioambientales causados por los productos químicos y/o de uso final, como los lubricantes basados en aceites minerales refinados petroquímicamente, han impulsado la demanda de componentes naturales en una gran variedad de productos manufacturados. En este sentido, algunas industrias de lubricantes han promovido el desarrollo de sus productos sustituyendo algunas materias primas no renovables por recursos naturales, para evitar la contaminación ambiental directa e indirecta causada por sus productos. Con este propósito, primero, se han introducido en diversas aplicaciones industriales y de consumo los aceites vegetales, en lugar de los aceites minerales, y después, las grasas lubricantes completamente biogénicas, que se obtienen utilizando aceites vegetales, así como sustituyendo los agentes espesantes tradicionalmente utilizados por espesantes biogénicos. En este sentido, el objetivo de este trabajo es investigar la respuesta tribológica y reológica de nuevas grasas lubricantes completamente biogénicas, dos grasas lubricantes semi-biogénicas de referencia y algunas

muestras de grasas lubricantes tradicionales, haciendo hincapié en los aspectos energéticos de los procesos de fricción y desgaste.

Con este objetivo, se utilizaron muestras de grasas lubricantes completamente biogénicas, formuladas con diferentes aceites naturales, por ejemplo, aceite de girasol de alto contenido en ácido oleico (HOSO), glicerol, aceite de ricino y una combinación de HOSO y aceite de ricino, así como diferentes agentes espesantes biodegradables, por ejemplo, cera de abejas, sémola de mazorca de maíz, celulosa natural y lignina, que se han estudiado tribológicamente en un nanotribómetro y en un tribómetro utilizando una combinación de materiales de bola de acero sobre disco de acero, y se han comparado con grasas tradicionales de 12-hidroxiestearato de litio/HOSO y de jabón de litio-calcio/éster sintético. De este modo, se ha obtenido una comprensión más completa de la influencia de la composición de estas grasas modelo en los procesos de fricción y desgaste en un contacto tribológico. Además, utilizando el modelo energético de desgaste, los procesos de fricción y desgaste pudieron interpretarse como una secuencia causa-efecto.

Además, se realizaron ensayos en rodamientos para investigar el comportamiento tribológico de algunas grasas biogénicas seleccionadas en un contacto real de maquinaria, evaluando su rendimiento de lubricación. Estos ensayos de aplicación real permitieron cuantificar el par de fricción del rodamiento completo en diferentes condiciones de funcionamiento y el desgaste producido mediante procedimientos de análisis del lubricante, cómo la ferrometría y ferrografía.

Además, las diferentes grasas modelo se investigaron reológicamente mediante ensayos de flujo transitorio rotacional, a diferentes temperaturas, midiendo la evolución del esfuerzo con el tiempo a una velocidad de cizalla constante, y caracterizando el fenómeno de la fricción interna mediante la cuantificación de la densidad de energía. Además, se estudió la relación entre la energía de activación y la degradación estructural de algunas muestras de grasas lubricantes tradicionales en diferentes situaciones de cizalla mediante ensayos de flujo transitorio rotacional y de barridos de amplitud en ensayos oscilatorios. Este trabajo experimental proporcionó información útil para una mejor comprensión del proceso de degradación estructural inducido por el cizallamiento en las grasas, lo que podría facilitar una mejora de la vida útil de las grasas lubricantes.

En definitiva, se han investigado una serie de nuevas grasas lubricantes biogénicas, completamente basadas en materias primas renovables, dos grasas lubricantes semi-biogénicas de referencia y algunas muestras de grasas lubricantes tradicionales para comprender mejor los

mecanismos de lubricación de las grasas en contactos tribológicos. Todos los resultados se analizaron desde un punto de vista energético, que puede ayudar a catalogar estas grasas lubricantes biogénicas como alternativas reales a las grasas lubricantes convencionales.

1.3. Objectives

The main objective of this Doctoral Thesis is to investigate new completely biogenic lubricating greases, two reference semi-biogenic lubricating greases and some traditional lubricating grease samples from a tribological and rheological point of view.

Regarding the specific goals of this research, the first target was the investigation of the frictional response, and also the wear volume produced on the steel plate, of new completely biogenic model greases as well as two reference semi-biogenic lubricating greases in a nanotribometer. In addition to this, the internal friction behaviour of the model greases was intended to be monitored by the evolution of the shear stress with time at a constant shear rate, quantifying the energy expenditure for a shearing process at the rheometer.

The second target of this research was to analyze the friction and wear processes of model greases according to Fleischer's energetic wear model, and assess the influence of the model grease composition on friction and wear processes, by means of tribological tests.

Investigating the tribological behaviour of some selected biogenic greases in real machine element contacts is also one of the important goals of this thesis. Therefore, the quantification of the friction torque behaviour of the full bearing and the evaluation of the wear obtained through lubricant analysis procedures compose the next purpose of this investigation.

Finally, the elucidation of the relationship between the activation energy and the structural degradation of model greases under different shear situations by means of rotational transient flow and oscillation amplitude sweep tests was another specific objective of this work.

1.4. Structure

This manuscript is structured into five main sections, including this present introductory chapter. Chapter 2 includes the state of scientific research on Tribology of lubricating greases. This state-of-the art includes first a general description of the tribological system and the frictional and wear states and types. Furthermore, a general review on lubricating greases, their composition, and microstructure is included, describing their typical rheological and

tribological behaviour. This section also highlights the fundamental notions and features of bio-based lubricating greases. With the purpose of completing the information that is necessary for the understanding of this work, an overview on energy-based wear models, friction energy density and activation energy regarding the structural degradation and wear of lubricating greases from a thermodynamic point of view, has been also provided.

Chapter 3 details the materials that have been used in this experimental work as well as the methods and conditions employed to characterize the rheological and tribological behaviour of the lubricating greases studied.

Chapter 4 constitutes the experimental results and their discussion, representing the core of this Doctoral Thesis, which is divided into three main blocks. Each block corresponds to the works published in several well-reputed scientific journals, which were conducted during this research. The first block refers to the tribological and rheological characterization of completely biogenic lubricating greases. The friction and wear behaviours of biogenic lubricating greases in steel-steel contact are evaluated in Block 2. In Block 3, shear-induced structural degradation of lubricating greases and associated activation energy are examined.

Finally, in Chapter 5, the most significant conclusions, which are deduced from the results experimentally obtained in this experimental work, are collected.

Chapter 2

State of the Art

2.1. Tribology

The term "tribology" originates from the greek verb, τρίβω, tribos, meaning rubbing and was first coined in the Jost Report “Lubrication (Tribology), Education and Research: A Report on the Present Position and Industry’s Needs” in 1966. Tribology is defined as “the science and technology of interacting surfaces in relative motion and of related subjects and practices”. Tribology mainly focusses on the study and application of the principles of friction, wear and lubrication.

The main task of tribology is to discover and describe the relationship between the friction process and the system reactions. Studies on tribology allow gaining a better understanding of cause and effect in the tribological process. In this sense, tribology plays a central role in many types of research and development. One major purpose of tribology is to reduce energy and material losses from technical systems due to friction and wear. In this way, trouble-free operation of the machines with a high degree of efficiency can be guaranteed. By optimizing the interacting surfaces in relative motion, it is possible to improve reliability and the service life of the machines and to save energy and material.

2.1.1. The tribological system

Basically, the tribological system is used for the systematic investigation and analysis of friction and wear processes. The general representation of a tribological system is shown in Figure 2.1. The tribological system consist of the collective stress, system structure and function. The system-structure is defined by the tribo-elements, which consist of the main body, the opposing body, the intermediate material and the ambient medium, the relevant properties and interactions of the tribo-elements. The collective stress determines the energy input in the tribological system and includes the physical and technical parameters such as normal force, the temperature and the duration of the stress. The function of a tribological system is to transform the input variables (X) into the output variables (Y), which is defined as the radiated energy of the tribological system and the mass flow of ejected wear particles. The loss variables (V) can occur as another output variable due to friction and wear.

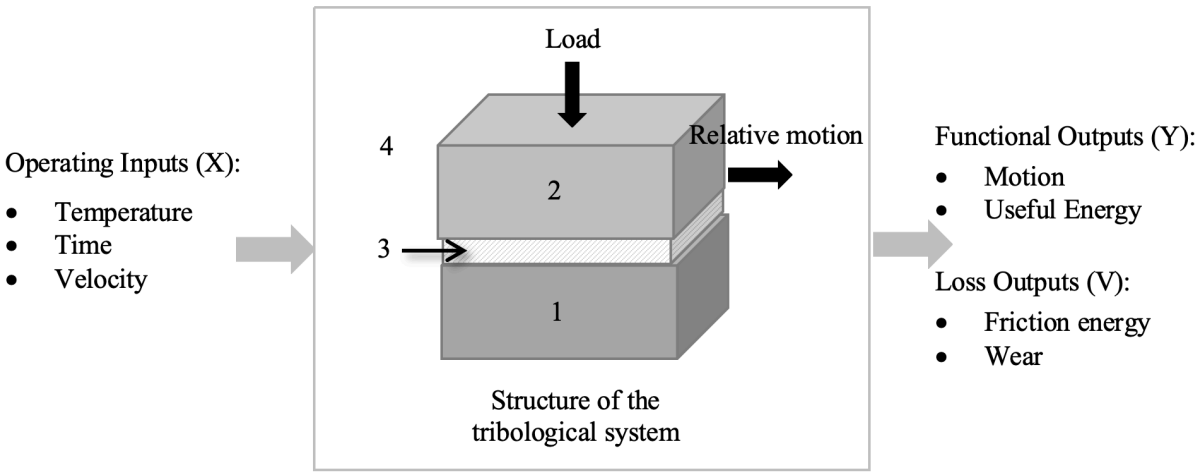

Figure 2.1 Representation of a tribological system. Note: 1–main body, 2–opposing body, 3–intermediate medium and 4–environment medium (adapted from H. Czichos [1,2])

2.2. Friction

Friction is defined as the loss of mechanical energy during the course, beginning or end of a relative motion of contacting material regions [2]. In other words, friction is the introduction of mechanical energy into a tribological system [3]. Friction process causes the loss of mechanical energy, i.e., the mechanical energy is transformed into other forms of energy such as thermal energy. Further, friction process that takes place in a friction point leads to irreversible changes, namely wear, which can affect the function/performance of machines. Friction should not generally be correlate with negative effects and results. Moreover, friction can also be desirable and important, for example: a high level of friction is desired when the tire comes into contact with the asphalt [4].

2.2.1. Friction types

As Fleischer et al. reported [2], friction is always related to the relative motion between two bodies in contact. Nevertheless, it should not be forgotten that friction process can also occur inside a viscous fluid such as a lubricating grease film, which separates the bodies in contact. Different types of relative motion of the contacting object lead to different types of friction. Depending on the relative movement of the bodies, friction is classified into static friction and dynamic friction. Static friction exists when two objects are not moving relative to each other. In the case of static friction, the acting force leads to microscopic movement which is not sufficient to initiate a relative movement of the body. In comparison to static friction, the

relative movement between bodies occurs with dynamic friction. The dynamic friction is divided into sliding friction, rolling friction and drilling friction. In the case of sliding friction, sliding occurs as a relative movement between the bodies which is present in a tribological contact as shown in Figure 2.2 (a). Sliding friction plays an important role in the function of tribological systems because, compared to other friction types, sliding friction is associated with major tribological stresses in the contact limit area, which relates to thermal processes and wear [1]. Figure 2.2 (b) shows a simple example of rolling friction, in which the cylinder rolls over a straight platform. Rolling friction occurs when one of the contacting bodies is rolling over the other. In the case of rolling friction, the axis of rotation of the rotating body is parallel to the friction surface. The drilling friction occurs between bodies in point contact when one of the contacting bodies executes a rotational motion. In the drilling friction, rotating motion takes place around an axis perpendicular to the friction surface as shown in Figure 2.2 (c). In addition, the mixed forms of friction types can arise from the superposition of the three kinematically defined types of movement. The form of combination of sliding and rolling friction is very well known, in which rolling and sliding occur simultaneously as a relative movement of contacting surfaces [2].

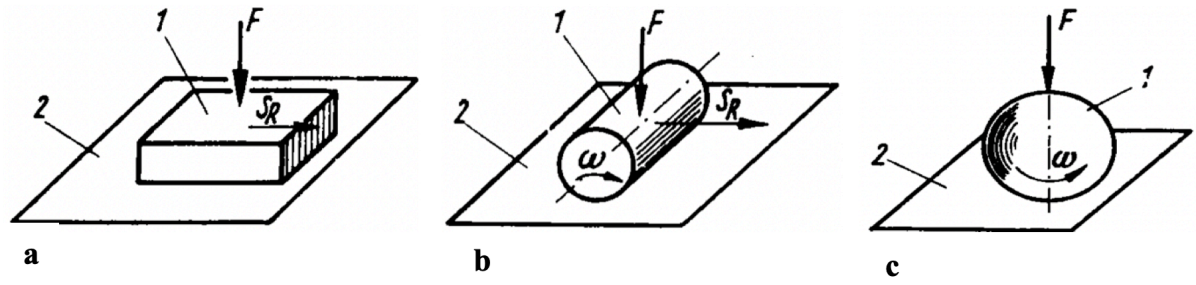

Figure 2.2 Model of sliding friction (a), rolling friction (b) and drilling friction (c) taken from [2]. Note: 1–moving friction body and 2–reference surface

2.2.2. Friction states

The friction states describe the friction process by means of material and energetic state variables. The aggregate state can be used to connection both state variables [2]. Depending on the aggregate state and the contact condition of the friction bodies, the friction is divided into the following four main friction states:

Solid body friction: Solid state friction is a state of friction, in which the relevant material region has solid state properties [2]. Figure 2.3 shows a model of solid friction state and the

contact situation of two rubbing surfaces. In the relative movement of the solid bodies, locally and temporally continuously changing contact points arise in the micro-range. When the solid body slides over the static body, friction process can lead to reversible and irreversible effects in the contacting bodies. Solid friction is related to separation and deformation processes occurring in the surface areas of contacting materials as energy expenditure in relative motion [2,5]. Most of the expended mechanical energy is converted into thermal energy, while the rest accumulates in the surface layer.

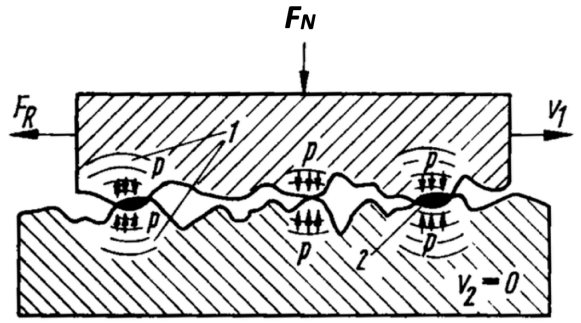

Figure 2.3 Model of solid body friction taken from [2]. Note: 1–elastic deformation, 2–plastic deformation, V_1 and V_2 – velocity of bodies, F_N – normal force, F_R – friction force and p – contact pressure

Fluid friction: Fluid friction is a state of friction in the material region with fluid properties [2]. Figure 2.4 shows a model of fluid friction, where the fluid separates two solid surfaces. In the fluid friction, the friction process occurs in the fluid layer such as lubricating film. In the case of fluid friction, irreversible effects as deformation are observed inside the fluid, which can lead to changes in the initial flow properties of fluids.

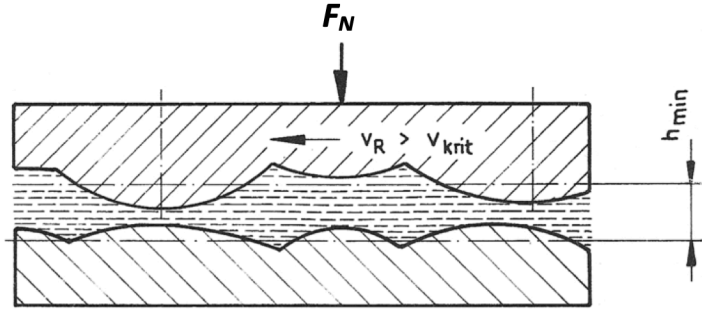

Figure 2.4 Model of fluid friction taken from [6]

Gas friction: Gas friction is a particular class of the fluid friction in which material region most significantly involved in friction has gas state properties [2].

Mixed friction: Mixed friction is a mixed form of at least two friction states that coexist temporally or locally [2]. Figure 2.5 shows a model of mixed friction state, which based on the solid and fluid friction. The idea that mixed friction requires the tribological contact, in which there are areas that are separated by a lubricant and other areas that have direct solid surface contact, is emphatically conflicted [5]. Direct contact areas can be only conceivable by high temperature peaks in the micro range or by a starved lubricated situation in the friction point, but not by a breakthrough of the lubricant film occurring as a result of maximum pressure [5].

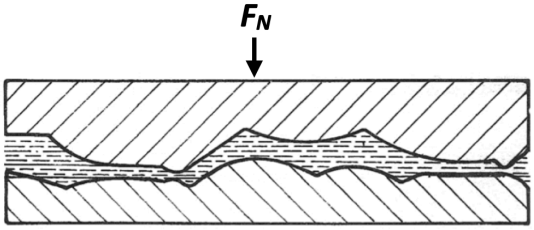

Figure 2.5 Model of mixed friction taken from [6]

To evaluate the tribological behaviour of friction pairings, friction states can be best characterized using the Stribeck curve shown in Figure 2.6. In the Stribeck curve, the friction coefficient, which is the ratio of friction force and normal force, is plotted versus the relative speed of the friction bodies. If the relative speed of both surfaces is zero, the friction coefficient is at its maximum value. As shown in Figure 2.6, the friction coefficient decreases with increasing relative velocity where the friction is considered as mixed friction. Moreover, the Stribeck curve shows that a minimum friction coefficient is reached during the transition from mixed friction to fluid friction. At this area, there is complete hydrodynamic separation of the friction surfaces. In the state of fluid friction, the solid bodies are completely separated with a lubricant and the friction coefficient increases with increasing relative velocity due to the increasing internal friction in the lubricant.

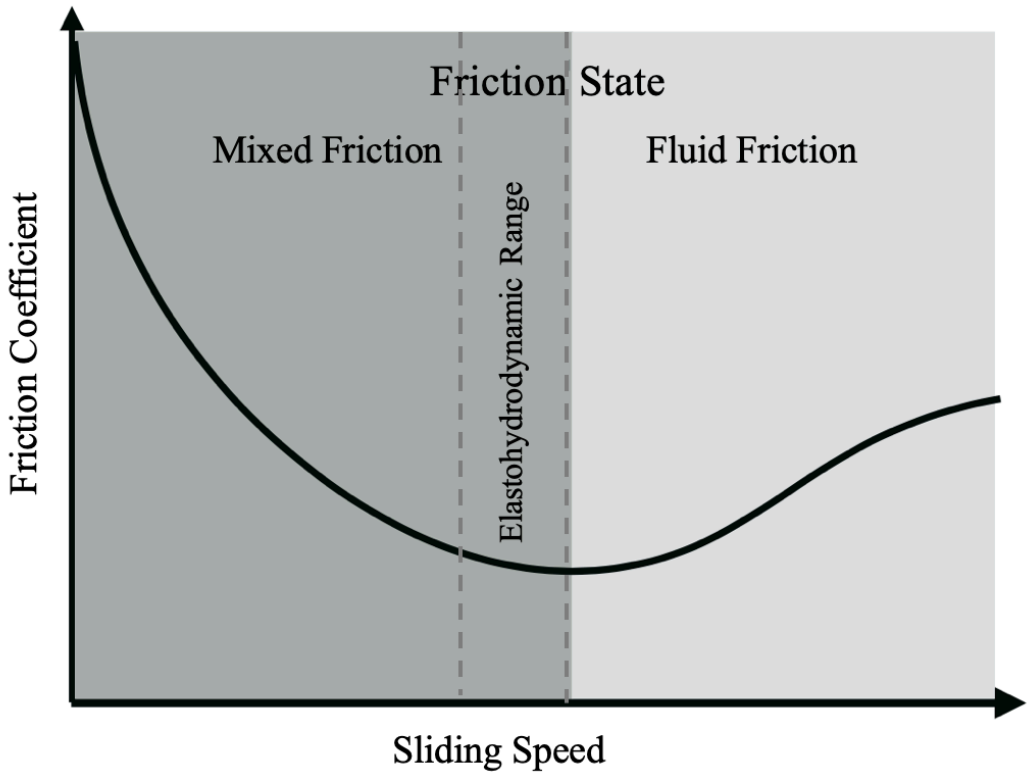

Figure 2.6 General behaviour of the friction over the sliding speed and friction states in the Stribeck curve (adapted from E. Kuhn [5])

2.2.3. Friction energy

The friction can be defined as the energy expenditure in the tribological system [7]. According to this definition, it is important to explain the term of friction energetically. The energetic approach plays an important role in making statements about the service life and reliability of friction pairings by calculating friction and wear. The basis of energetic considerations is the dual nature of friction [2]. The dual nature means that the frictional energy is composed of two parts which are the deformation part and the adhesion part as displayed in Figure 2.7 [8].

The friction consists of the energy required to overcome the overlap, which represents the mechanical or deformation component of the friction, and the energy to separate the material connections, which represents the molecular part of the friction [2]. Overcoming can take place both by elastic or plastic deformations or by chipping deformation in the friction body 1, 2 or by deformation in the lubricant 3 as intermediate material [2]. It can also occur by separating the material connection in the contact surfaces of the friction bodies. The friction bodies are usually stressed differently and this difference is taken into account when considering the friction process from an energetic point of view [5].

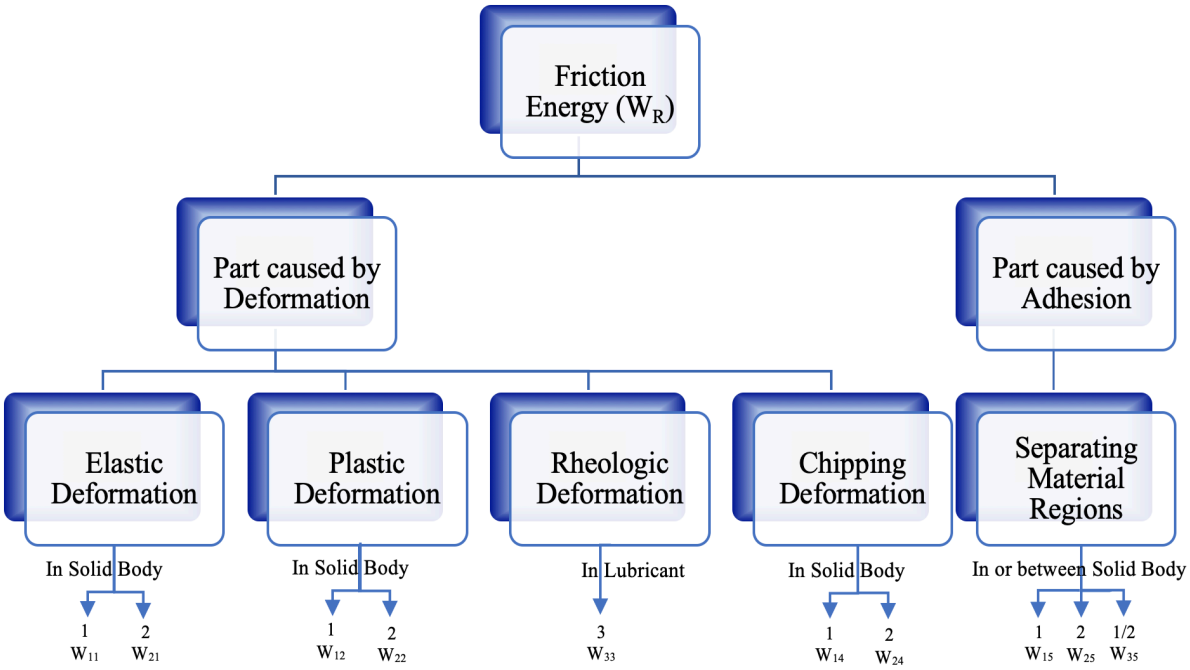

Figure 2.7 Possible components of the friction energy - dual nature of friction. Note: W_{ij} with i–friction body and j–mechanism (adapted from G. Fleischer [8])

The friction energy expenditure consists of the sum of the friction energy proportions, as shown in Figure 2.7 and can be calculated as follows [2]:

$$W_R = \sum_{(i,j)} W_{ij} \tag{2.1}$$

where index i is the number of the friction element and index j is the number of the type of energy component.

To estimate the components of single friction energy in the solid body friction state, it is necessary to determine the energy density ($e_{i,j}$), the volume of the involved contact (V_{ij}) and the number of similar energy components (n_{ij}) [2]:

$$W_R = \sum_{(i,j)} e_{i,j} \cdot n_{ij} \cdot V_{ij} \tag{2.2}$$

The energy density (e) is a material parameter. In order to calculate the energy density, the mechanical properties of the friction body materials and the intermediate materials in the deformation or separation process must be known. In general, the energy density can be obtained using:

$$e = \frac{W}{V} \tag{2.3}$$

where W is the friction energy and V is the volume of the involved contact.

The friction energy density for single system elements involved can be estimated as follows [2]:

$$e_{R,i} = \frac{\sum_j e_j \cdot n_j \cdot V_j}{\sum_j n_j \cdot V_j} \tag{2.4}$$

2.3. Wear

In the tribological system, the friction process causes wear, which is the result of friction energy input into a tribological system [9]. In more recent work, e.g. [5], the definition for wear can be found in the following form:

Wear is the dissipation of the supplied frictional energy with simultaneous production of entropy.

This definition extends the wear beyond the solid body. Wear is influenced by the material, shape and surface of the body and by the type, particle size and properties of the intermediate material. In addition, the load conditions such as the size and time course of the load and also the temperature, as well as the type of ambient medium play an important role.

During the wear process, the physical and chemical process take place because of the mechanical and energetic interaction in contact area. These processes are known as wear mechanisms and cause the material changes and material loss of the friction partners. The wear mechanisms can occur individually, successively or superimposed depending on the structure of the tribological system and the operating variables. The wear mechanism is divided into adhesion, abrasion, surface fatigue and tribochemical reaction.

2.3.1. Wear states

The states of wear result from the friction states. According to the physical states of the stressed material involved in wear, wear is divided into solid body wear and lubricant wear, as shown in Figure 2.8. In the case of solid body wear, wear occurs in solid material regions due to friction process and direct contact of surfaces. Moreover, the solid body wear is also differentiated into abrasive, adhesive, deformation wear and property wear. Abrasive wear is defined as a loss of material in the solid-state material regions due to submicroscopic, microscopic, macroscopic fracture processes or separation processes [2]. Adhesive wear refers to unwanted material transfer from one friction surface to another due to micro-adhesion and macro-adhesion as a result of the friction process. In contrast to abrasive and adhesive wear, a deformation wear may

occur as a result of plastic deformation without material loss in the relevant material region. In the case of property wear, an increase in internal energy leads to a change in the physical and chemical properties in the friction bodies. In addition to solid body wear, the lubricant wear refers to the removal of lubricant layer in tribological contact. Kuhn describes the rheological wear as irreversible structural change due to tribological stress in material areas of a pseudoplastic lubricant [5].

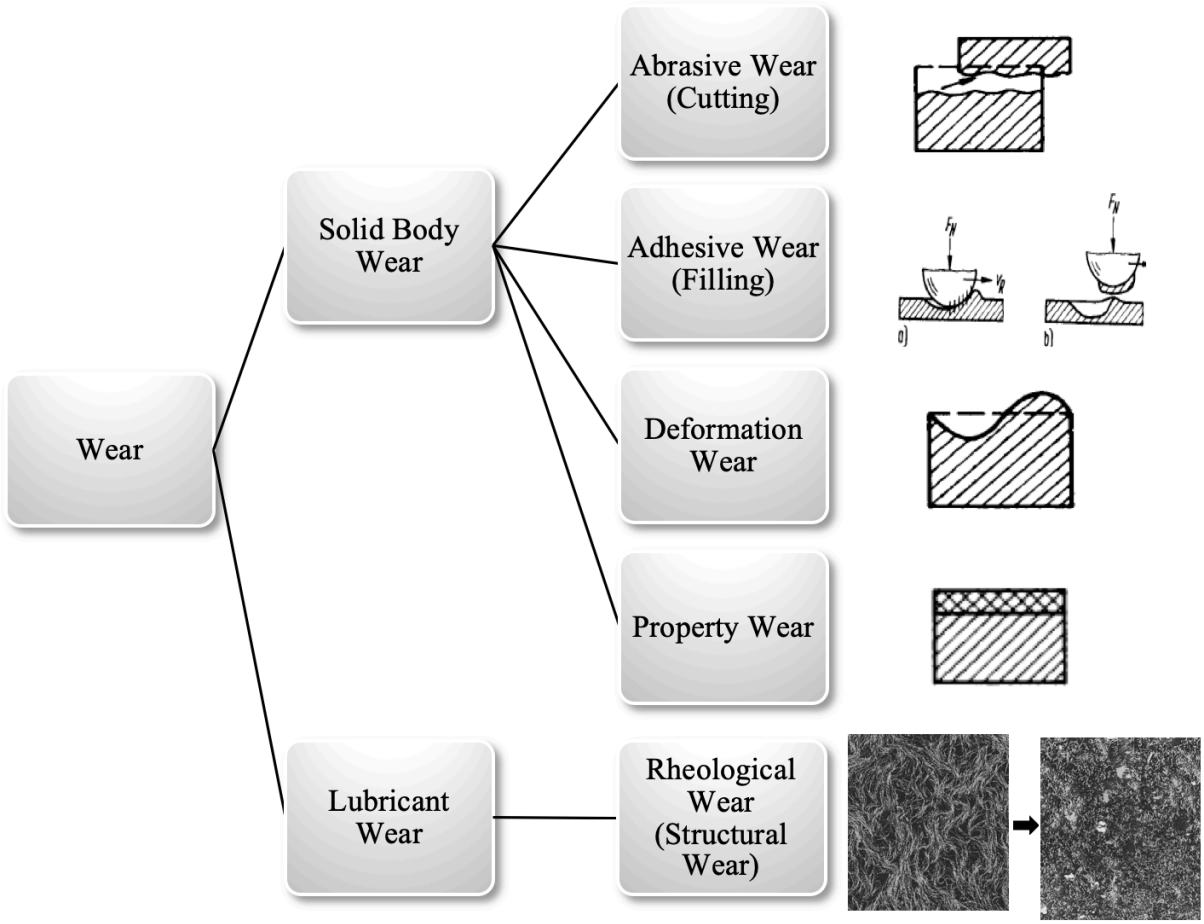

Figure 2.8 Classification of tribological wear (adapted from E. Kuhn and G. Fleischer [2,5])

2.3.2. Wear types

Depending on the type of motion of the friction bodies und the structure of the tribological system, different wear types can be observed in analogy to friction types. The wear is divided into the sliding, rolling and drilling wear as solid wear types.

2.4. Lubricating greases

The use of a thin layers of gas, liquid or solid called lubricant between two surfaces improves the smoothness of movement of one surface over another that is observed as lubrication [10]. In general, the lubricant prevents the direct contact of the two solid bodies which leads to reduce the friction energy and the loss of material as one type of wear.

The applications of the lubricants to machine elements play important roles in protecting the friction spot from corrosion, controlling temperature, avoiding the penetration of contaminants and other substances from the exterior into friction contact and providing a fluid seal [11]. Operating conditions and the material type influence the efficiency of the lubricants in the lubricating contact [10]. For instance, a gaseous film is used for low contact stress while solid films are usually preferred at slow speed contacts [10].

Generally, lubricants can be divided into two major types depending on the applications [12,13]:

- automotive lubricants used in the automobile and transportation industry like engine oils, gear oils and hydraulic fluids,
- industrial lubricants used for industrial purposes and special purposes according to specific operations like industrial oils, greases, metalworking lubricants, solid lubricant films and process oils.

Figure 2.9 gives information about how many lubricants were consumed worldwide over an eleven-year period between 2007 and 2017, and the breakdown by product groups in 2017. It can be seen that the consumption of lubricants has increased with time and the worldwide lubricant consumption peaked with 36,1 million tons in 2017. Moreover, as shown in Figure 2.9, automobile oils make up the highest lubricant consumption with a share of 57 percent and follow industrial oils with a share of 26 percent in 2017.

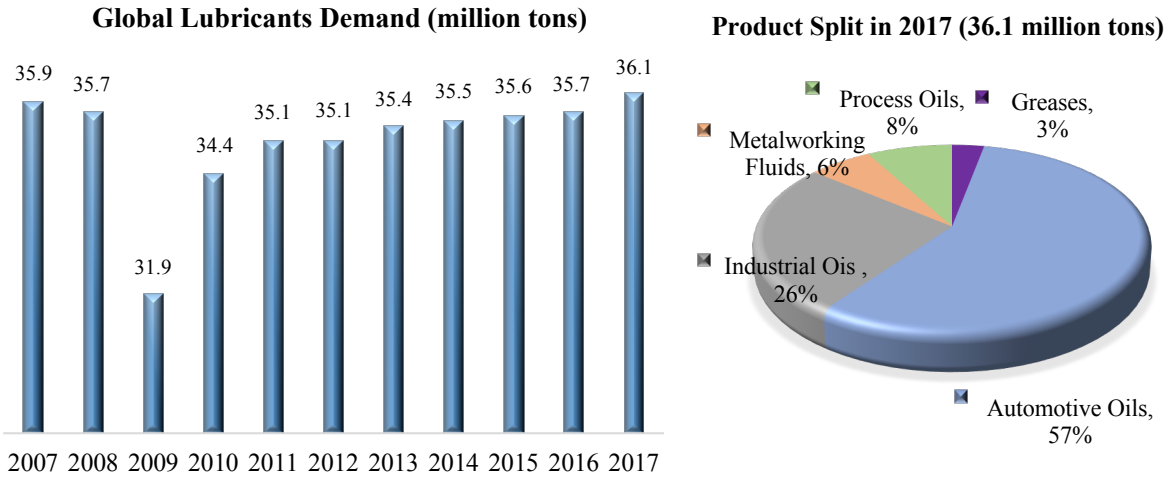

Figure 2.9 Global lubricants demand (without marine oils) and product split in 2017 [14]

The most widely used lubricant are liquids such as oils; however, due to the physical stability and rheological properties of lubricating greases, the use of these instead of liquid lubricants can provide an advantage in several applications, where lubricating lubricants would not stay or adhere in the contact, in order to handle some factors like fluctuations with temperature, loads, vibrations and surrounding environment conditions [15]. Moreover, lubricating greases can be employed in hard-to-reach contacts in order to reduce the leakage and frequency of lubrication [16]. Lubricating greases can additionally provide more water-resistance, act as seals against dirt and help to reduce noise [12,17]. On the other hand, the use of lubricating greases shows some disadvantages over oils, when heat transfer is a problem or since they are more sensitive to oxidation. In addition, lubricating greases exhibit a lower speed limit due to their higher effective viscosity [12].

Grease is defined as a semisolid lubricant, in which a thickener is dispersed in a lubricating oil [10]. In addition to base oil and thickener, some chemical or physical additives can be used in grease formulations in order to improve specific properties and functions like the mechanical stability and the oxidative stability of the grease.

2.4.1. Grease classification

In general, the classification of the lubricating greases is associated with their consistency which is established by the National Lubricating Grease Institute (NLGI). The grease consistency is determined by penetration of a standard cone, according to ASTM D 217, and is classified into nine grades according to their penetration depth as shown in Table 2.1. The

smallest NLGI class is designated as 000 and corresponds to the highest penetration depth in the penetration test. On the other hand, Class 6 has the lowest penetration depth. In other words, with increasing NLGI classes, the consistency becomes stiffer and the penetration depth in the penetration test decreases.

Depending on the application in the tribological contact grease grade is chosen. Soft greases, i.e. 000 ,00, 0 and 1 grades, are preferred for low viscosity applications, while grades 0, 1 and 2 are used in highly loaded gearing [10]. Greases 1, 2, 3 and 4, are usually applied to rolling contact bearings. In addition, harder greases, 5 and 6, are chosen for higher speed applications or applications in which leakage is a concern [10]. However, the NLGI grade alone is insufficient to specify the grease required by a particular application. Besides consistency, the selection of a grease for a specific application also depends on the other properties such as mechanical stability, application temperature limit and oxidation resistance.

Table 2.1 Grease classification according to DIN 51818

NLGI classes according to DIN 51818	**Worked penetration values according to DIN ISO 2137 [0.1 mm]**	**Description of nature**	**Application**
000	445 to 475	Watery	Gear
00	400 to 430	Liquid	
0	335 to 385	Semi fluid	
1	310 to 340	Very soft	Gear Roller bearing Slide bearing
2	265 to 295	Soft	
3	220 to 250	Supple	
4	175 to 205	Nearly firm	
5	130 to 160	Firm	Block greases
6	85 to 115	Very firm	

2.4.2. Composition of lubricating greases

Lubricating greases principally consist of a base oil and a thickener. Base oil comprises the largest ingredient of a grease, which may take a share of 65-95% by weigh. Base oil viscosity plays important role in determining application conditions of a grease. Thickener in combination with the base oil provides the solid to semi-fluid structure, which may take a share of between 5 to 35 wt. %. The grease consistency is dependent on the thickener content. In addition to base oil and thickener, the lubricating grease can also contain additives, usually additive packages, to enhance the tribological characteristics of greases. Each of the three components can change the properties of the grease considerably, depending on the type and amount. Overall, the operating behaviour and the intended use of lubricating greases are determined by the concentration and type of the three components.

2.4.2.1. Base oils

Mineral and synthetic oils and esters are used as base oils. Vegetable oils are also used for special applications. Since the proportion of the base oil in the composition of the lubricating greases is quite large, the base oil significantly influences the properties of the lubricating grease. Base oils must not only have good lubrication properties, but must also have good flow properties and high thermal and oxidative resistance.

To produce a lubricating grease, mineral oils are most widely used as base oil, the kinematic viscosity of which is in a range of between 40mm^2/s and 3400mm^2/s at 20°C [5]. About 99% of greases are formulated with mineral oils [10]. Mineral oils are derived from crude oil-vacuum distillation and subsequent refining. The base oils can be differentiated according to the nature of the crude oil, i.e. naphthenic, paraffinic or aromatic. Naphthenic oils have low viscosity index; however, they are the most common. In addition, naphthenic oils maintain the fluid properties at low temperatures and can easily combine with soaps [10]. Paraffinic oils can present a higher viscosity index than naphthenic oils. In addition, they can be used for high-temperature applications and in applications requiring a longer lubricant life [18]. The aromatic oil is present as a minor component of naphthenic or paraffinic oils [10].

Polyalphaolefin (PAO), synthetic esters, phosphate esters and silicones are the most widely used synthetic oils. Synthetic oils are mostly employed for special applications such as in high performance aircraft, missiles and in space [10]. In general, the use of synthetic oil instead of mineral oil as a base oil shows some advantages such as higher viscosity index, excellent low-

and high-temperature performance and good oxidative stability, as well as some disadvantages, such as the higher cost [18]. Vegetable oils as base oils are obtained from renewable resources and used in greases intended for the food and pharmaceutical industries.

2.4.2.2. Thickeners

Thickener confers the semi-solid character to the lubricating grease and forms a tridimensional structure inside the lubricating fluid. The thickener has the ability of storing energy within the structure and provides the lubricant an elastic behaviour [19,20]. Moreover, thickeners do not only determine the consistency of the lubricating grease, which is dependent on the concentration of the thickener, but they also offer the suitable rheological and tribological behaviour to the lubricating grease [21,22]. In this sense, thickener dependent properties are rheological behaviour, mechanical stability, speed characteristics, oxidation stability, water and acid resistance and operating temperature range [23]. The characteristics of a grease relate to the type of thickener used. Therefore, the grease type can be classified according to type of thickening agents used during manufacture. In general, the thickeners can be divided into the three groups: soap-thickeners, complex-soap thickeners and non-soap-thickeners, as shown in Figure 2.10.

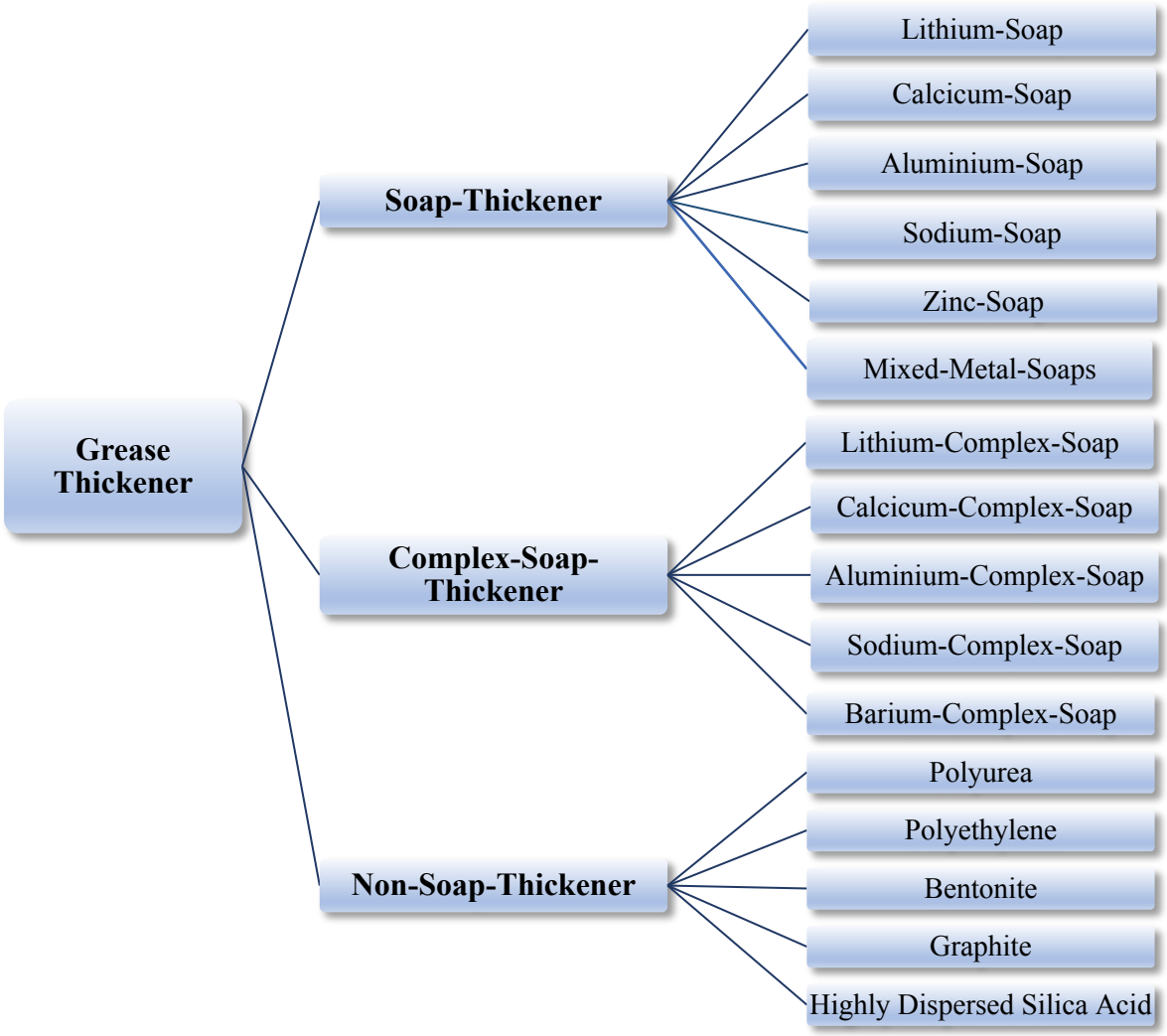

Figure 2.10 Common thickeners used to produce lubricating greases

Simple soaps are the most common type of grease thickeners. From a chemical point of view, soap thickener is derived from the saponification reaction of animal or vegetable fatty acids. The most frequently employed soap type greases are lithium, calcium and aluminium in which soap are based on metal salts of fatty acids [10]. Lithium greases have high dropping point (melting point) at 180°C, good water resistance, good adhesive characteristic, very well structural and shear stability. In addition, some properties of lithium greases such as corrosion protection and oxidation resistance can be improved by suitable additives. Calcium soap greases have the lowest raw material costs compared to other simple metal soaps. In general, they have very good water-resistance and good adhesion characteristics. The considerable disadvantages of these greases are poor shear stability and the comparatively low upper operating temperature limit (80°C). However, with the use of 12-hydroxy stearate the dropping point of calcium greases can be raised up to 120°C.

In contrast to simple soap greases, complex soap greases are composed of a simple soap and a complexing agent such as short chain carboxylic acids or inorganic acids. This combination leads to complex mixtures of thickener molecules of different chain lengths. Moreover, these complexes can provide very good properties to the thickener such as high temperature resistance, increase in dropping point and ability to use in high stress. Complex greases based on lithium, aluminum, calcium and barium show a high dropping point of 218°C for barium greases and 260°C for others [10,24]. In addition, complex soap greases exhibit very good oxidation resistance [24].

According to the thickener types, lubricating greases can also be thickened with non-soap materials which consist of organic or inorganic materials. The silica and bentonite clays are most commonly used as inorganic thickening agents [10]. These types of lubricating greases can be employed in high temperature applications and their maximum operating temperature is determined by the oxidation stability of the base oil and other grease components, because they have no defined melting point [10]. The greases based on organic thickeners such as polyurea and polyethylene offer superior performance in extreme temperature conditions and ideal properties such as resistance to loads. The most commonly used is polyurea thickener which is derived from urea derivatives and don't comprise any metallic components [25]. They exhibit excellent mechanical and thermal stability, outstanding service life and high dropping point of 270°C [10].

2.4.2.3. Additives in lubricating greases

Lubricating grease additives are chemical compounds and substances that are added to improve certain properties of grease. In general, additives are divided into two groups [26]:

- Additives which change the physical and chemical properties of the lubricants, e.g. viscosity modifier and anti-oxidants,
- Additives which change the physical and chemical properties of friction surfaces, e.g. extreme pressure and anti-wear additives.

Additives commonly used in lubricating greases are oxidation, rust and corrosion inhibitors, tackiness, anti-wear agents and extreme pressure (EP) additives [10].

2.4.3. Bio-based lubricating greases

It is estimated that about 40-50 % of the around 5 million tonnes of applied lubricants in Europe annually return to the environment due to losses during operation, spillages during topping-up, leaks or accident losses [12]. The environmental damage, which is caused by lubricants, has increased the need for renewable and biodegradable lubricants. Therefore, the use of biodegradable greases for different industrial applications is remarkably important for avoiding direct and indirect environmental pollution [27-29]. In this sense, some lubricant industries focus on developing their products from renewable resources in order to minimize adverse impacts on the environment and avoid indirect impact on human health.

In general, biolubricants can be defined as lubricants, obtained from bio-based raw materials i.e. vegetable oils, animal fats or any other environmentally benign hydrocarbons, which are rapidly biodegradable and/or non-toxic to humans and the environment [30]. Biodegradability can be described as a measure of the breakdown of the chemical structure of the substance by microorganisms [31]. Biodegradability is evaluated for each component in the lubricant separately [32]. According to biodegradability, the substance is considered into three categories [32-34]:

- **readily biodegradable substances**, in which the level of biodegradation is achieved by more than 70% within 28-day period in tests based upon dissolved organic carbon or by more than 60 % of the theoretical maximum value in tests based upon oxygen consumption or carbon dioxide generation,
- **inherently biodegradable substances**, when they show biodegradation higher than 70% after 28 days in an inherent degradation test or higher than 20% but less than 60% of the theoretical maximum value after 28 days in the test based upon oxygen consumption or carbon dioxide generation,
- **non-biodegradable substances**, which comply neither with easy nor with inherent biodegradability.

In order to characterize and label environmentally acceptable products e.g. biodegradable lubricants, several eco-labels and standards like Blue Angel by Germany, European Eco-label by the European Union and Swedish Standard by Sweden have been developed in different countries [12,27,31,32]. In general, the main objective of these eco-labelling programs for biodegradable lubricants is to draw attention to products that consist of renewable raw materials and have the potential to reduce the negative environmental impact due to low toxicological

hazard potential and good biodegradability [12,33]. In order to grant the environment label, there are several the ecological criteria for the biodegradable lubricants which include a series of test and verification requirements regarding some properties like the toxicological effect and the degradation behaviour of the components used in the lubricant [33].

A consequence of intensive research and development in the past is the number of the so-called bio-grease formulations reported in the scientific literature or even industrially produced. These lubricants consist of a vegetable-derived oil like castor oil or sunflower oil and traditional thickeners like metal soaps [17,35-39]. The use of vegetable oil instead of mineral oil as a liquid lubricant is widely spread [40-42] and shows some advantages, such as good lubricity, the ability to adhere to metal surfaces, non-toxicity, high biodegradability, weak viscosity-temperature dependence, solvency for lubricant additives and low volatility, as well as some disadvantages and certain limitations that restrict their applicability such as poor oxidative stability which is dependent on the unsaturation degree, deficient low temperature flow properties, and small range of viscosities, as discussed and reported in previous works [43-48]. However, these negative features can be overcome or minimized by using additives or inducing chemical modifications [44,45,49-52]. Erhan et al. [46]. sought to improve the oxidation behaviour and low temperature flow property of soybean oil as vegetable oil by using a combination of chemical additives, diluent (PAO) and high-oleic vegetable oils. Moreover, the effectiveness of using epoxidized soybean oil (ESBO) over soybean oil (SBO) and genetically modified high oleic soybean oil (HOSBO) for high temperature lubricant applications was investigated by Adhvaryu and Erhan [44]. The research [44] showed that ESBO provided good response to antioxidant additives at low concentration (1%) and preserves a low thermal and oxidative behaviour compared with other examined test oils.

Completely biogenic lubricating greases can be obtained by replacing the mineral base oil with a vegetable oil, as well as by substituting traditionally used thickener agents (metallic soaps or polyurea compounds) with biogenic thickeners. In previous research [53-60], some formulations, such as those based on castor or soybean oil used as a biodegradable base oil, and natural thickeners like cellulose derivatives, chitin, glyceryl stearates, or sorbitan stearates, were rheologically and tribologically investigated and compared with some traditional greases, such as lithium-12-hydroxysteate lubricating grease. The results of these works showed that some formulations provided similar or better thermal, rheological, and mechanical properties than traditional lubricating greases for potential lubricating applications. Moreover, bio-grease formulations, based on castor oil as the base oil and sorbitan and glyceryl monostearate or

acylated chitosan as the thickener agents, generally yielded lower friction coefficient values than the reference lithium greases in some tribological tests [55].

2.4.4. Grease microstructure

In a grease, the thickener forms a three-dimensional network composed of fibres, fibre agglomerates or other structural units such as rods. Microstructure of lubricating greases may be obtained by crystallization of the thickener particle inside the lubricating oil [61]. The geometry and the distribution of the thickener, the interactions of the thickeners with tribological system and the ability of storing energy qualify the grease structure [7]. Moreover, the lubricating grease microstructure depends on nature and concentration of the thickener employed, nature and viscosity of the base oil, and process of the grease production [62-66]. Regarding the influence of thickener concentration on the lubricating grease microstructure, Delgado et al. [62] showed that large particles in form of platelets were observed for lithium lubricating grease with the low thickener concentration, while an increase in thickener concentration leads to a high density of physical entanglements among fibers. In addition, lithium grease prepared with a high viscosity base oil exhibited longer fibers and larger hollow spaces among fibers, in which base oil is trapped, compared to lithium grease prepared with low viscosity base oil [62].

Lubricating grease microstructures can be observed by means of scanning electron microscopy (SEM) and atomic force microscopy (AFM). Important difference in these techniques is that SEM technique is vacuum based, in which lubricating oil must be removed or its volatility reduced before experiments, while in AFM technique the tests can be performed under atmospheric pressure, in which grease sample is not submitted to any physical modification [63,67]. Figure 2.11 shows SEM images exhibiting the different shape of lithium, lithium complex and polyurea greases. As can be observed, much more twisted and entangled fibers appear in the microstructure of lithium grease compared to lithium complex grease, while polyurea grease shows thickener particles in the form of platelets.

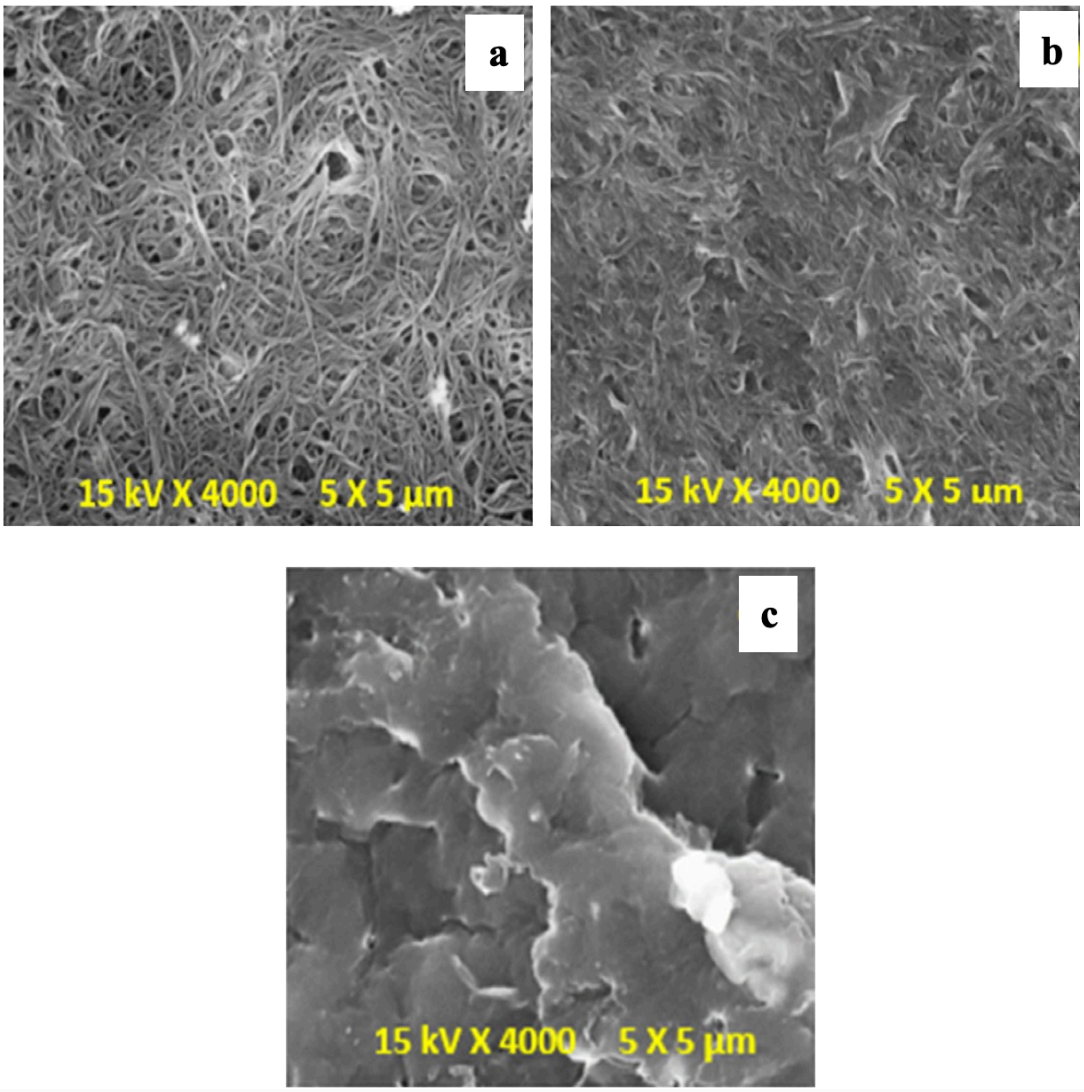

Figure 2.11 SEM (15 kV and × 4000 magnification) photomicrographs for various lubricating greases: (a) lithium grease, (b) lithium complex grease and (c) polyurea grease (window sizes of 5 µm × 5 µm) [68]

Figure 2.12 displays the microstructure obtained using AFM for aluminium complex, calcium complex and lithium-calcium complex greases. Aluminium complex grease shows a fibrous microstructure with small and fine fibers, and calcium complex grease thickeners appear to be in the form of large aggregates often separated by a larger distance. Moreover, the lithium-calcium based complex grease exhibits a connecting fibrous-granular microstructure [63]. As can be seen in Figure 2.11 and Figure 2.12, SEM and AFM photomicrographs show an apparent difference in the microstructure of the lubricating greases, depending on the kind of thickener used and the particles' size. The shape and distribution of thickener particles and the percentage in the full volume of the grease affect the physical properties of the lubricating grease [69].

Lubricating greases having too high particles distribution of the thickener, cannot exhibit enough capability of making spatial, three-dimensional structures due to the physicochemical interactions, which leads to negatively influence on lubricating properties [69]. Moreover, too large particles of the thickener produce an increase in the consistency of the lubricating grease, resulting in their easy disruption inside the tribological contact [69].

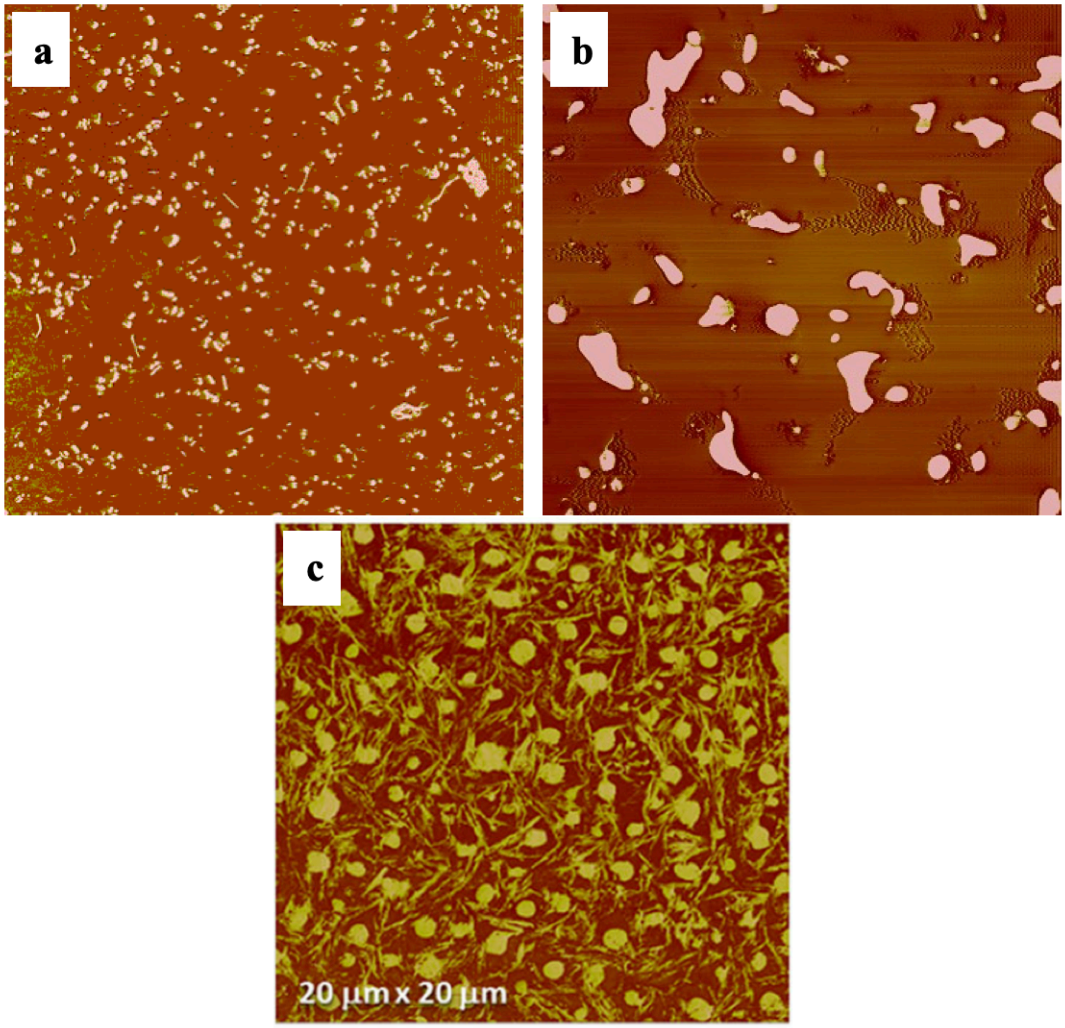

Figure 2.12 AFM micrographs for various lubricating greases: (a) aluminium complex grease, (b) calcium complex grease and (c) lithium-calcium complex grease (window sizes of 20 µm × 20 µm) [63,70]

The base oil is connected to the thickener through a combination of van der Waals and capillary forces. In theories of grease structure, the flow properties of greases are primarily related to the interactions between thickener molecules, i.e. inter- and intramolecular van der Waals forces, and the geometry of the structural units [71]. Degradation of the thickener microstructure and a reduction in particle interactions lead to changes in the flow properties of greases during the

shearing process [71-73], mainly caused by the flow orientation of particles (mostly fibres) and/or particle breakdown [63]. The occurrence of these changes in the thickener structure when relatively low shear stresses are applied is responsible for the complex yielding flow behaviour of greases. This behaviour is characterized by a discontinuity in the flow curve associated with an apparent yield stress, which is also associated with a sudden drop in viscosity [70]. Therefore, the stability of the thickener microstructure in lubricating greases influences their friction reduction, ability to flow, grease performance, and protection of lubricated surfaces in a tribological system [69].

2.4.5. Rheological behaviour of lubricating greases

The rheology deals with the flow behaviour of liquids and with the deformation behaviour of solids. The rheological behaviour of lubricating greases plays an important role to predict the flow and deformation of lubricating greases under operating conditions and to understand the microstructure of the lubricating greases and grease reactions in the tribological system [66,74].

The rheological behaviour of lubricating greases can be characterized by [5]:

- A yield stress must be overcome to flow.
- The viscosity decreases with the increase of shear rate, i.e. shear-thinning flow behaviour.
- Lubricating greases are partly thixotropic. This means that the viscosity decreases with the shear time and after the shearing process and a rest period, the viscosity increases again, partially recovery the initial viscosity.

Lubricating greases are viscoelastic substances. This means that lubricating greases exhibit both solid and liquid properties, as a function of the applied stress. The elasticity is related to the internal microstructure formed by the thickening agent and its properties allow lubricating greases to remain in contact with the moving surfaces and not to leak out from the tribological contact. In addition to this, elasticity of lubricating greases enables the ability to store the elastic energy [5]. The viscosity characteristic is mainly related to the base oil and allows lubricating greases to flow under the shearing process.

The viscoelastic behaviour of lubricating greases can be investigated by means of the oscillatory shear experiments in the rheometer. The amplitude sweep tests are usually used to characterize the linear viscoelastic behaviour (LVE-behaviour) but also to investigate the fluid friction inside the grease film within the linear viscoelastic range. Moreover, the amplitude sweeps tests allow to determine the yielding point as the value of the shear stress at the limit of LVE-range,

which is often associated with the yield stress, and the flow point, as the value of the shear stress at the crossover point. In amplitude sweep tests, the lubricating grease is sheared in the gap between an oscillating plate and a fixed plate, and the amplitude of the oscillation is increased step wise at a constant frequency. To evaluate the measured results of the amplitude sweeps, the values of the storage (G') and the loss (G'') moduli are usually plotted on the y-axis against the corresponding deformation, γ, or shear stress, τ, as depicted in Figure 2.13. It has been established that G' represents the elastic component of the viscoelastic response and takes into account the reversibly stored deformation energy. In contrast, G'' describes the viscous component and is a measure of the irreversible energy expended. Typically, in the first region of the curve in Figure 2.13, G' and G'' are constant at low deformations, corresponding to the so-called linear viscoelastic regime (LVE), which describes the behaviour of lubricating greases under applied oscillatory stress below their yield stress. In LVE-range, lubricating greases behave like a viscoelastic solid and their structure is undisturbed. According to DIN 51810–2 [75], the limit of the LVE range, is determined by a change in either G' or G'' of more than 10% from the LVE-plateau values; this "critical point" is denoted by the first vertical line in Figure 2.13. At this point, a critical energy level is reached, which initiates the degradation of the grease structure. This critical level of energy is named the critical energy density ($e_{rheo-critical}$) and can be determined with [76]:

$$e_{rheo-crtical} = \frac{G' \cdot \gamma_{critical}^2}{\cos \delta} \tag{2.5}$$

where δ [-] is the phase shift angle. Another characteristic point in the amplitude sweep tests is the crossover point between G' and G'' outside the LVE. This crossover point is typically called the flow point because it is assumed that the whole grease sample starts to flow at this point. At this point, the viscoelastic behaviour of the grease changes irreversibly, inducing a transition from the solid state ($G' > G''$) to the fluid state ($G' < G''$) [77]. The indirect measure for the structural degradation of a lubricating grease caused by liquid friction can be the expended energy to reach the crossover point in an oscillating measurement [78,79]. The expended energy at the crossover point can be estimated as follows [80]:

$$e_{rheo-cross} = \frac{G' \cdot \gamma_{cross}^2}{\cos \delta} = \tau_{cross} \cdot \gamma_{cross} \tag{2.6}$$

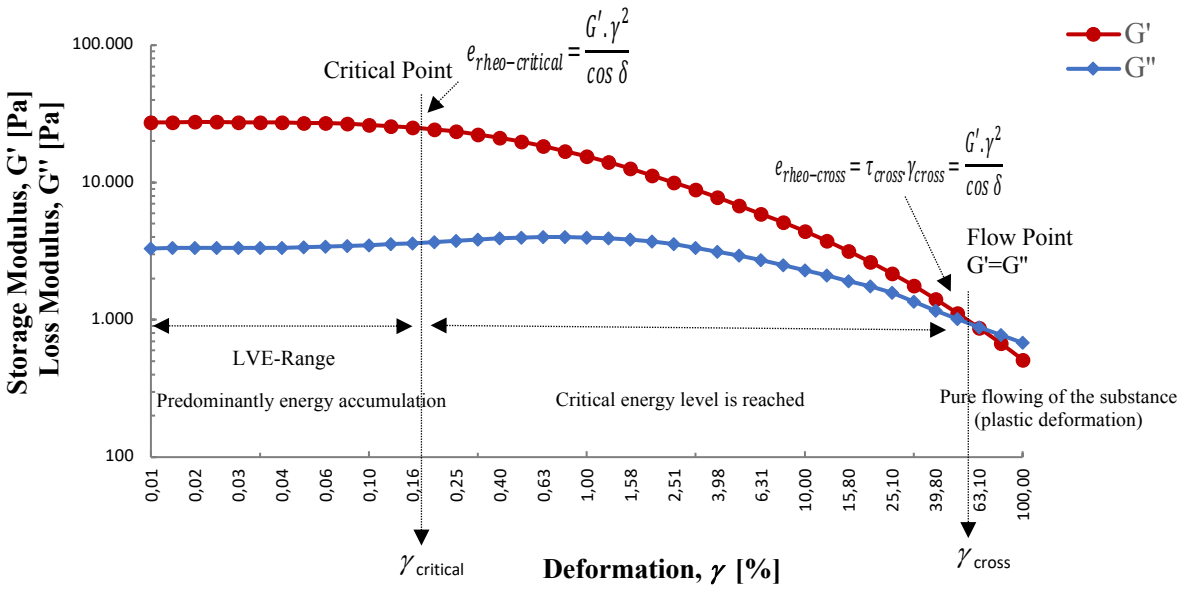

Figure 2.13 Typical evolution and characteristic points of the storage and loss moduli during an amplitude sweep

In frequency sweep tests at a constant amplitude inside the LVE, the evolution of viscoelastic moduli versus frequency represents the mechanical spectrum of lubricating greases. Typically, the values of the storage modulus G' are higher than values of the loss G'' modulus in the whole measured frequency range, as shown in Figure 2.14 [62,81-84]. Figure 2.14 displays the mechanical spectrum for a lithium lubricating grease, which corresponds to the gel-like response of colloidal structures and highly entangled polymeric systems [85].

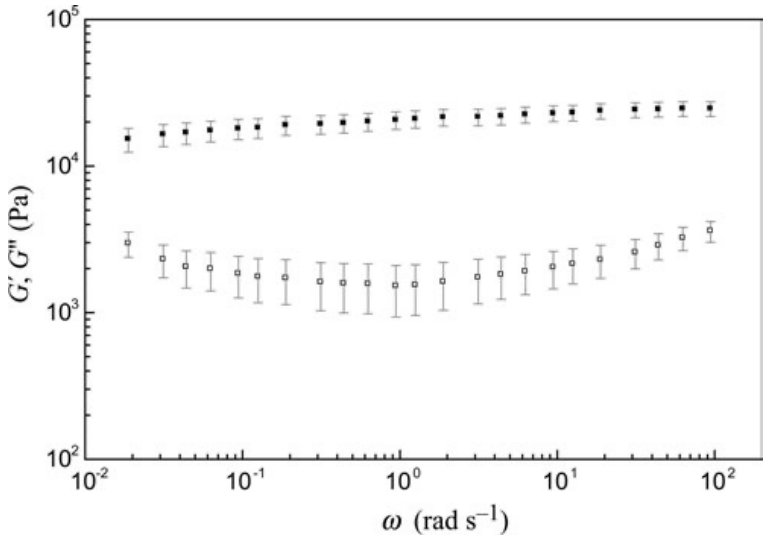

Figure 2.14 Typical evolution of the storage and loss moduli during a small amplitude oscillatory shear test for lubricating greases [22]

The study of rheological properties provides some useful information for understanding of how several parameters like thickener concentration, base oil viscosity and temperature influence the lubricating grease rheological properties. [62,69,86-89]. Delgado et al. [62] investigated the influences that thickener concentration and base oil viscosity exert on the rheology of lubricating greases and its relationship with microstructure of grease. The results of this study showed that an increase in thickener concentration, which provides a more compact and/or entangled microstructural network, leads to an increase in the values of the viscoelastic functions in the linear viscoelastic regime (Figure 2.15) [62]. As can be observed in Figure 2.15 (b), the values of loss tangent (tan δ), which is described as the ratio of the viscoelastic moduli, remain almost stable in the whole examined frequency range. This reveals that the relative elasticity is not influenced by thickener concentration [62].

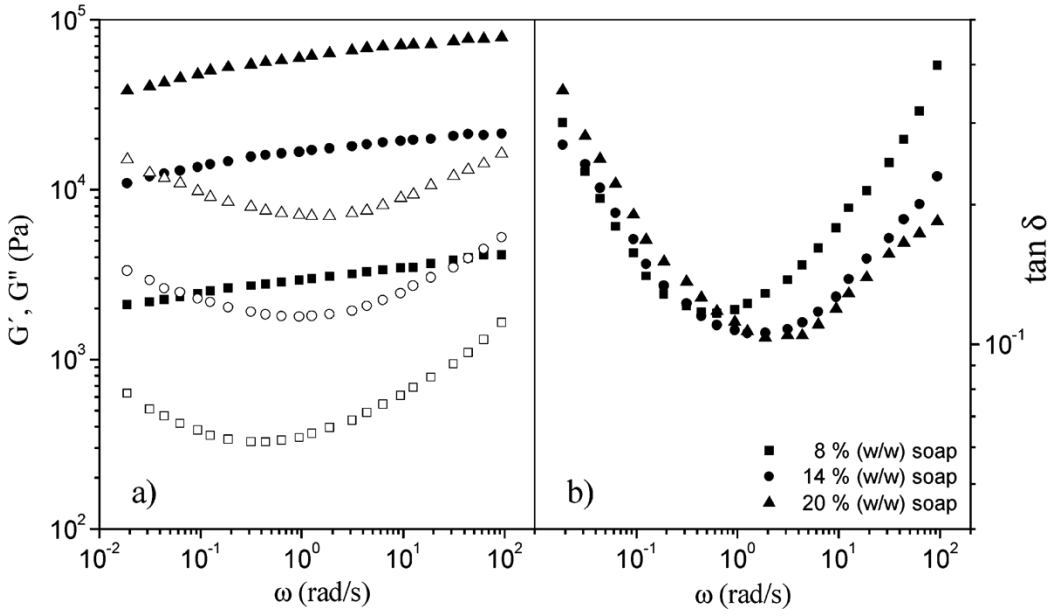

Figure 2.15 Effect of the thickener concentration of lubricating greases on (a) the storage G' and loss G" moduli and (b) the loss tangent tan δ [62]

Moreover, Paszkowski [69] analyzed the influence of soap thickener (lithium 12-hydroxystearate) concentration on the critical strain (γ_c) value and shear stress (τ) value in the critical point by means of a stress/strain controlled rotational rheometer. As a result, an increase in soap thickener concentration leads to a decrease in the value of critical strain and an increase in the value of shear stress in the critical point, as shown in Figure 2.16. This result reveals that the range of the linear viscoelasticity depends on the thickener concentration in the lubricating grease.

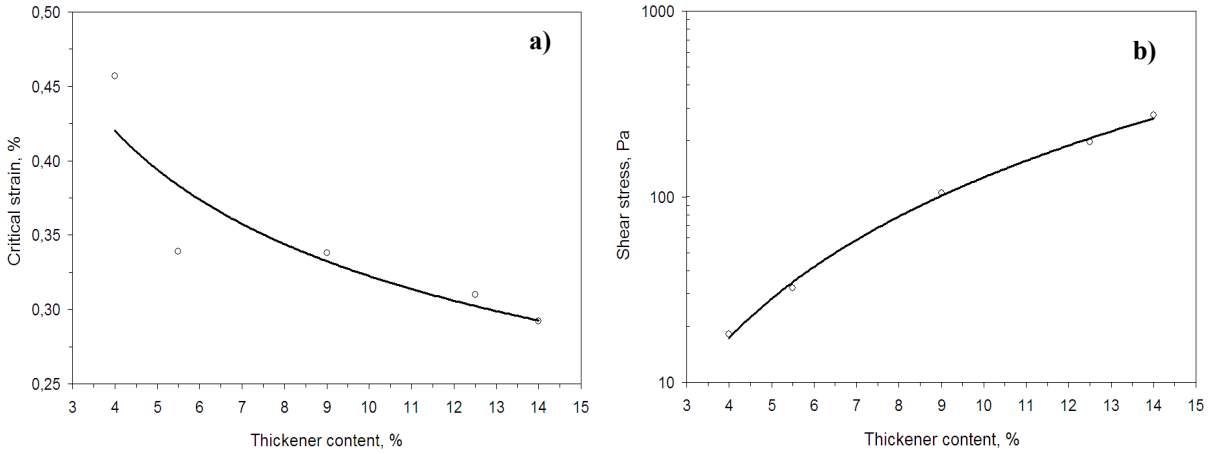

Figure 2.16 Influence of thickener concentration of lubricating greases on (a) the critical strain and (b) shear stress in the critical point [69]

Regarding the effects of base oil viscosity on the rheological properties of the lubricating greases, the results obtained by Delgado et al. in [62] showed that the values of the storage, *G'*, and loss, *G''*, moduli decrease with the increasing oil viscosity (Figure 2.17-a) while the values of loss tangent decrease with decreasing oil viscosity (Figure 2.17-b), which indicates that the relative elastic characteristics of a grease decrease by increasing oil viscosity [62].

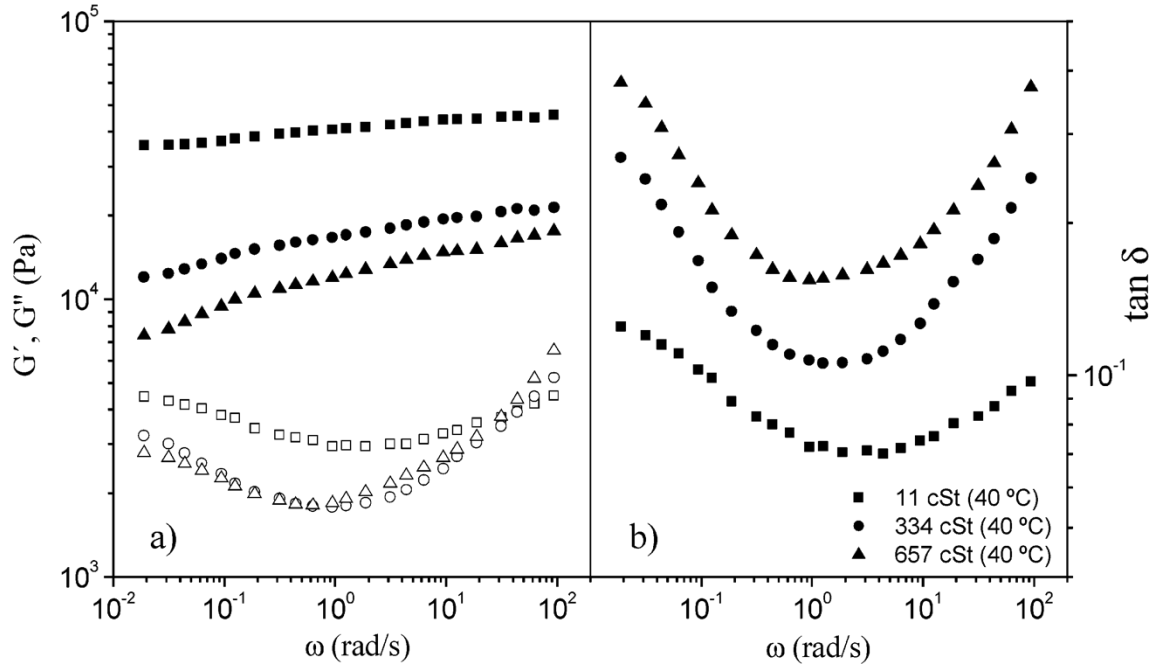

Figure 2.17 Effect of the oil viscosity of lubricating greases on (a) the storage G' and loss G'' moduli and (b) the loss tangent tan δ [62]

Regarding the viscous flow behaviour, in comparison with Newtonian liquid oils, lubricating greases do not show a linear relationship between applied shear stress (τ) and resulting shear rate ($\dot{\gamma}$). For typical lubricating greases, when the applied shear stress exceeds the yield stress, the microstructure of lubricating grease is progressively destroyed and then the grease begins to behave like a viscous fluid, i.e. to flow [15,69]. When the shear stress is ceased, the microstructure will be partially reconstructed [15,69]. Therefore, shear stress can be related to mechanical degradation of lubricating grease. [90]. The measurement of the yield stress value in the lubricating grease can aid the determining of usefulness of lubricating grease for the application in tribological systems [69]. However, the non-Newtonian behaviour of lubricating greases is referred to as the shear-thinning behaviour. In other words, the lubricating greases exhibit a decrease in apparent viscosity with increasing shear rate [69] (pseudoplastic behaviour), caused by the degradation of the grease microstructure and the flow orientation of particles. Figure 2.18 illustrates the viscous flow curves for lubricating greases of various thickener concentrations, showing the viscosity changes as a function of the shear rate. As can be observed, an increase in thickener concentration lead to an increase in viscosity (Figure 2.18-a). On the other hand, the base oil viscosity does not affect nearly the viscosity of the lubricating grease (Figure 2.18-b), despite an opposite tendency than that found on the viscoelastic functions is observed at sufficiently high shear rates, as a result of degradation of grease microstructure [62].

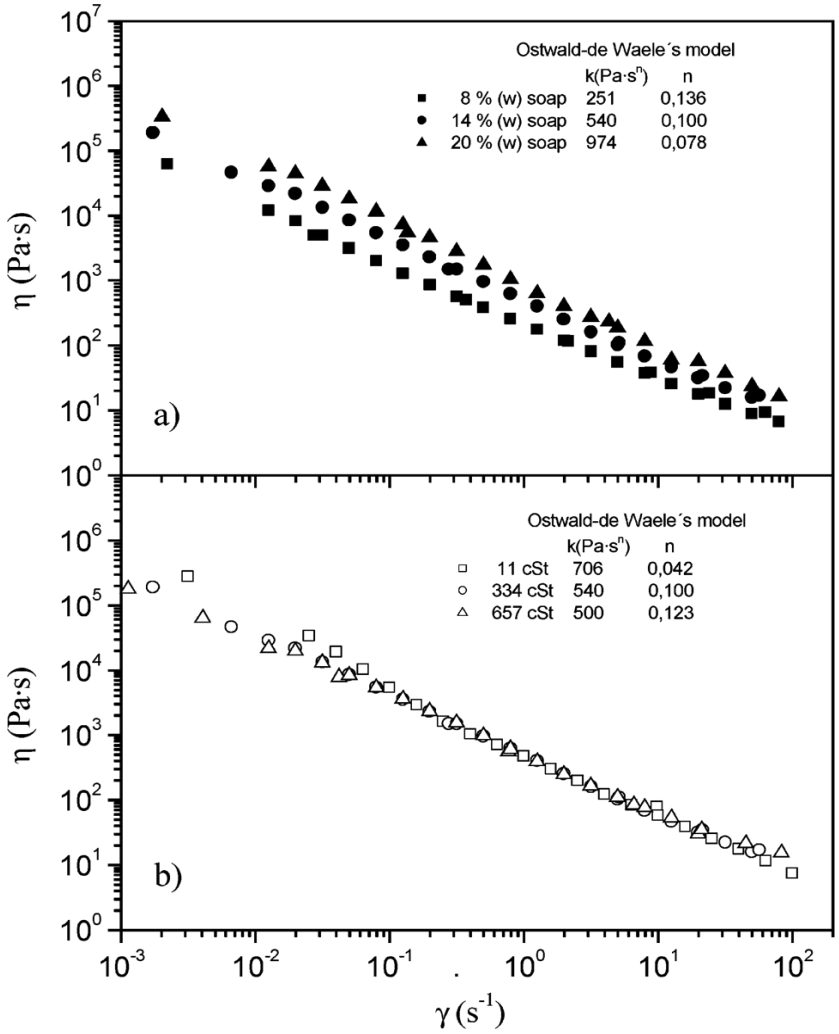

Figure 2.18 Shear-thinning behaviour of lubricating greases (a) with various thickener concentrations and (b) based on oils with various viscosities [62]

In relation to the influence of temperature on the lubricating grease rheological properties, as reported in previous works [66,87,88,91], viscoelastic functions tend to decrease as temperature increases. Figure 2.19 displays the evolution of the viscoelastic moduli with frequency, within the linear viscoelasticity range, for two different lubricating greases, at different temperatures [66]. It is obvious that the values of the storage G' and loss G'' moduli decrease with the increasing temperature. Moreover, the values of the viscoelastic moduli for the lubricating grease based on lithium 12-hydroxystearate remain almost unaffected by temperature below 50°C, and then progressively decrease (Figure 2.19-a), while the values of the viscoelastic moduli for the calcium sulphonate grease significantly decrease at temperatures above 100°C (Figure 2.19-b) [66]. These results indicate that the viscoelastic functions significantly decrease above a specific temperature, and the effect of temperature on the lubricating grease rheological properties depends on nature of the lubricating grease studied [66].

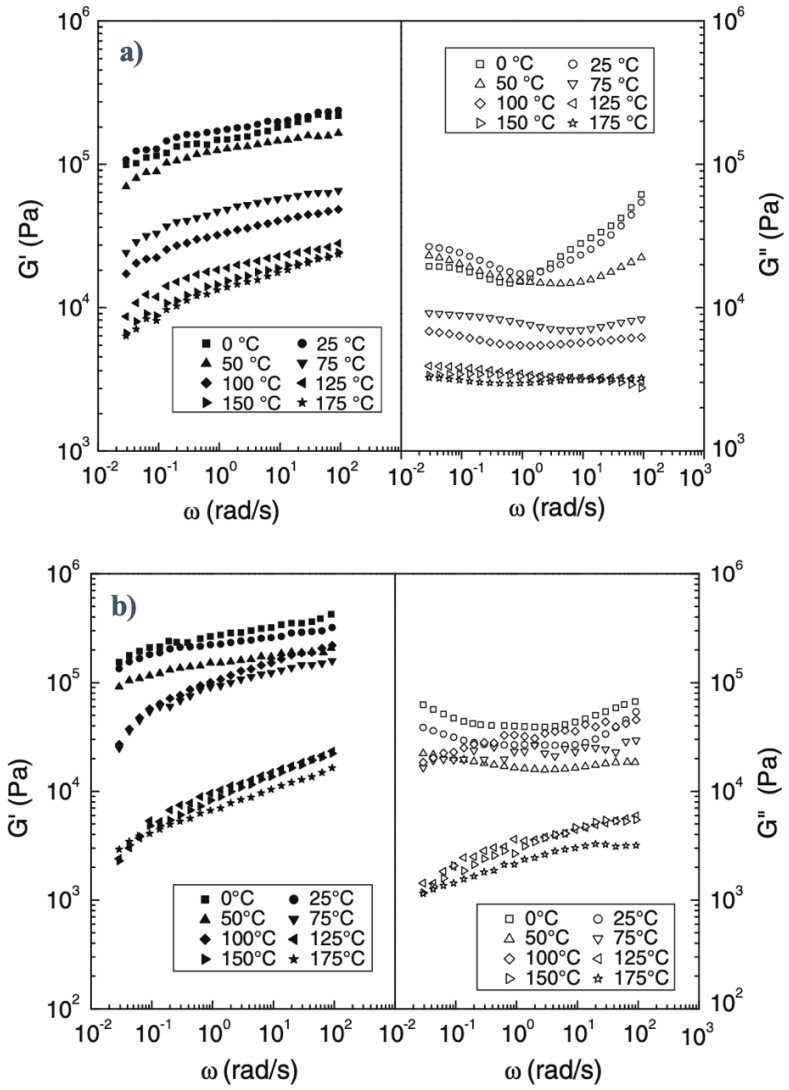

Figure 2.19 Influence of temperature on the viscoelastic moduli (G' and G'') for lubricating greases (a) lithium 12-hydroxystearate and (b) calcium sulphonate complex [66]

Regarding the influence of temperature on the flow behaviour of the lubricating greases, Åström H. et al. [92] showed that shear stress decreased with increase in temperature. Reasons for this effect are the increasing solubility of the thickener in the base oil as the temperature increases, the generally decreasing viscosity of the base oil and changes in crystal lattice [5,93].

Moreover, lubricating greases exhibit time-dependent behaviours which can be defined as thixotropy. Thixotropic behaviour is present when the viscosity of a substance decreases with time of shearing at constant conditions and progressively regenerates after a rest period or a reduction in the shear rate [5]. During the process of shearing, microstructural changes in the lubricating greases occur which causes a reduction in viscosity. Physical interactions between particles which result in the formation of a cross-linked structure during the relaxation of the

substance lead to an increase in viscosity [94]. The regeneration extent of the lubricating grease microstructure is affected by the physical state of the microstructure at the moment of stress relaxation in the grease and by the shearing conditions like temperature and shear rate [95]. In general, the lubricating greases exhibit partly thixotropic behaviour due to their viscoelastic character [5]. This means that when the shearing stops or during standstill, the re-solidification of the substance takes place but the properties do not completely return to their initial level [94]. An example curve of the partly thixotropic behaviour for a lubricating grease is given in Figure 2.20, showing the relationship of viscosity versus time. As can be observed in Figure 2.20, the viscosity decreases faster under shear and then it increases again in the rest phase [96]. This indicates that the thickener structure is destroyed faster than reconstruction.

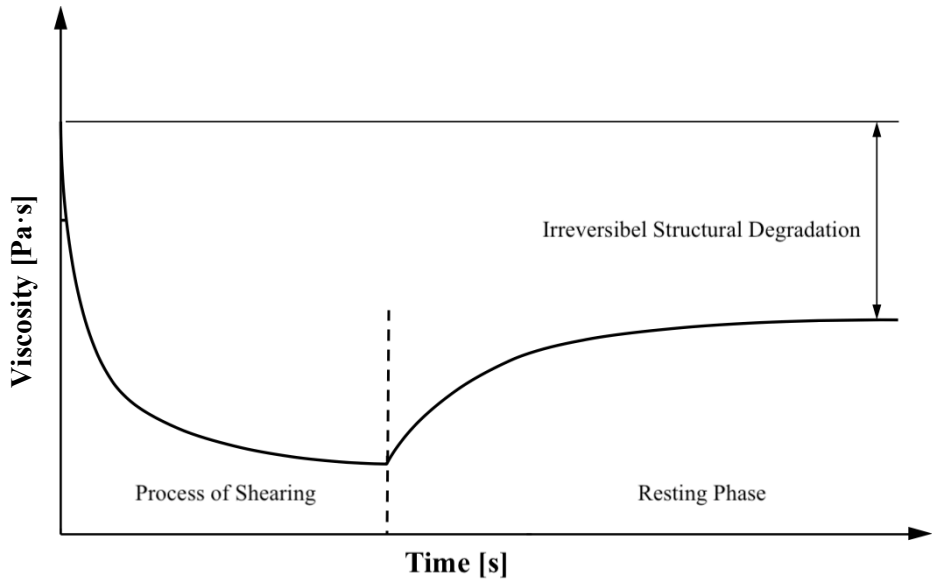

Figure 2.20 Example of a viscosity vs. time curve

From the rheological point of view, the time-dependent shear-induced evolution of lubricating grease microstructure can be studied by means of rotational transient flow tests, as previously reported in many investigations [20,97-100]. Figure 2.21 shows the evolution of the shear stress with time in which a non-linear viscoelastic response is observed with two distinct regions. In principle, the grease behaviour in rotational tests with constant shear rates presents a peak of maximum shear stress, the so-called stress overshoot (τ_{max}), which is mainly result of the viscoelastic response of the grease structure [98,99]. After reaching the stress overshoot (τ_{max}), the shear stress decreases continuously with the time, which is explained with the structural degradation of the grease and loss of the viscosity due to the shear flow process [98,99]. This

shear stress decreases continues until the steady–state level, in which is indicated an equilibrium between structural degradation and recovery [98,99].

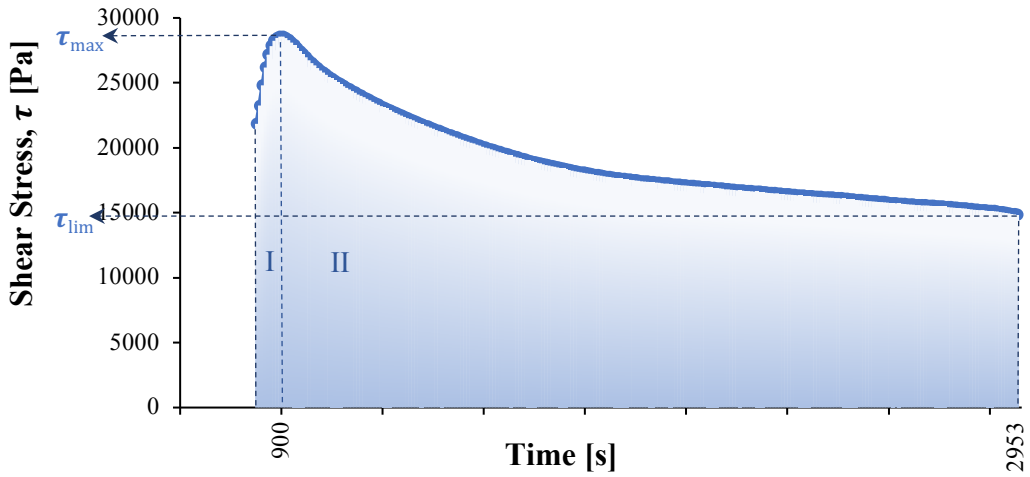

Figure 2.21 Example of a shear stress vs. time curve obtained in rotational transient flow tests

As previously reported [99], rheological parameters, related to the viscoelastic response and the structural breakdown of lubricating greases, are affected by thickener concentration and base oil viscosity, depending on the shear rate. Delgado et al. [99], showed that an increase in the thickener concentration led to an increase in the value of the maximum shear stress (τ_{max}), which is related to the maximum elastic resistance of grease microstructure, and in the time necessary to reach the maximum shear stress (t_{max}), which is related to the beginning of significant grease structural breakdown process. On the other hand, a decrease of the maximum shear stress (τ_{max}) was observed by increasing base oil viscosity at low hear rates, although an opposite tendency has been found at high shear rates. Moreover, t_{max} tended to increase as base oil viscosity increases.

Figure 2.21 illustrates the effect of time-dependent rheological response, which is the result of shear-induced structural degradation. As can be observed in Figure 2.22, dramatic changes in the fibre network occur after 15 h of shearing in a rheometer with a shear rate of 5000 s^{-1} in 25 °C, resulting shorter and thinner fibers than the same fresh grease sample.

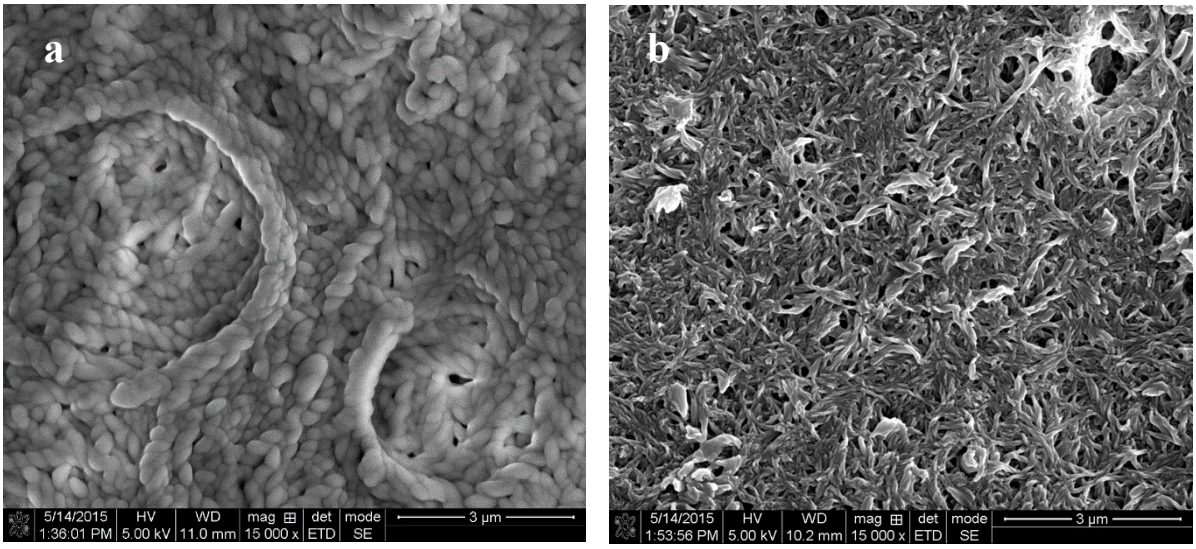

Figure 2.22 Microstructural changes of a lithium-complex grease: (a) fresh grease and (b) after 15 h shearing with a shear rate of 5000 s^{-1} at 25°C [101]

2.4.6. Tribological behaviour of lubricating greases

In general, the tribological behaviour of lubricating greases is meant by the capability to lubricate a contact [100]. The lubricating efficiency of grease is affected by physical and chemical deteriorations, which are resulted by shear stresses, pressure, and the extreme operating conditions, particularly temperature [102]. The physical degradation includes the destruction of grease thickener's microstructure, increased base oil separation and associated viscosity changes, while chemical degradation includes base oil and thickener oxidation [87,102,103]. As lubrication is basically a flow and deformation phenomenon, a full rheological characterization of greases, related to the viscoelastic properties and the structural degradation of lubricating greases, provide useful information that help to understand grease behaviour under working conditions [99]. This leads to look for a correlation between the rheological behaviour and tribological parameters such as the friction coefficient. Delgado et al. [98] studied the influence of some rheological parameters of lubricating greases on the friction process, i.e. the friction coefficient obtained from a ball-disc tribometer. The research showed that the higher the plateau modulus (G_N^0), which is related to elastic behaviour and mechanical resistance of greases [62], the strain (γ,) at $\tan\delta = G''/G' = 1$, the consistency index and the viscosity at high-shear stress, as well as more the relative elastic component, the lower was the friction coefficient value. In addition, Delgado et al. [98] found that the relationship between rheological parameters and the friction coefficient was dependent on processing conditions by isolating the effect of composition in greases obtained with different processing protocols.

Moreover, as previously reported [98,99,104], the study of the structural degradation of greases in the friction process from an energetic point of view may also provide some information about the tribological behaviour of greases. In one study [98], the friction coefficient obtained from a ball-disc tribometer was correlated with the energy densities obtained from rotational transient test i.e. the storage energy density, which is related to the grease capacity to accumulate energy in the elastic deformation, and the limiting energy density, which is also called rheological energy density and represents the energy expenditure per stressed grease volume. The results of this research showed that greases with a high capacity to accumulate energy and greases with less energy expenditure during the flow process exhibited low values of the friction coefficient.

The thickener and its structure play an important role in the lubrication process i.e. friction and wear processes [19,20]. The presence of the thickener particles in the tribological contact provides an increase in the viscosity and thickness of the elastohydrodynamic lubrication film which leads to a significant reduction in the friction coefficient in comparison with those found for the liquid lubricants i.e. base oil alone [105-108]. Regarding the effect of grease contents on the frictional behaviour, Kuhn [100] showed that the influence of the base oil viscosity was stronger than the influence of thickener component in a tribological contact. Overall, tribological and rheological properties of lubricating greases are influenced by properties of the base oil (viscosity and polarity), the type and concentration of the thickeners and the properties of the three-dimensional network arisen as a consequence of interactions between the base oil and thickener [98].

Apart from the evaluation of the friction coefficient, it is also interesting the examination of wear responses of surfaces obtained as result of friction in the lubricated contacts. The wear of the solid body, described as a loss of materials, arises as a result of a gradual energy accumulation within the stressed volume [20]. The wear can be considered a process associated with exceeding a critical energy level [19,20]. This accumulation process is affected by the applied energy and the ability to accumulate energy [20]. In general, to reduce the friction energy and wear, various types of lubricants are applied to machine elements [109]. There are many studies found in the literature, which investigate the influence of lubricating grease components on frictional and wear behaviour. Regarding the effect of thickener content on wear behaviour, Kuhn [110] showed that greases with high soap contents produced lower wear track, obtained after performing the frictional tests in a tribometer, than that obtained for the lower thickener contents. Moreover, Fiedler et al. [111] found that the influence of the base oil on wear, obtained after carrying out frictional tests on a nanotribometer using a sapphire ball on a steel disc material combination, was much smaller than that of the thickening agent, and

differed according to the thickening agent in grease formulations. Based on experimental research, Sanchez et al. [55] showed that wear behaviour in the ball-on disc contact related to the balance between the frictional behaviour and the mechanical stability of grease structures. Some special greases like those based on ∝-cellulose as thickener produced significantly high wear in the tribological contact, although they exhibited optimum frictional behaviour. This result could be explained by the poor mechanical stability of the greases, which favours that the microstructure of the grease is destroyed inside the tribological contact and therefore reduces their efficiency in the lubricating contact [55].

The frictional behaviour in lubricated contacts is often characterized by means of the Stribeck curve, in which the evolution of the friction coefficient is evaluated as a function of the relative speed of the friction bodies, as described in section 2.2.2. In addition to this, there are other variations of the Stribeck curve in which the friction coefficient is plotted versus the Stribeck parameter, which is defined as the product of dynamic viscosity (η) and tangential speed (U) divided by the normal contact load applied (F_N), or the film parameter (Λ), which is lubrication film thickness divided by the composite surface roughness, as shown in Figure 2.23 [112]. In general, the relationship between friction and lubrication is characterized on basis of the Stribeck parameter, which affects the fluid film formation between the friction surfaces in a tribological contact and allows to divide the lubrication regimes into the boundary, mixed and hydrodynamic [113]. On the other hand, the film parameter plays an important role to understand the relationship between the lubrication film thickness (h) and the roughness of the intervening surfaces (σ_1, σ_2) [114]. The Stribeck curve is commonly used to investigate the lubrication regimes of lubricating oils, which exhibits Newtonian behaviour [115-119]. However, in some studies [120,121], it was assumed that the base oil is main responsible for lubrication as a result of degradation of the grease microstructure under highly stressed conditions. In this way, the Stribeck parameter was utilized by including the value of base oil viscosity for lubricating greases, which are non-Newtonian materials [120,121].

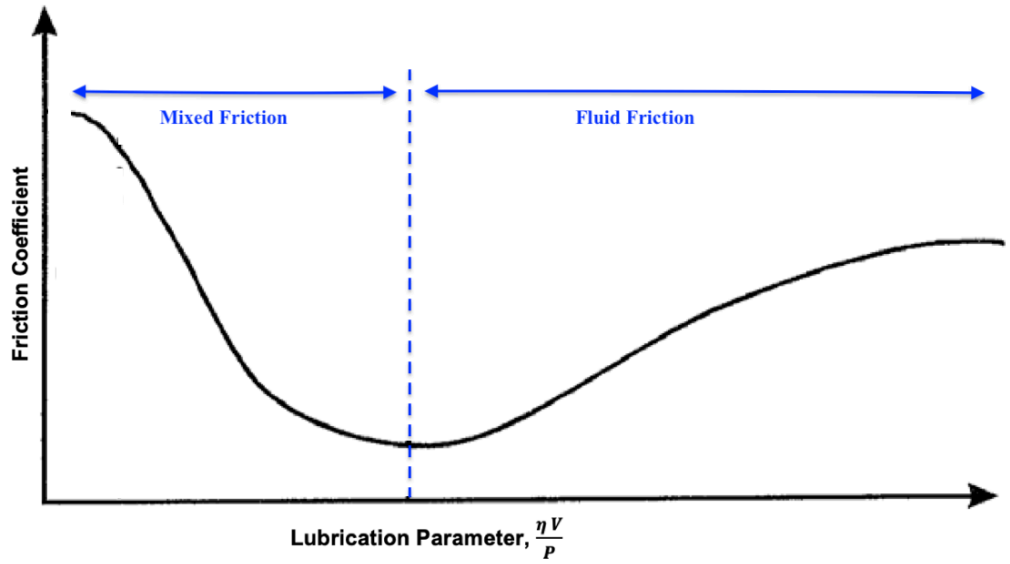

Figure 2.23 Lubrication regimes of the Stribeck curve [100]

2.5. Energy-based wear model and (apparent) friction energy density

Friction energy causes wear effects on a tribocontact (on the contacting surfaces). In the energy-based wear model, Fleischer [2] defined the term "apparent friction energy density, e_R^*" in order to describe the relationship between friction and wear. The apparent friction energy density (e_R^*) represents the amount of friction work (W_R) in relation to the wear volume (V_V):

$$e_R^* = \frac{W_R}{V_V} \tag{2.7}$$

Assuming that the friction shear stress (τ_R) can be determined from the friction coefficient (f) and the nominal contact pressure (P_a):

$$\tau_R = f \cdot P_a \tag{2.8}$$

the linear wear intensity (I_h) [122] according to Fleischer's fundamental equation of wear can be obtained using:

$$I_h = \frac{\tau_R}{e_R^*} \tag{2.9}$$

In general, the expended energy consists of several components; therefore, there are also several components of wear [2]. Therefore, the apparent energy density can be extended to:

$$\frac{1}{e_R^*} = \frac{\alpha_1}{e_{R1}^*} + \frac{\alpha_2}{e_{R2}^*} + \frac{\alpha_3}{e_{R3}^*} \tag{2.10}$$

by considering the applied lubricant as a friction body. The parameters α_1, α_2, and α_3 represent the energy proportion factors, which represent the distribution of the friction energy to the respective friction bodies in a tribological system [5].

If the apparent friction energy density is considered in the steady-state phase of solid-state wear, Equation (2.7) can be rewritten as follows:

$$e_R^* = \frac{W_R}{V_V} = \frac{F_R \cdot s_R}{A_R \cdot h_v} = \tau_R \cdot \frac{1}{I_h} = \frac{\tau_R}{I_h} \tag{2.11}$$

where F_R is the fiction force, s_R is the friction distance, A_R is the frictional contact area (wear area), and h_v is the wear depth.

Fleischer's energetic wear model was based on the so-called hypothesis of energy storage [2,8]. This hypothesis considered that the formation of a wear particle would occur only after repeated contacting since the critical energy level is usually not exceeded by the energy impulse of contact [2]. According to the energy accumulation hypothesis, a part of the energy of each impulse would be stored in a tribologically stressed material [2]. When the accumulated energy reached the critical energy value, a wear particle would form, i.e., particle separation from the contacting surface would occur and the accumulated energy would dissipate, indicating that the energy of a single contact (W_{R_e}) in the friction process partly accumulates and partly dissipates [2]:

$$W_{R_e} = W_{store_e} + W_{Diss_e} \tag{2.12}$$

Fleischer et al. [2] described the critical energy level required for the formation of the wear particle by identifying the average fracture energy density with the application of a critical number of contacts (n_k):

$$\overline{e_B} = \zeta_R \cdot e_{R_e} \cdot (n_k - 1) + e_{R_e} \tag{2.13}$$

where ζ_R is the energy accumulation number and e_{R_e} is the energy density of a single contact.

The previously given equation of the apparent frictional energy density (Equation (2.7)) can be rewritten as [2]:

$$e_R^* = \frac{n_k}{\upsilon_V} \cdot \frac{\overline{e_B}}{1 + \zeta_R \cdot (n_k - 1)} \tag{2.14}$$

by introducing the wear number (υ_V):

$$\upsilon_V = \frac{V_V}{V_R} \tag{2.15}$$

where V_R is the frictional volume.

Figure 2.24 shows the graph of the basic energy equation of wear and allows for visualization of the relationship between the apparent energy density (e_R^*), the intensity of wear (I_h), and the friction shear stress (τ_R). Fleischer [8] divided this plot into five different friction and wear states (areas 0–4) according to the occurring mechanisms, as shown in Figure 2.24 and Table 2.2. Range 1 is hydrodynamic lubrication, which leads to negligible wear intensities and zero wear in fluid friction. The other remarkable friction state is solid friction i.e., range 4, which leads to the immediate separation of material. The middle ranges, namely quasi-fluid friction, mixed friction, and solid friction with elastic and/or plastic deformation mechanisms, are also considered.

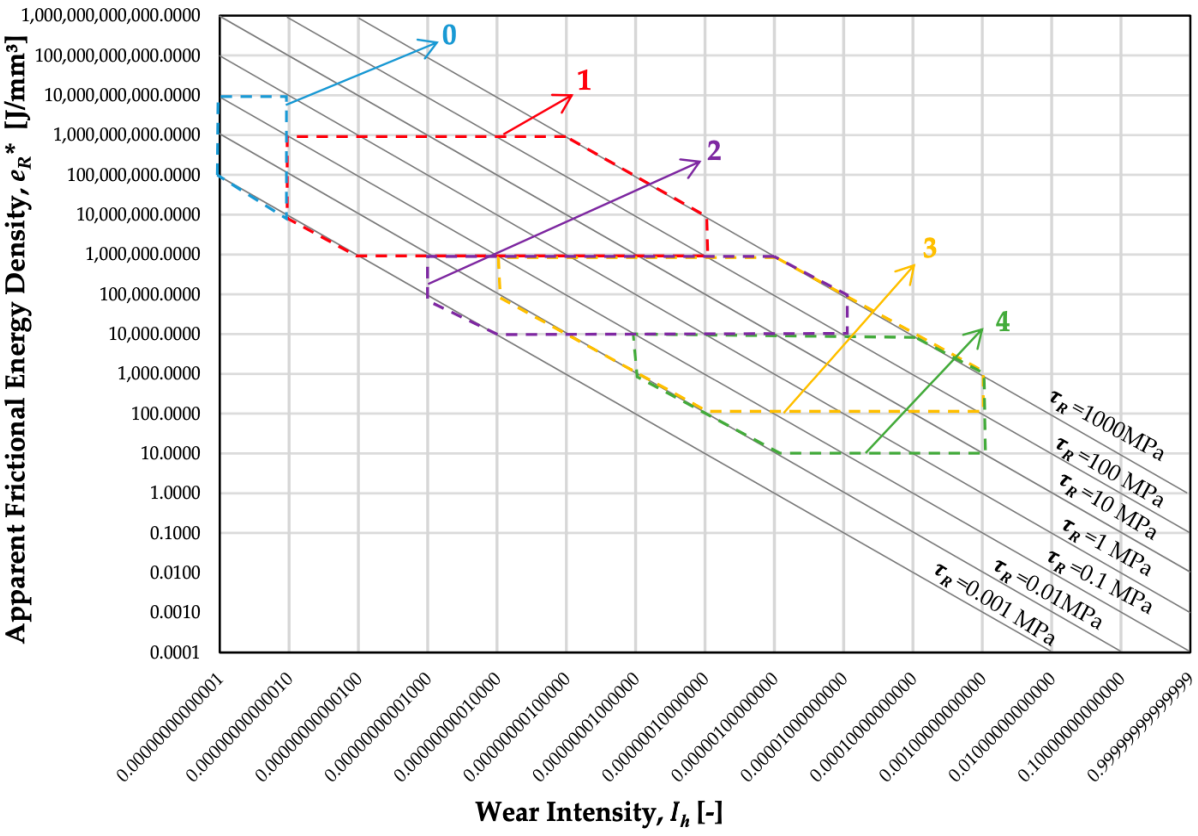

Figure 2.24 Graph of the basic energy equation of wear (adapted from G. Fleischer [8])

Table 2.2 Friction and wear conditions with associated tribological process parameters (adapted from G. Fleischer [8])

Range	Friction State	Wear State	Process Parameter		
			e_R^* (J/mm^3)	τ_R (MPa)	I_h (−)
0	Fluid friction (rheological deformation and shear)	Zero wear	10^{10}–10^{7}	10^{0}–10^{-3}	$<10^{-13}$
1	Fluid friction/mixed friction (rheological and elastic deformation and shear)	Solid body wear level 1	10^{9}–10^{6}	10^{3}–10^{-3}	10^{-13}–10^{-7}
2	Mixed friction (rheological and plastic deformation and shear)	Solid body wear level 2	10^{6}–10^{4}	10^{3}–10^{-3}	10^{-11}–10^{-5}
3	Solid friction (elastic and plastic deformation and shear)	Solid body wear level 3	10^{6}–10^{2}	10^{3}–10^{-2}	10^{-10}–10^{-3}
4	Solid friction (separating deformation and shear)	Solid body wear level 4	10^{4}–10^{1}	10^{3}–10^{-2}	10^{-8}–10^{-3}

2.6. Interpretation of activation energy in the structural degradation of lubricating greases

For a better understanding of the structural degradation process in greases, it is necessary to consider the friction inside the grease microstructure. This can be studied through rheological tests, interpreted as fluid friction experiments. In this study, the fluid friction can be defined as the energy expenditure during the relative motion of greases in a shearing process. Fluid friction inside a grease film leads to an irreversible change in the thickener structure, which is herein referred to as lubricant wear. This irreversible change in the grease structure due to a shearing process requires exceeding a critical energy level [7]: the activation energy, E_a. In other words, the activation energy (E_a) refers to the amount of energy that must be overcome to produce a shear-induced structural degradation (frictional degradation) of the grease. Some previous studies [123-130] have attempted to predict the shelf life or the oxidation induction time of lubricants using the concept of the activation energy by analysing the temperature dependence of the aging (degradation) process using the Arrhenius equation. Ide et al. [123] reported that a relationship between the activation energy and the estimated service life of a grease could be inferred. In other recent studies, the E_a concept was used to evaluate the thermal stability of novel bio-based lubricating greases in terms of changes in the linear viscoelastic functions [131,132].

Rotational transient tests are usually performed to monitor the evolution of shear stress (or viscosity) with time at a constant shear rate; however, they can also provide information about the energy of the internal fluid friction behaviour, as previously reported [80,99,100,133,134]. As shown in Figure 2.21, the typical grease behaviour in transient tests at a constant shear rate presents two distinct regions. In the first part of the curve, the lubricating grease accumulates mechanical energy, and the shear stress increases with time until reaching the maximum shear stress (τ_{max}) as a result of the viscoelastic response of the grease structure [70]. The second part of the shear stress versus time curve comprises the region between the maximum shear stress (τ_{max}) and the equilibrium or steady-state shear stress (τ_{lim}). At τ_{max}, the level of accumulated energy is sufficiently high to produce structural degradation of the grease. Afterwards, the energy is dissipated by the frictional force between the layers of flowing grease. As a result of the structural breakdown, the shear stress decreases with time until a steady state is reached, corresponding to an equilibrium between the structural degradation and the rearrangement of the grease microstructure [98].

An energetic interpretation of the second part of the shear stress versus time curve can provide some useful information about the rheological and tribological behaviour of the lubricating grease in the flow process [5]. In this sense, the rheological energy density, e_{rheo}, which represents the energy expenditure per stressed grease volume during shear-induced structural degradation, can be calculated by integrating the second part of the τ vs. t curve at a constant shear rate ($\dot{\gamma}$), as follows [98]:

$$e_{rheo} = \dot{\gamma} . \int_{t_{max}}^{t_{lim}} \tau(t) . dt \tag{2.16}$$

where t_{max} is the time necessary to reach the maximum shear stress (τ_{max}), and t_{lim} is the time necessary to reach the steady-state shear stress (τ_{lim}).

Moreover, the following empirical model was introduced for the shear stress as a function of time [100]:

$$\tau(t) = \tau_{lim} . \left(\frac{t}{t_{lim}}\right)^{-n} \tag{2.17}$$

where t_{lim} is the time necessary to reach the steady-state shear stress (τ_{lim}), and n is the dimensionless exponent which describes the intensity of the structure degradation and can be determined with the help of a potential regression. An important explanation here is that τ_{lim} and t_{lim} represent the stationary state of the grease. Using Equations (2.16) and (2.17), the energy expenditure per stressed volume can be estimated for a defined stress period.

As previously reported [9], owing to the temperature dependence of the rheological functions, the energy expenditure (e_{rheo}) strongly depends on the temperature applied during the shearing of greases at a constant shear rate. As a result, at high test temperatures, less energy expenditure is generally needed to stress the thickener structure. Analogous to other rheological functions [71,124,135-139], the temperature dependent behaviour of the energy density can be described using an Arrhenius-type equation:

$$e_{rheo} = A.exp\left(\frac{E_a}{R.T}\right) \tag{2.18}$$

where R is the gas constant (8.314 J/mol·K); T is the absolute temperature (K); A (J/m3) is the pre-exponential factor, which also represents the theoretical limit value of the rheological energy density when the temperature approaches infinity ($T \rightarrow \infty$); and E_a (J/mol) is the activation energy, which in this case represents the amount of energy required for the thickener molecules to achieve a certain shear-induced structural degradation.

As shown in Figure 2.25, if the logarithm of the rheological energy density (e_{rheo}) is plotted versus the reciprocal of the temperature, the ratio of E_a to R can be obtained as the slope of the linear relationship.

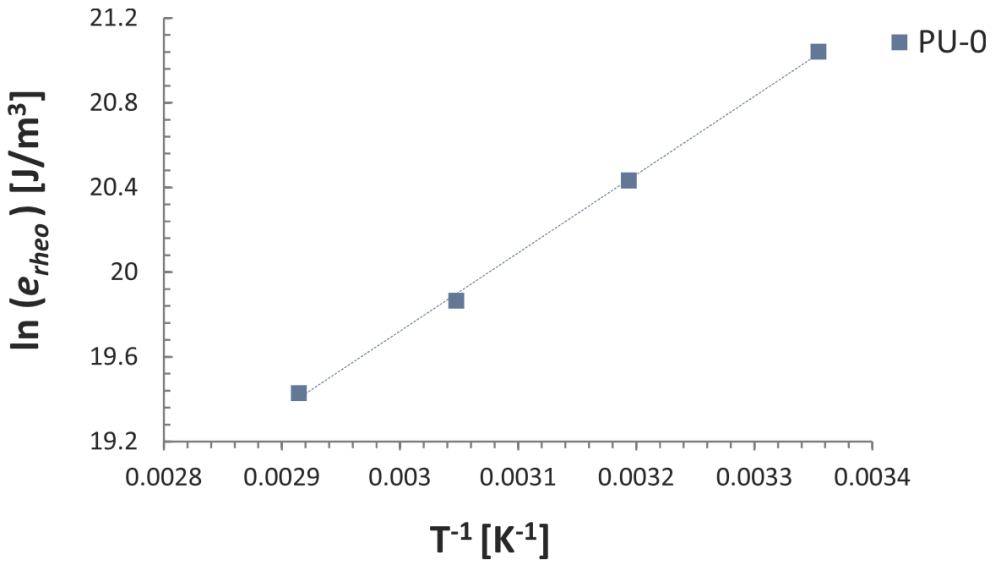

Figure 2.25 Example of an Arrhenius plot

Moreover, if two values of the energy density (e_{rheo-1} and e_{rheo-2}) at two corresponding temperatures (T_1 and T_2) are known for a grease, the energy density (e_{rheo}) at any other temperature (T) can then be estimated. In other words, once the activation energy for a given

grease sample and e_{rheo} at a given reference temperature (T_{ref}) is known, the energy density for any other temperature, T, can be deduced as follows:

$$\frac{E_a}{R} = \frac{\Delta(\ln e_{rheo})}{\Delta(T^{-1})} \equiv \frac{\ln(e_{rheo}(T)) - \ln(e_{rheo}(T_{ref}))}{(T^{-1}) - (T_{ref}^{-1})} \equiv \frac{\ln\left(\frac{e_{rheo}(T)}{e_{rheo}(T_{ref})}\right)}{(T^{-1}) - (T_{ref}^{-1})} \equiv \frac{\ln(e_T)}{(T^{-1}) - (T_{ref}^{-1})} \quad (2.19)$$

Rearranging Equation (2.19) yields the following:

$$e_T = \exp\left(\frac{E_a}{R}\left((T^{-1}) - \left(T_{ref}^{-1}\right)\right)\right) \quad (2.20)$$

where e_T is the ratio of the energy densities at a temperature T and a reference temperature T_{ref} :

$$e_T = \frac{e_{rheo}(T)}{e_{rheo}(T_{ref})} \quad (2.21)$$

Taking these considerations into account, the structural degradation of lubricating greases during the friction process is analysed in this study from an energetic point of view by focusing on the second part of the $\tau(t)$ curve at different temperatures, which is used to determine the activation energy.

As an example, to illustrate the effect of shear-induced structural degradation, Figure 2.26 shows the microstructure of a lithium grease sample before (left) and after (right) 4 h of shearing in a rheometer at a constant shear rate of 1000 s^{-1}. Atomic Force Microscopy (AFM) micrographs shown in Figure 2.26 allow to observe changes in the microstructure of the Li grease sample due to shearing. The change in the thickener structure caused by the liquid friction is obvious in Figure 2.26. As can be observed, the shear stress causes a significant decrease in the size of fibres and fibre agglomerates. To achieve this shear-induced structural degradation in a lubricating grease, the amount of energy that must be overcome by the thickener molecules under these shear conditions can be interpreted as the activation energy, E_a (Eq. (2.18)).

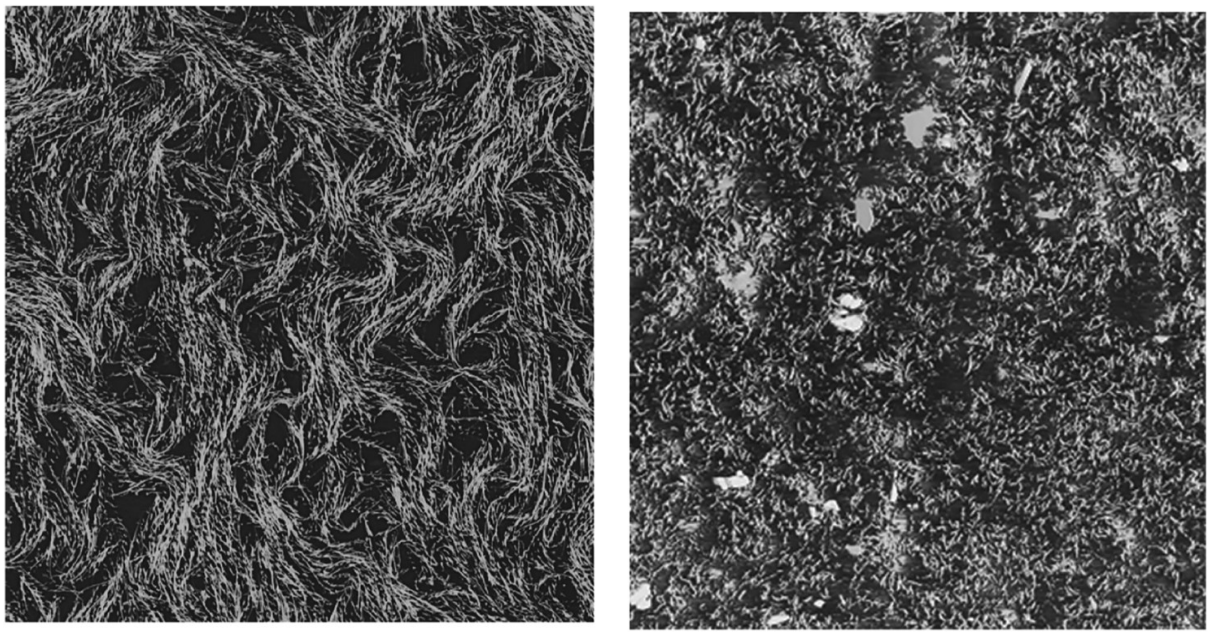

Figure 2.26 Atomic Force Microscopy (AFM) micrographs of a selected lithium sample: the left side shows the fresh Li grease sample and the right side shows the Li grease sample sheared in a rheometer for 4 h at $\dot{\gamma}=1000\ s^{-1}$ (window size: 20 μm x 20 μm)

2.7. Considerations on lubricating grease wear by means of thermodynamic studies

Generally, grease degradation, namely grease wear, can be categorized into two regimes: physical degradation and chemical degradation [102,140]. Physical degradation includes the destruction of the thickener structure due to the mechanical working of the grease, which is called grease mechanical degradation, and the oil separation (loss of base oil) resulting from the evaporation of the oil at high temperatures or the increase in the bleeding rate and the oil leakage [90,102,140]. Chemical degradation is mainly due to the oxidation reactions which involves base oil and thickener oxidation as well as additive depletion [102,128]. As can be visualized in Figure 2.27, chemical degradation predominates at high operating temperature, while mechanical degradation is generally dominant at high velocity (shear rate) and low operating temperature [90,102,141]. This dissertation is focused on the lubricating grease mechanical degradation under shearing.

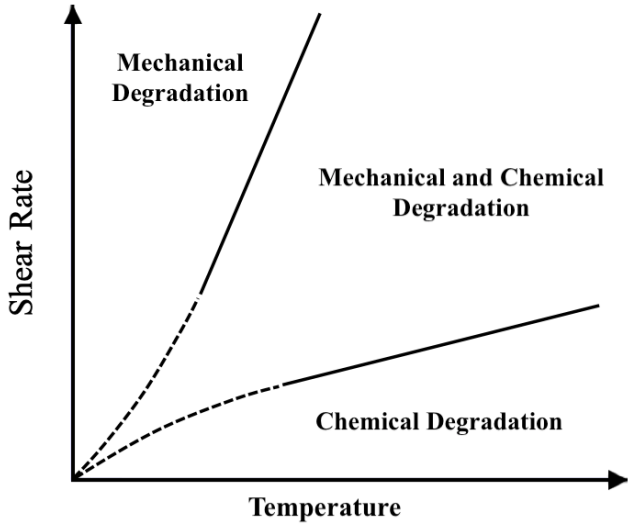

Figure 2.27 Grease degradation mechanism remade from [142]

Mechanical degradation of lubricating grease is an irreversible process which is related to the production of entropy associated with the energy dissipation [102,140,143]. When a grease undergoes mechanical shear, the shear process, i.e. friction process, dissipates energy, while the wear process generates entropy. In other words, energy is dissipated inside the grease which causes a deterioration of the thickener structure, heat and entropy generation [76,78,102,140,143]. As previously reported [78,79], application of thermodynamics laws allows to investigate a correlation between grease degradation and entropy. According to the first law of thermodynamics based on the principle of energy conservation, the change in the internal energy (ΔU) is equal to the difference between the heat (Q) added to the system and the work (W) by the system as follows:

$$\Delta U = Q - W \tag{2.22}$$

when a lubricating grease experiences mechanical shear in a closed tribological system and it is assumed that the temperature of a grease sample remains constant, the change of internal energy (ΔU) is considered as zero [140]. In this case, the work done on the lubricating grease during shear action is equivalent to the heat transferred from the lubricating grease to the surroundings as follows [140]:

$$\Delta U = 0 = Q - W \quad \rightarrow \quad W = Q \tag{2.23}$$

According to the second law of thermodynamics based on the irreversibility of natural processes, in which entropy of the system increases, the amount of the generated entropy (dS)

is equal to the amount of produced heat (δQ) divided by the temperature of the system (T) as follows:

$$\mathrm{d}S = \frac{\delta Q}{T} \tag{2.24}$$

According to the equation 2.23, equation (2.24) can be rewritten as:

$$\mathrm{d}S = \frac{\delta Q}{T} = \frac{\delta W}{T} \tag{2.25}$$

Since the mechanical energy i.e. the accumulated energy dissipates inside the grease sample, the work (W) is considered as the accumulated energy at constant temperature during the shear process [140,144]. In this case, the entropy density generated inside the grease sample (S_g) can be expressed by the accumulated energy divided by the shearing temperature as follows [140,143]:

$$S_g = \frac{\int \tau(\mathrm{t}) \,.\, \dot{\gamma}(t) \,.\, \mathrm{dt}}{T} \tag{2.26}$$

where $\tau(\mathrm{t})$ is the shear stress and $\dot{\gamma}(\mathrm{t})$ is the shear rate. If the shear rate is constant during the shearing of a grease at constant temperature, rearranging Equation (2.26) yields the following:

$$S_g = \dot{\gamma}(t) \,.\frac{\int \tau(\mathrm{t}) \,.\mathrm{dt}}{T} \tag{2.27}$$

To obtain information about the correlation of structural degradation of lubricating grease and entropy, interesting investigations come from [3,73,78,79,90,140,143,145,146].

Rezasoltani and Khonsari [140] made experimental work by using a rheometer to monitor the amount of mechanical degradation due to structural damages inside the grease, and to quantify the accumulated energy and entropy generation. The research showed that the shearing process breaks down the grease structure and causes heat and entropy generation. Moreover, Rezasoltani and Khonsari [140] found a linear relationship between the mechanical degradation and entropy generation, and also between mechanical degradation and energy dissipation, which remains valid regardless of the applied shear rate or the grease temperature. In addition, they defined a degradation coefficient by correlating rate of accumulated energy, and rate of entropy generation with mechanical degradation, that can help to estimate the grease mechanical life prediction in the application.

Zhou et al. [73] extended the work of Rezasoltani and Khonsari [140], in which investigated the process of structural change of a grease sample by observing the change of net penetration vs. the entropy density generation (S_g). They concluded that there occur two phases of degradation, first a rapid drop of rheological properties and second a more slowly process of

degradation, as shown in Figure 2.28. In the first phase, mainly reorientation and breakage of the thickener structure occur, which causes a progressive drop in rheological properties of the grease, while in the second phase, the aging is dominated by the breakage of smaller fiber fragments, and the grease degrades at a much slower rate [73]. To describe these two-phase behaviours, a grease- aging equation was developed [73]:

$$Y = \frac{Y_i - Y_\infty}{1 + K \cdot S_g^m} + Y_\infty \tag{2.28}$$

where Y presents the rheological properties, Y_i presents the initial rheological value for fresh grease, Y_∞ presents the second-stage value for the long time-aged sample, K is the coefficient of degradation and m is the exponent of degradation [73]. They reported that this aging behaviour is in relation with the entropy generation rate and the change in the thickener structure during aging process because of breakage of the thickener structure, grease degrades.

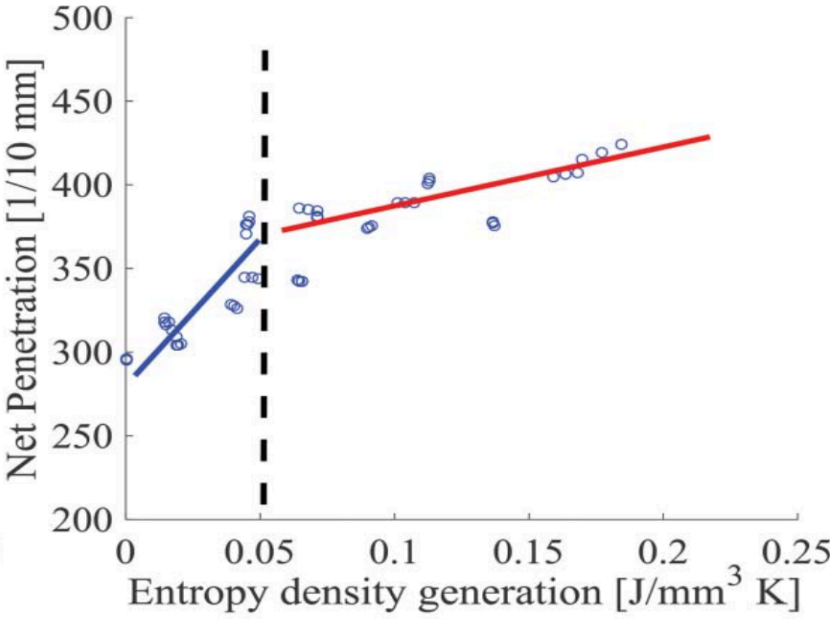

Figure 2.28 Net penetration values against entropy generation density during the aging process for Li/M grease (lithium 12-hydroxy stearate und mineral oil) [73]

Lijesh and Khonsari [145] presented a methodology to determine the life of grease experiencing mechanical degradation. The authors tried to evaluate the grease degradation by continuously measuring the entropy generation rate from the values of friction torque and angular velocity. The time for the degradation rate of a higher-grade grease to drop to a lower-grade grease was determined with the help of entropy generation rate and a description for the practice of working the grease 60 s in the double-stroke grease worker was given [145].

An alternative approach for the analysis of grease degradation using the entropy concept was provided by Kuhn [3,143]. Kuhn [3] investigates the ability of a tribosystem to start a self-optimization process applied stressed lubricating grease. The condition to start a self-optimization is the loss of stability. For that case Kuhn investigated the probability for self-optimization with criterion:

$$\frac{1}{2}\frac{\partial}{\partial t}(\delta^2 S) = \sum_i X_i \cdot J_i > 0 \tag{2.29}$$

where X is the thermodynamic force and J is the thermodynamic flux [3]. As Kuhn reported [3,143], rotational rheometer test at a constant shear rate delivers the possibility to observe the structural changes of grease during a friction process and self-organization of stressed grease. Figure 2.29 shows the shear stress versus the shear time curve in which grease behaviour is observed with two distinct regions. In the first part, shear stress decreases with shear time which is explained by the structural degradation of the grease, while in the second part, which is defined as stationary period, solid inside the grease achieves a more or less stable structure or equilibrium state [3,143]. This behaviour can indicate self-optimization as a reaction of the system to an arising instability. To check these assumptions, Kuhn took friction, fragmentation and coagulation into account in his stability studies to create an entropy balance equation.

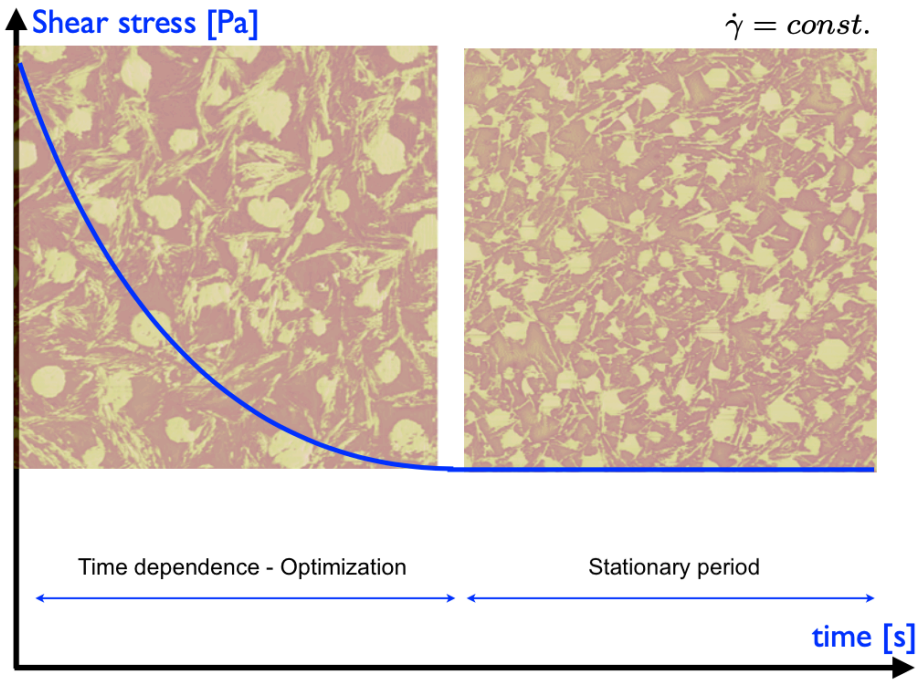

Figure 2.29 Grease behaviour obtained in rotational rheometer test at a constant shear rate (AFM-pictures obtained by J.M. Franco, University of Huelva, Huelva, Spain) [143]

The entropy variation of the observed grease volume element, dS, is composed of the following components:

$$\mathrm{d}S = \mathrm{d}S_i + \mathrm{d}S_e \tag{2.30}$$

where $\mathrm{d}S_i$ is the entropy production and $\mathrm{d}S_e$ is the entropy flow.

According to Eq. 2.29 the disturbance of the thermodynamic force and flux has to be investigate. Using the proposal [143]:

$$J_i = \tau + \dot{\gamma} \tag{2.31}$$

Equation (2.29) can be rewritten for the stability criterion as:

$$\frac{1}{2}\frac{\partial}{\partial t}(\delta^2 S) = \delta\left[\frac{\tau\cdot\dot{\gamma}}{-\lambda T^2}\right]\delta(\tau\cdot\dot{\gamma}) = \frac{\dot{\gamma}^2}{T^2}\left[\frac{1}{\lambda}\left(\left(\frac{\delta\tau}{\delta\varepsilon}\right)^2\frac{\tau}{\lambda^2}\frac{\delta\tau}{\delta\varepsilon}\frac{\delta\lambda}{\delta\varepsilon}\right)\delta\varepsilon^2\right] \tag{2.32}$$

Here λ is the thermal conductivity and ε is a parameter that describes the distance from equilibrium. For example, the difference between equilibrium structure and temporary structure. The right side of the equation (2.32) must become negative if instability is to arise:

$$\frac{\delta\tau}{\delta\varepsilon}\frac{\delta\lambda}{\delta\varepsilon} < 0 \tag{2.33}$$

That means an increase or decrease of shear stress τ and heat conductivity λ simultaneously with ε increments. From rheological experiments, see Figure 2.29, we know that there is a decreasing shear stress for a constant shear rate if wear happens. The same process behaviour can be assumed for heat conductivity. The tribological process produces more small particles covered by an oil coat [143]. For a detailed presentation considering mechanisms as fragmentation and coagulation see [143].

2.8. References

1. Czichos, H.; Habig, K.H. Tribologie-Handbuch. *Vieweg und Teubner Verlag*, Springer Fachmedien Wiesbaden GmbH, Germany, 2010.
2. Fleischer, G.; Gröger, H.; Thum, H. Verschleiß und Zuverlässigkeit. *VEB Verlag Technik*, Berlin, Germany, 1980.
3. Kuhn, E. Aspects of Self-Organization of Tribological Stressed Lubricating Greases. *Lubricants*, 2020, 8, 28, doi:10.3390/lubricants8030028.
4. Bartz, W.J. Einführung in die Tribologie der Schmierungstechnik - Tribologie-Schmierstoffe – Anwendungen. *Expert Verlag GmbH*, 2010.
5. Kuhn, E. Zur Tribologie der Schmierfette: Eine Energetische Betrachtungsweise des Reibungs-und Verschleißprozesses. *Expert Verlag*, Renningen, Germany, 2017.
6. Fleischer, G. Probleme und Kriterien der Mischreibung. *Schmierungstechnik*, Berlin, 1982, 13, 12.
7. Kuhn, E. Friction and Wear of a Grease Lubricated Contact- An Energetic Approach. Tribology - Fundamentals and Advancements; Gegner, J., Ed.; *IntechOpen*, 2013, DOI: 10.5772/55837.
8. Fleischer, G. Zum energetischen Niveau von Reibpaarungen. *Schmierungstechnik* 16, VEB Verlag Technik, Berlin, Germany, 1985.
9. Acar, N.; Kuhn, E.; Franco, J.M. Tribological and rheological characterization of new completely biogenic lubricating greases: a comparative experimental investigation. *Lubricants*, 2018, 6, 2, 45, https://doi.org/10.3390/lubricants6020045.
10. Stachowiak, G.W.; Batchelor, A.W. Engineering Tribology. *Elsevier* Butterworth-Heinemann, 2011.
11. Klamann, D. Schmierstoffe und verwandte Produkte - Herstellung, Eigenschaften, Anwendungen. *Verlag Chemie*, Weinheim, 1982.
12. Mang, T.; Dresel, W. Lubricants and Lubrication. *WILEY-VCH Verlag GmbH & Co. KGaA*, Weinheim, 2007.
13. Mobarak, H.M.; Niza Mohamad, E.; Masjuki, H.H.; Kalam, M.A.; Al Mahmud, K.A.H.; Habibullah, M.; Ashraful, A.M. The prospects of biolubricants as alternatives in

automotive applications. *Renewable and Sustainable Energy Reviews*, 2014, 33, 34–43, http://dx.doi.org/10.1016/j.rser.2014.01.062

14. Lindemann, L. Future Challenges of the Lubricants Industry. *Fuchs Capital Market Day* 2018, Available online: https://www.fuchs.com/fileadmin/Home/Praesentation/2018/180618_FCMD_CTO.pdf (accessed on 22.11.2021).
15. Hamnelid, L. Introduction to rheology of lubricating grease Publication. *ELGI Rheology Book Publicatio*n, 2005, 1–20.
16. Lugt, P.M. A review on grease lubrication in rolling bearings. *Tribology Transactions*, 2009, 52, 4, 470–480.
17. Abdulbari, H.A.; Rosli, M. Y.; Abdurrahman, H. N.; Nizam M. K. Lubricating grease from spent bleaching earth and waste cooking oil: Tribology properties. *International Journal of the Physical Sciences*, 2011, 6, 20, 4695–4699.
18. Fitch, B.; Corporation, N. Understanding the Differences Between Base Oil Formulations. Available online: https://www.machinerylubrication.com/Read/30730/base-oil-formulations. (accessed on 22.11.2021).
19. Kuhn, E.; Delgado, M. Description of the structural degradation of lubricating greases as a reaction of the tribological system. *Eurogrease*, 2010, 12–15.
20. Kuhn, E. Influence of the soap content of lubricating greases on the tribological process. *Eurogrease*, 2007, 7–11.
21. Mas, R.; Magnin, A. Rheology of colloidal suspensions: case of lubricating greases. *Journal of Rheology*, 1994, 38, 4, 889–908.
22. Delgado, M.A.; Sánchez, M.C.; Valencia, C.; Franco, J.M.; Gallegos, C. Relationship among microstructure, rheology and processing of a lithium lubricating grease. *Chemical Engineering Research and Design*, 2005, 83, 9, 1085–1092.
23. Goerz, T. Schmierfette auf Seifenbasis, Zusammensetzung-Herstellung-Eigenschaften. *Tribologie und Schmierungstechnik*, 56. Jahrgang, 1/2009.
24. Corporation, N. How to Identify Different Types of Grease. Available online: https://www.machinerylubrication.com/Read/29062/different-grease-types. (accessed on 22.11.2021).

25. Casserly, E.; Langlais, T.; Springer, S.P.; Kumar, A.; Mallory, B. The Effect of Base Oils on Thickening and Physical Properties of Lubricating Greases. *Lube-Tech*, The European Lubricants Industry Magazine, 2018, No.115.

26. Bartz, W.J. Additive für Schmierstoffe. Kontakt und Studium, *Expert-Verlag GmbH*, Renningen-Malmsheim, 1994.

27. Bartz, J.W. Lubricants and the environment. *Tribology International*, 1998, 31, 35–47.

28. Wilson, B. Lubricants and functional fluids from renewable resources. *Industrial Lubrication and Tribology*, 1998, 50, 6–15.

29. Boyde, S. Green lubricants: Environmental benefits and impacts of lubrication. *Green Chemistry*, 2002, 4, 293–307.

30. Salimon, J.; Salih, N.; Yousif, E. Biolubricants: Raw materials, chemical modifications and environmental benefits. *European Journal of Lipid Science and Technology*, 2010, 112, 519–530, https://doi.org/10.1002/ejlt.200900205.

31. Medina, V.F. Evaluation of Environmentally Acceptable Lubricants (EALS) for Dams Managed by the U.S. Army Corps of Engineers. *U.S. Army Engineer Research and Development Center*, 2015.

32. Theodori, D.; Saft, R.J.; Krop, H.; Broekhuizen, P.V. Development of criteria for the award of the European Eco-label to lubricants. *IVAM research and consultancy on sustainability*, 2004.

33. BLUE ANGEL, The German Ecolabel. Biodegradable Lubricants and Hydraulic Fluids (DE-UZ 178). Basic Award Criteria, 2014, https://produktinfo.blauer-engel.de/uploads/criteriafile/en/DE-UZ%20178-201407-en%20Criteria-V5.pdf.

34. Candela, V.A.G.; Renata, K.; Oyeshola, K.; Oliver, W.; Rosa, R.M.; Carme, H.; Natalia, F.; Marta, E.; Gemma, J.; Jaume, J.; Elisabet, B. Revision of the European Ecolabel Criteria for Lubricants. *Publications Office of the European Union*, 2018, DOI: 10.2760/58736.

35. Sukirno, R.F.; Setijo, B.; Mohammad, N. Biogrease based on palm oil and lithium soap thickener: Evaluation of antiwear property. *World Applied Sciences Journal*, 2009, 6, 3, 401–407.

36. Fajar, R. Nasikin. Anti-wear properties of bio-grease from modified palm oil and calcium soap thickener. *CIGR Journal*, 2010, 12, 64–69.

37. El-Adly, R.A.; Bedier, A.H.; Modather, F.H.; Enas, A.I.; Mahmmoud, M.E. Jojoba and Castor Oils as Fluids for the preparation of bio greases: A Comparative Study. *International Journal of Scientific and Engineering Research*, 2014, 5, ISSN 2229–5518.

38. Panchal, T.; Chauhan, D.; Thomas, M.; Patel, J. Bio based grease a value added product from renewable resources. *Industrial Crops and Products*, 2015, 63, 48–52.

39. Nagendramma, P.; Kumar, P. Eco-Friendly Multipurpose Lubricating Greases from Vegetable Residual Oils. *Lubricants*, 2015, 3, 628–636.

40. Asadauskas, S.; Perez, J.M.; Duda, J.L. Oxidative stability and antiwear properties of high oleic vegetable oils. *Lubrication Engineering*, 1996, 52, 877–882.

41. Randles, S.J.; Wright, M. Environmentally considerate ester lubrication for the automotive and engineering industries. *Journal of Synthetic Lubrication*,1992, 9, 145–161.

42. Wu, X.; Zhang, X.; Yang, S.; Chen, H.; Wang, D. The study of epoxidized rapeseed oil used as a potential biodegradable lubricant. *Journal of the American Oil Chemists´ Society*, 2000, 77, 561–563.

43. Erhan, S.Z.; Asadauskas, S. Lubricant basestocks from vegetable oils. *Industrial Crops and Products*, 2000, 11, 277–282.

44. Adhvaryu, A.; Erhan, S.Z. Epoxidized soybean oil as a potential source of high-temperature lubricants. *Industrial Crops and Products*, 2002, 15, 247–254.

45. Adhvaryu, A.; Erhan, S.Z.; Perez, J.M. Tribological studies of thermally and chemically modified vegetable oils for use as environmentally friendly lubricants. *Wear*, 2004, 257, 359–367.

46. Erhan, S.Z.; Sharma, B.K.; Perez, J.M. Oxidation and low temperature stability of vegetable oil-based lubricants. *Industrial Crops and Products*, 2006, 24, 292–299.

47. Lea, C.W. European development of lubricants derived from renewable resources. *Industrial Lubrication and Tribology*, 2002, 54, 268–274.

48. Maleque, M.A.; Masjuki, H.H.; Sapuan, S.M. Vegetable-based biodegradable lubricating oil additives. *Industrial Lubrication and Tribology*, 2003, 55, 137–143.

49. Adhvaryu, A.; Sung, C.; Erhan, S.Z. Fatty acids and antioxidant effects on grease microstructures. *Industrial Crops and Products*, 2005, 21, 285–291.

50. Quinchia, L.A.; Delgado, M.A.; Valencia, C.; Franco, J.M.; Gallegos, C. Viscosity Modification of High-Oleic Sunflower Oil with Polymeric Additives for the Design of New Biolubricant Formulations. *Environmental Science and Technology*, 2009, 43, 6, 2060–2065.

51. Quinchia, L.A.; Delgado, M.A.; Valencia, C.; Franco, J.M.; Gallegos, C. Viscosity modification of different vegetable oils with EVA copolymer for lubricant applications. *Industrial Crops and Products*, 2010, 32, 3, 607–612.

52. García-Zapateiro, L.A.; Delgado, M.A.; Franco, J.M.; Valencia, C.; Ruiz-Méndez, M.V.; Garcés, R.; Gallegos, C. Oleins as a source of estolides for biolubricant applications. *Grasas Y Aceites*, 2010, 61, 171-174, DOI: 10.3989/gya.075209.

53. Sánchez, R.; Franco, J.M.; Delgado, M.A.; Valencia, C.; Gallegos, C. Effect of thermo-mechanical processing on the rheology of oleogels potentially applicable as biodegradable lubricating greases. *Chemical Engineering Research and Design*, 2008, 86, 1073–1082.

54. Sánchez, R.; Franco, J.M.; Delgado, M.A.; Valencia, C.; Gallegos, C. Development of new green lubricating greases formulations based on cellulosic derivatives and castor oil. *Green Chemistry*, 2009, 11, 686–693.

55. Sánchez, R.; Franco, J.M.; Kuhn, E.; Fiedler, M. Tribological characterization of green lubricating greases formulated with castor oil and different biogenic thickener agents: A comparative experimental study. *Industrial Lubrication and Tribology*, 2011, 63, 446–452.

56. Sánchez, R.; Franco, J.M.; Delgado, M.A.; Valencia, C.; Gallegos, C. Thermal and mechanical characterization of cellulosic derivatives-based oleogels potentially applicable as bio-lubricating greases: Influence of ethyl cellulose molecular weight. *Carbohydrate Polymers*, 2011, 83, 151–158.

57. Sánchez, R.; Stringari, G.B.; Franco, J.M.; Delgado, M.A.; Valencia, C.; Gallegos, C. Use of chitin, chitosan and acylated derivatives as thickener agents of vegetable oils for bio lubricant applications. *Carbohydrate Polymers*, 2011, 85, 705–714.

58. Martin Alfonso, J.E.; Yañez, R.; Valencia, C.; Franco, J.M.; Díaz, M.J. Optimization of the Methylation Conditions of Kraft Cellulose Pulp for Its Use As a Thickener Agent in Biodegradable Lubricating Greases. *Industrial and Engineering Chemistry Research*, 2009, 48, 6765–6771.

59. Núñez, N.; Martin Alfonso, J.E.; Valencia, C.; Sánchez, M.C.; Franco, J.M. Rheology of new green lubricating grease formulations containing cellulose pulp and its methylated derivative as thickener agents. *Industrial Crops and Products*, 2012, 37, 500–507.

60. Sánchez, R.; Franco, J.M.; Delgado, M.A.; Valencia, C.; Gallegos, C. Rheological and mechanical properties of oleogels based on castor oil and cellulosic derivatives potentially applicable as bio-lubricating greases: Influence of cellulosic derivatives concentration ratio. *Journal of Industrial and Engineering Chemistry*, 2011, 17, 705–711.

61. NLGI. Lubricating grease guide. *National Lubricating Grease Institute (ed)*, 2006, Kansas.

62. Delgado, M.; Valencia, C.; Sánchez, M.; Franco, J.; Gallegos, C. Influence of soap concentration and oil viscosity on the rheology and microstructure of lubricating greases. *Industrial and Engineering Chemistry Research*, 2006, 45, 1902–1910.

63. Roman, C.; Valencia, C.; Franco, J.M. AFM and SEM Assessment of Lubricating Grease Microstructures: Influence of Sample Preparation Protocol, Frictional Working Conditions and Composition. *Tribology Letters*, 2016, 63, 20, DOI: 10.1007/s11249-016-0710-y.

64. Ishchuk, Yu.L. Lubricating Grease Manufacturing Technology. *New Delhi: New Age International,* 2005.

65. Boner, C.J. Modern Lubricating Greases. *Broseley: Scientific Publication (GB) Ltd*, 1976.

66. Sánchez, M.C.; Franco, J.M.; Valencia, C.; Gallegos, C.; Urquiola, F.; Urchegui, R. Atomic Force Microscopy and Thermo-Rheological Characterisation of Lubricating Greases. *Tribology Letters*, 2011, 41, 463–470.

67. Moreno, G.; Valencia, C.; Franco, J.M.; Gallegos, C.; Diogo, A.; Bordado, J.C.M. Influence of molecular weight and free NCO content on the rheological properties of lithium lubricating greases modified with NCO-terminated prepolymers. *European Polymer Journal*, 2008, 44, 2262–2274.

68. Cyriac, F.; Lugt, P.M.; Bosman, R.; Padberg, C.J.; Venner, C.H. Effect of Thickener Particle Geometry and Concentration on the Grease EHL Film Thickness at Medium Speeds. *Tribology Letters*, 2016, 61, 18.

69. Paszkowski, M. Some aspects of grease flow in lubrication systems and friction nodes. In: Gegner J, editor. *Tribology—Fundamentals and Advancements*, 2013, 77–106, https://doi.org/10.5772/55929.

70. Delgado, M.A.; Secouard, S.; Valencia, C.; Franco, J.M. On the steady-state flow and yielding behaviour of lubricating greases. *Fluid*, 2019, 4, 6.

71. Bauer, W.H.; Finkelstein, A.P.; Wiberley, S.E. Flow properties of lithium stearate-oil model greases as functions of soap concentration and temperature. *ASLE Trans*, 1960, 3, 215–224.

72. Lin, C.L.; Meehan, P.A. Microstructure characterization of degraded grease in axle roller bearings. *Tribology Transactions*, 2019, 62, 667–87.

73. Zhou, Y.; Bosman, R.; Lugt, P.M. A model for shear degradation of lithium soap grease at ambient temperature. *Tribology Transactions*, 2018, 61, 61–70. https://doi.org/10.1080/10402004.2016.1272730.

74. Balan, C. The rheology of lubricating greases. *ELGI (ed)*, Amsterdam, 2000.

75. DIN 51810-2. Testing of lubricants - testing rheological properties of lubricating greases – part2: determination of flow point using an oscillatory rheometer with a parallel-plate measuring system. 2011, 04.

76. Kuhn, E. Investigation of the structural degradation of lubricating greases from an energy point of view. *SCAD*, University of Ghent, Belgium, 2013.

77. Litters, T.; Koch, B. Einfluss der Basisöl polarität auf das viskoelastische Verhalten von Schmierfetten. *German Tribology Conference*, Göttingen, Germany, 2008.

78. Kuhn, E. Tribological Stress of Lubricating Greases in the Light of System Entropy. *Lubricants*, 2016, 4, 37.

79. Kuhn, E. Correlation between System Entropy and Structural Changes in Lubricating Grease. *Lubricants*, 2015, 3, 332–345.

80. Kuhn, E. Energetic investigations of the structural degradation of lubricating greases caused by friction. *5th World Tribology Congress*, Turin, Italy, 2013.

81. Franco, J.; Delgado, M.; Valencia, C.; Sánchez, M.; Gallegos, C. Mixing rheometry for studying the manufacture of lubricating greases. *Chemical Engineering Science*, 2005, 60, 2409–2418.

82. Martin-Alfonso, J.E.; Valencia, C.; Sánchez, M.C.; Franco, J.M.; Gallegos, C. Development of new lubricating grease formulations using recycled LDPE as rheology modifier additive. *European Polymer Journal*, 2007, 43, 139–149.

83. Martin-Alfonso, J.E.; Valencia, C.; Sánchez, M.C.; Franco, J.M.; Gallegos, C. Recycled and virgin ldpe as rheology modifiers of lithium lubricating greases: A comparative study. *Polymer Engineering and Science*, 2008, 48, 1112–1119.

84. Martin-Alfonso, J.E.; Valencia, C.; Sánchez, M.C.; Franco, J.M. Evaluation of thermal and rheological properties of lubricating greases modified with recycled ldpe. *Tribology Transactions*, 2012, 55, 518–528.

85. Ferry, J.D. Viscoelastic properties of polymers. *John Wiley & Sons (ed)*, New York, 1980.

86. Couronne, I.; Blettner, G.; Vergne, P. Rheological Behavior of Greases - Part I: Effects of Composition and Structure. *Tribology Transactions*, 2000, 43, 4, 619–626.

87. Delgado, M.A.; Valencia, C.; Sánchez, M.C.; Franco, J.M.; Gallegos, C. Thermorheological behaviour of a lithium lubricating grease. *Tribology Letters*, 2006, 23, 47–54.

88. Cheng, Y.; Pan, J.; Yang, J. Effect of Thermorheological Properties on Shear Flow of Grease in Pipes. *Journal of Chemical Engineering of Japan*, 2016, 49, 9, 815–823.

89. Karis, T.E.; Kono, R.N.; Jhon, M.S. Harmonic analysis in grease rheology. J*ournal of Applied Polymer Science*, 2003, 90, 334–343.

90. Gurt, A.; Khonsari, M. The Use of Entropy in Modeling the Mechanical Degradation of Grease. *Lubricants*, 2019, 7, 82.

91. Jiabao, P.; Guangxin, Y.; Jianping W. Effect of Thermorheological Properties on tribological behaviors of lubricating grease. *Materials Research Express*, 2020, 7, 3, id.035509.

92. Åström, H.; Höglund, E. Rheological properties of six greases and their two base oils. *Research report*, Luleå University, 1990.

93. Mader, W. Hinweise zur Anwendung von Schmierfetten. *Curt Vincent Verlag*, Hannover, 1979.

94. Paszkowski, M.; Olsztynska-Janus S. Grease thixotropy: evaluation of grease microstructure change due to shear and relaxation. *Industrial Lubrication and Tribology*, 2014, 66, 223-237.

95. Paszkowski, M. Assessment of the effect of temperature, shear rate and thickener content on the thixotropy of lithium lubricating greases. *Proc IMechE Part J, Engineering Tribology*, 2012, 227, 3, 209–219.

96. Czarny, R. Effects of changes in grease structure on sliding friction. *Industrial Lubrication and Tribology*, 1995, 47, 1, 3–7.

97. Fiedler, M.; Sánchez, R.; Valencia, C.; Leopold, C.S.; Kuhn, E.; Franco, J.M. Influence of Base Oil Polarity on the Transient Shear Flow of Biodegradable Lubricating Greases. *Lubricants*, 2015, 3, 611–627.

98. Delgado, M.A.; Franco, J.M.; Kuhn, E. Effect of rheological behaviour of lithium greases on the friction process. *Industrial Lubrication and Tribology*, 2008, 60, 37–45.

99. Delgado, M.A.; Franco, J.M.; Valencia, C.; Kuhn, E.; Gallegos, C. Transient shear flow of model lithium lubricating greases. *Mech Time-Dependent Mater*, 2009, 13, 63–80.

100. Kuhn, E. Experimental grease investigations from an energy point of view. *Industrial Lubrication and Tribology*, 1999, 51, 5.

101. Rezasoltani, A.; Khonsari, M.M. On the Correlation Between Mechanical Degradation of Lubricating Grease and Entropy. *Arnold Tross Colloquium*, Hamburg University of Applied Sciences, Hamburg, Germany, 2016, ISBN 978-3-8440-4962-6.

102. Rezasoltani, A.; Khonsari, M. On monitoring physical and chemical degradation and life estimation models for lubricating greases. *Lubricants*, 2016, 4, 3, 34.

103. Cann, P.M.; Webster, M.N.; Doner, J.P.; Lugt, P.; Wikstrom, V. Grease degradation in R0F bearing test. *Tribolgy Transactions*, 2006, Preprint No. (AM) 06-06.

104. Kuhn, E. Investigations into the degradation of the structure of lubricating greases. *Tribology Transactions*, 1998, 41, 247–250.

105. Gonçalves, D.; Graça, B.; Campos, A.V.; Seabra, J.; Leckner, J.; Westbroek, R. On the film thickness behaviour of polymer greases at low and high speeds. *Tribology International*, 2015, 90, 435–444.

106. Cen, H.; Lugt, P.M.; Morales-Espejel, G.E. On the film thickness of grease-lubricated contacts at low speeds. *Tribology Transactions*, 2014, 57, 668–678.

107. Hurley, S.; Cann, P.M. The influence of grease composition on film thickness in rolling contacts. *NLGI Spokesm* 1999, 63, 12–22.

108. Palacios, J.M.; Cameron, A.; Arizmendi, L. Film thickness of grease in rolling contacts. *ASLE Transactions*, 1981, 24, 474–478.

109. Acar, N.; Franco, J.M.; Kuhn, E. On the shear-induced structural degradation of lubricating greases and associated activation energy: An experimental rheological study. *Tribology International,* 2020, 144, 106105.

110. Kuhn, E. Zur Tribologie der Schmierfette, Eine Energetische Betrachtungsweise des Reibungs- und Verschleißprozesses. *Expert Verlag*, Renningen, 2009.

111. Fiedler, M.; Kuhn, E.; Franco, J.M.; Litters, T. Tribological Properties of Greases Based on Biogenic Base Oils and Traditional Thickeners in Sapphire-Steel Contact. *Tribology Letters*, 2011, 44, 293–304.

112. Khonsari, M.M.; Booser, E.R. On the Stribeck curve. *Friction and Lubrication*, 2010, 263–278.

113. Hutchings, I.M. Tribology: Friction and wear of engineering materials. *Edward Arnold*, Great Britain, 1992.

114. Gonçalves, D.; Vieira, A.; Carneiro, A.; Campos, A.V.; Seabra, J.H.O. Film Thickness and Friction Relationship in Grease Lubricated Rough Contacts. *Lubricants*, 2017, 5, 34.

115. Goh, S.M.; Versluis, P.; Appelqvbist, I.A.M.; Bialek, L. Tribological measurements of foods using a rheometer. *Food Research International*, 2010, 43, 183–186.

116. Galda, L.; Pawlus, P.; Sep, J. Dimples shape and distribution effect on characteristics of Stribeck curve. *Tribology International*, 2009, 42, 1505–1512.

117. Kalin, M.; Velkavrh, I.; Vizintin, J. The Stribeck curve and lubrication design for non-fully wetted surfaces. *Wear* 2009, 267, 1232–1240.

118. García-Zapateiro, L.A.; Franco, J.M.; Valencia, C.; Delgado, M.A.; Gallegos, C. Viscous, thermal and tribological characterization of oleic and ricinoleic acidsderived estolides and their blends with vegetable oils. *Journal of Industrial and Engineering Chemistry*, 2013,19, 1289–1298.

119. Sulek, M.W.; Kulczycki, A.; Malysa, A. Assessment of lubricity of compositions of fuel oil with biocomponents derived from rape-seed. *Wear*, 2010, 268, 104–108.

120. Lu, X.; Khonsari, M.M. An experimental investigation of grease-lubricated journal bearings. *Journal of Tribology Transactions of the ASME*, 2007, 129, 84–90.

121. Gonçalves, D.; Graça, B.; Campos, A.V.; Seabra, J.; Leckner, J.; Westbroek R. Formulation, rheology and thermal ageing of polymer greases—Part I: influence of the thickener content. *Tribology International*, 2015, 87, 160–70.

122. Kragelski, I.P.; Dobicin, M.N.; Kombalov, V.S. Reibung und Verschleiß. *Verlag Technik*, Germany, 1982.

123. Ide, A.; Asai, Y.; Takayama, A.; Akiyama, M. New life prediction method of the grease by the activation energy. *Tribology Online*, 2011, 6, 45–49.

124. Dornhöfer, G. Ermittlung der Schmierfettgebrauchsdauer mit zeitraffender Prüfmethode und Übertragbarkeit auf reales Temperaturkollektiv. *Tribologie und Schmierungstechnik*, 2018, 65, 1, 7–13.

125. Gimzewski, E. The relationship between oxidation induction temperatures and times for petroleum products. *Thermochimica Acta*, 1992, 198, 133–140.

126. Rhee, I.S. Development of a new oxidation stability test method for greases using a pressure differential scanning calorimeter. *NLGI's 57th annual meeting*, Denver, Colorado, USA, 1990.

127. Rhee, I.S. Decomposition kinetic of greases by thermal analysis. *DTIC Document*, 2007.

128. Rezasoltani, A.; Khonsari, M. Experimental investigation of the chemical degradation of lubricating grease from an energy point of view. *Tribology International*, 2019, 137, 289–302.

129. Matzke, M.; Dornhöfer, G.; Schöfer, J. Quantitatively-accelerated testing of grease oxidation- a parameter study with RapidOxy. *60. German Tribology Conference*, Göttingen, Germany 2019.

130. Zhou, Y.; Bosman, R.; Lugt, P.M. A master curve for the shear degradation of lubricating greases with a fibrous structure. *Tribology Transactions*, 2019, 62, 78–87.

131. Cortés-Triviño, E.; Valencia, C.; Delgado, M.A.; Franco J.M. Thermo-rheological and tribological properties of novel bio-lubricating greases thickened with epoxidized lignocellulosic materials. *Journal of Industrial and Engineering Chemistry*, 2019, 80, 626–632. https://doi.org/ 10.1016/j.jiec.2019.08.052.

132. Borrero-Lopez, A.M.; Blanquez, A.; Valencia, C.; Hernandez, M.; Arias, M.E.; Franco, J.M. Influence of solid-state fermentation with Streptomyces on the ability of wheat and barley straws to thicken castor oil for lubricating purposes. *Industrial Crops and Products*, 2019, 140, 111625.

133. Kuhn, E.; Balan, C. Experimental procedure for the evaluation of the friction energy of lubricating greases. *Wear*, 1997, 209, 237–240.

134. Kuhn, E. Effects of fluid friction on lubricating greases. *LUBMAT Conference*, Bilbao, Spain, 2016.

135. Müller, M. Bestimmung der Aktivierungsenergie von Fluiden mit hilfe der Viskositätsmessung. *Tribologie und Schmierungstechnik*, 2016, 63, 42–51.

136. Müller, M. Klassifizierung von Schmierstoffen basierend auf der Aktivierungsenergie. *Tribologie und Schmierungstechnik*, 2017, 64, 41–45.

137. Sánchez, R.; Franco, J.M.; Delgado, M.A.; Valencia, C.; Gallegos, C. Rheology of oleogels based on sorbitan and glyceryl monostearates and vegetable oils for lubricating applications. *Grasas Aceites*, 2011, 62, 328–336.

138. Ike, E. The study of viscosity-temperature dependence and activation energy for palm oil and soybean oil. *Global Journal of Pure and Applied Sciences*, 2019, 25, 209–217.

139. Idrees, S.A.; Mustafa, L.L.; Saleem, S.S. Improvement viscosity index of lubricating engine oil using low molecular weight compounds. *Science Journal of University of Zakho*, 2019, 7, 14–17.

140. Rezasoltani, A.; Khonsari, M.M. On the correlation between mechanical degradation of lubricating grease and entropy. *Tribology Letters*, 2014, 56, 2, 197–204.

141. Zhou, Y. On the mechanical aging of lubricating greases. *PhD thesis*, the University of Twente, Netherlands, 2018.

142. Ito, H.; Tomaru, M.; Suzuki, T. Physical and chemical aspects of grease deterioration in sealed ball bearings. *Lubrication Engineering (STLE)*, 1988, 44, 10, 872–879.

143. Kuhn, E. Application of a thermodynamic concept for the analysis of structural degradation of soap thickened lubricating greases. *Lubricants*, 2018, 6, 7.

144. Kuhn, E. Description of the energy level of tribologically stressed greases. *Wear*, 1995, 188, 138–141.

145. Lijesh, K.P.; Khonsari, M.M. On the assessment of mechanical degradation of grease using entropy generation rate. *Tribology Letters*, 2019, 67, 50.

146. Osara, J.A.; Bryant, M.D. Thermodynamics of Grease Degradation. *Tribology International*, 2019, 137, 433–445.

Chapter 3

Materials

&

Experimental Methods

3.1. Materials

In this study, fully or partially biogenic and traditional lubricating greases were investigated by means of suitable series of tribological and rheological experiments.

Completely biogenic lubricating greases (1–13) and two reference semi-biogenic lubricating greases (R1, R2) were produced by *Fuchs Europe Schmierstoffe* (Mannheim, Germany) and *Fuchs Lubritech* (Kaiserslautern, Germany). Moreover, four completely biogenic lubricating greases (S1–S4) from *Pro²TecS* (University of Huelva, Huelva, Spain) were investigated in this study. All biogenic lubricating grease samples were formulated with different biogenic oils, e.g., high-oleic sunflower oil (HOSO), glycerol, castor oil, and a combination of HOSO and castor oil, as the base oils. Moreover, different natural products, e.g., beeswax, corncob grits, natural cellulose, and lignin, were used as thickener agents. For confidentiality reasons, information on the percentage of each thickener in *Fuchs* greases cannot be provided here. The second group of biogenic grease samples used castor oil as the base oil and lignin as the thickener agent, once chemically modified with an epoxy compound (polyethylene glycol diglycidyl ether (PEGDGE)) or hexamethylene diisocyanate (HMDI) to promote the chemical interaction with the base oil [1-3]. The compositions of all the biogenic grease samples are depicted in Table 3.1.

Table 3.1 Compositions of biogenic lubricating greases

Grease Sample (Code)	Base Oil	Substance of Content
R1	Synthetic ester	Lithium/calcium soap
R2	HOSO [1]	Lithium-12-hydroxystearate
1	HOSO and castor oil	Beeswax, glyceryl monostearate, and cetyl alcohol
2	HOSO and castor oil	Glyceryl monostearate, cetyl alcohol, and sorbitan monostearate
3	HOSO and glycerol	Cellulose ether
4	HOSO	Isoprene derivative
5	HOSO	Lignosulfonate
6	HOSO	Natural cellulose fibers, 18 µm
7	HOSO	Corncob grits, 80–120 µm
8	HOSO	Natural cellulose, 20–40 µm
9	HOSO	Natural wood pulp from softwood, 70–150 µm
10	HOSO	Natural cellulose fibers, 120 µm
11	HOSO and castor oil	Ethyl cellulose, carnauba wax, and cetyl alcohol
12	Castor oil, HOSO and MCT oil (triglyceride of C8/C10 fatty acids)	Polyhydroxybutyric acid and ethyl cellulose
13	Glycerol and sorbitan monooleate	Chitosan, glyceryl monostearate, and calcium phosphates
S1	Castor oil	Lignin/PEGDGE [2] (weight ratio of 1/0.25)
S2	Castor oil	Lignin/PEGDGE (weight ratio of 1/1)
S3	Castor oil	Lignin/HMDI [3] (weight ratio of 1/2)
S4	Castor oil	Lignin/HMDI (weight ratio of 1/1)

[1] HOSO: high-oleic sunflower oil; [2] PEGDGE: polyethylene glycol diglycidyl ether; [3] HMDI: hexamethylene diisocyanate.

In addition, six traditional lubricating greases were specifically manufactured by *Fuchs Europe Schmierstoffe* (Mannheim, Germany), by applying the traditional method in a pilot plant. The greases were composed of the same base oil, a mixture of polyalpha olefin (PAO, approx. 31 mm^2/s kinematic viscosity at 40°C) and a paraffinic mineral oil (approx. 500 mm^2/s kinematic viscosity at 40°C) in a ratio of 1:1, and two different thickener types, lithium-12-

hydroxystearate (Li) and polyurea (PU). The thickener content varied from 4.5% to 11.1%. The criterion for selecting thickener concentrations was to fit the NLGI grade to 0, 1 and 2 for each thickener type. More detailed information for the base oil, and compositions and NLGI grades of these grease samples are summarised in Table 3.2.

Table 3.2 Grease compositions and NLGI grades [4]

Grease Sample (Code)	Thickener Type	Thickener Concentration [%]	Base Oil			NLGI[3] Class
			Type	v40[1] [mm²/s]	PP[2] [°C]	
Li-0	Lithium-12-Hydroxystearate	4.5	PAO/Paraffinic mineral oil[4]	100	-24	0
Li-1		6.5				1
Li-2		9.5				2
PU-0	Polyurea	7.9				0
PU-1		8.6				1
PU-2		11.1				2

[1] v40: Kinematic viscosity at 40°C, [2] PP: Pour Point, [3] NLGI: National Lubricating Grease Institute, [4] PAO6/ paraffinic bright stock

3.2. Experimental methods

3.2.1. Tribological tests

In order to investigate the friction and wear processes, completely biogenic lubricating greases and two reference semi-biogenic lubricating greases (R1, R2) were examined using a nanotribometer, a ball on a disc tribometer and a rolling bearing test rig.

3.2.1.1. Tribological tests on the nanotribometer

A nanotribometer from CSM Instruments (Peseux, Switzerland), shown in Figure 3.1, was used to determine the friction values of tribologically stressed material combinations. The test set-up consists of a static ball, which is fixed to a cantilever to avoid rolling, and a rotating disc. In the nanotribometer, the disc is stressed by pressure caused by applying a normal force. The ball-on-disc apparatus works in rotational mode. The fiber-optic sensors measure the deflection of the cantilever in radial (frictional force) and normal (normal force) directions, and by the

precise calibration of the spring constant of the cantilever in both directions determined into frictional and normal forces.

In the Tribology Research Center (TREC) at the Hamburg University of Applied Sciences (HAW-Hamburg, Germany), all tests were performed using a material combination of a steel ball (100Cr6) with 1 mm diameter on a steel disc (115CrV3, hardness 60–62 HRC, Zentrale Laborwerkstatt at the HAW-Hamburg, Hamburg, Germany) in rotational mode. All the steel discs were metallographically grinded and polished with a soft finish diamond paste of particle size 3 μm in the last polishing step. Normal load was kept constant at 200 mN with resulting Hertzian stress values of 1.2 GPa, and relative speed was varied with values of 40 $mm \cdot s^{-1}$ and 60 $mm \cdot s^{-1}$. Under these conditions, a mixed-friction lubricated contact was achieved. The evolution of the friction coefficient with time was followed during 34 min (with relative speed 40 $mm \cdot s^{-1}$) and 22 min (with relative speed 60 $mm \cdot s^{-1}$). Each test was performed with model grease samples (1-9 and S1-S4) and two reference grease samples (R1 and R2) and repeated three times at an ambient temperature of 22 ± 1 °C to calculate a quite accurate average friction coefficient.

The wear marks, which were produced from the three-times repetition of the measurement in the same track at the nanotribometer, were analyzed by means of white light Interferometry (by Zygo Nexview, Middlefield, OH USA). In this investigation, biogenic grease samples were examined to quantify the wear in the solids.

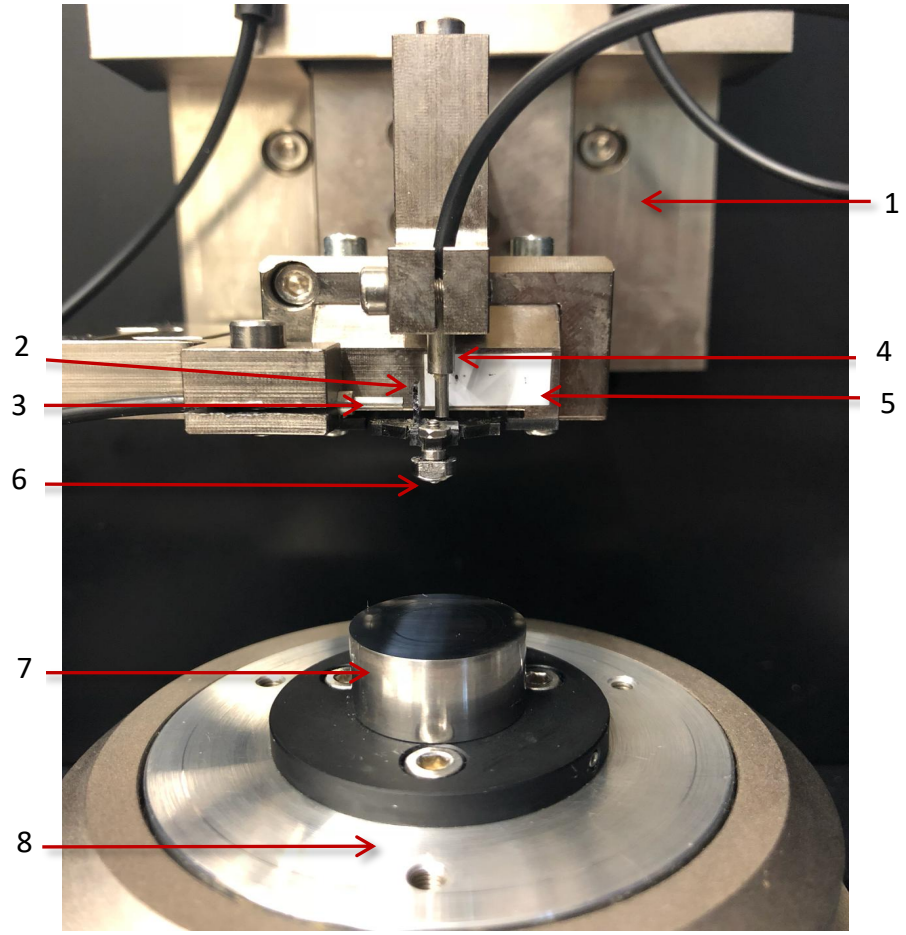

Figure 3.1 Nanotribometer from CSM Instruments (Peseux, Switzerland). Note: 1–Z-step-motor-axis with integrated piezo-axis, 2–Mirrors of optical sensors, 3–Interferometrical sensor, 4–Interferometrical sensor, 5–Cantilever, 6–Steel ball, 7–Steel disk, and 8–Rotational axis

3.2.1.2. Tribological tests on the ball-on-disc tribometer

A tribometer designed by the Tribology Research Center (TREC) at the Hamburg University of Applied Sciences (HAW-Hamburg, Germany), as shown in Figure 3.2, was used to determine the friction coefficient values of tribologically stressed material combinations. The test set-up was composed of a rotatory plate and a fixed ball. In the tribometer, the steel plate was lubricated with a grease sample and stressed by applying a normal force. By means of a load cell, the friction force was measured during the test, thereby allowing the friction coefficient to be determined.

All tests were carried out in rotational mode with a relative speed of 0.129 $m \cdot s^{-1}$, using a steel ball (100Cr6) 12.7 mm in diameter and steel plates (S235JR (St37), Zentrale Laborwerkstatt at the HAW-Hamburg, Hamburg, Germany). In order to achieve comparable results, frictional and wear behaviours of the completely biogenic lubricating greases (1-13 and S1-S4) and two

reference greases (R1 and R2) were investigated using the same test parameters and conditions for the tribometer. All the steel plates were metallographically grinded and polished with a soft finish diamond paste of particle size 3 μm in order to significantly reduce surface roughness. Grease layers of the same thickness were applied to the steel plates, as shown in Figure 3.2. The normal load was kept constant at 12.62 N, with a resulting Hertzian stress value of 930.76 MPa during 5 min. Each test was replicated ten times on the same track at an ambient temperature of 22 ± 1 °C in order to get a representative average friction coefficient value.

To quantify the wear of the solids, the wear marks on the steel plates created after the ten repetitions of the test on the same track of the tribometer were investigated using white light interferometry with a Zygo Nexview apparatus (Middlefield, OH, USA). Wear depths were quantified by means of the Zygo Mx software.

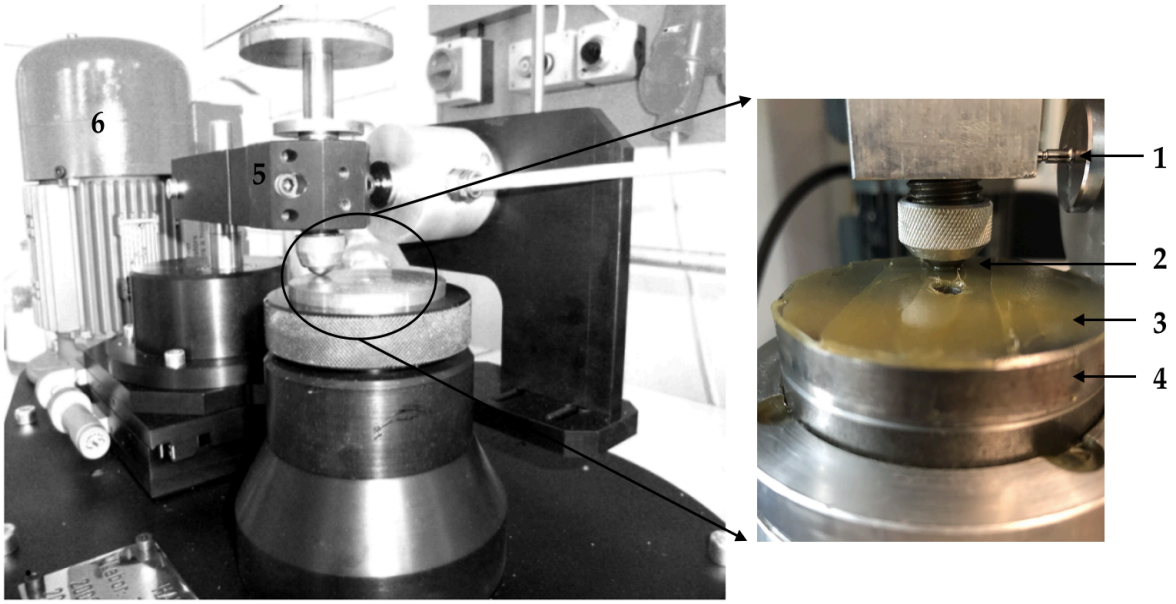

Figure 3.2 Tribometer designed by the Tribology Research Center (TREC) at Hamburg University of Applied Sciences (HAW-Hamburg, Germany). Note: 1–Friction force-sensor, 2–steel ball, 3–lubricating grease, 4–steel disc, 5–swivel arm, and 6–electromotor (adapted from E. Kuhn [5])

3.2.1.3. Rolling bearing's friction torque tests

In order to assess the tribological behaviour of the biogenic greases on real machine element contacts, rolling bearing (RB) tests were performed with selected model greases 1 and 2 in a dedicated rolling bearing test rig, as seen in Figure 3.3. In this test rig, the rolling bearing was

subjected to a constant axial load (P) applied from bottom to top; the thrust roller bearing tested in this work operated in a vertical arrangement [6-9].

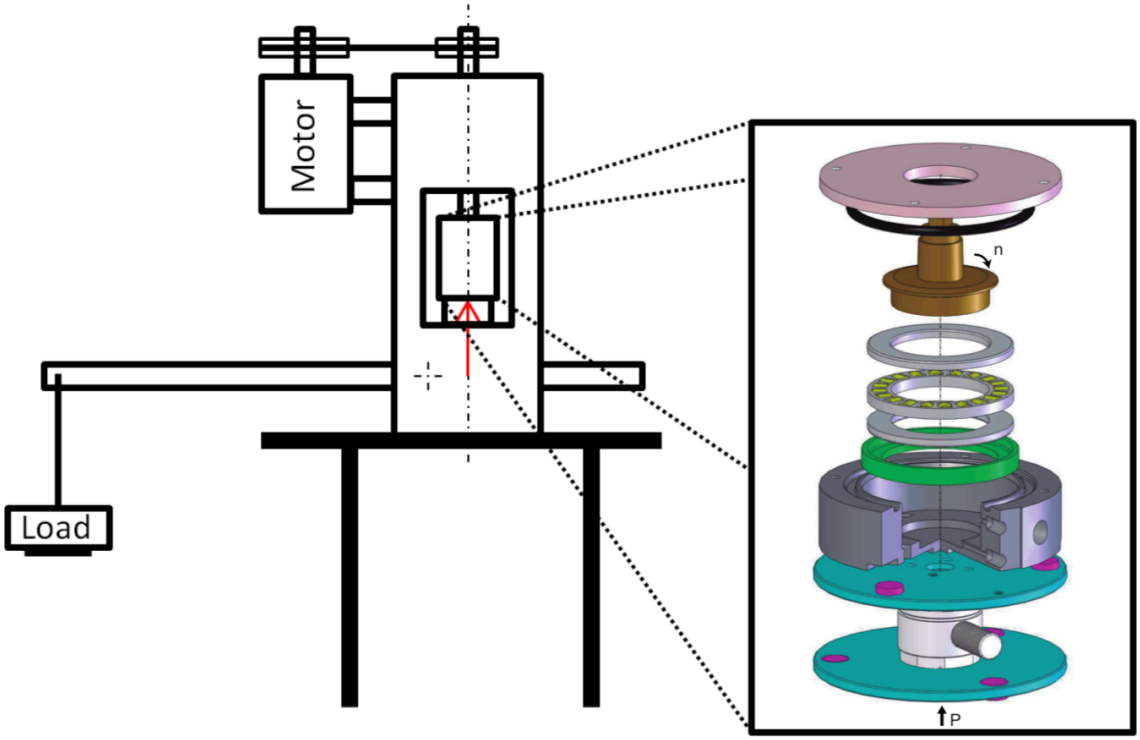

Figure 3.3 Rolling bearing test rig scheme

An electrical motor provided the necessary power to overcome the power loss of the system and keep the rotational speed steady. A belt-pulley arrangement transmitted the power from the motor to the rolling bearing shaft, forcing the upper raceway to rotate. The lower raceway was fixed to the bearing house and the torque cell, while the rolling elements' cage rotated due to the motion imposed by the upper raceway. A piezoelectric reaction torque cell KISTLER® 9339A (Kistler Group, Winterthur, Switzerland) was used to measure the friction torque. For each speed step tested, five torque measurements were performed.

The tests were performed with a thrust ball bearing (TBB) 51107 from SKF (SKF Group, Gothenburg, Sweden). The TBB had 21 rolling elements that were 6 mm in diameter and the raceways had a mean diameter of 43.5 mm. Regarding the thrust load, the tests were performed with approximately 5 kN. Given the number of rolling elements of the TBB and the radius of curvature, the maximum Hertzian pressure was around 2 GPa during the ball–raceway contact. Since the melting temperature of the thickeners was around 60 °C, it was decided to control the temperature inside the TBB at 50 °C. Since the temperature did not reach 60 °C, the thickener

did not melt and therefore the structure should have only been affected by the mechanical working, avoiding a premature degradation of the grease structure.

3.2.1.3.1. Power loss tests

The operating conditions chosen for the power loss tests are shown in Table 3.3. The tests performed were well above the minimum required load (0.02C) while also not exceeding the maximum dynamic load rating (P/C ≈ 25%, P: equivalent dynamic bearing load (kN), C: basic dynamic load rating (kN)).

Table 3.3 Operating conditions of the power loss tests. TBB: Thrust ball bearing

Parameter	**TBB 51107**
Mean diameter (mm)	43.5
Number of rolling elements	21
Height (mm)	12
Composite roughness (nm)	155
Rotational speed (rpm)	100, 200, 400, 800, 1600
Axial Load (N)	5 kN (≈2.08 GPa)
Temperature (°C)	Controlled at 50 °C

The friction torque measuring procedure involved the following steps:

1. The machine was loaded with 5 kg (load on the bearing ≈1000 N) and the motor was started, with the speed increasing to 500 rpm for 5 min.
2. The load was increased to 25 kg (5 kN) and the speed was set at 100 rpm.
3. Temperature stabilization was undertaken (less than 1°C degree variation in a time window of 10 min).
4. The friction torque was measured five times at constant operating conditions.
5. The rotational speed was increased. Steps 3 and 4 were repeated to reach the required rotational speed.
6. The test was stopped.

The total test duration was between 6 and 7 h to allow for the temperature to stabilize at 50 °C every time the speed was increased. The rolling bearing test rig was able to maintain the temperature at 50 °C with less than 1 °C deviation for all rotational speeds by using an external thermal bath.

3.2.1.3.2. Wear tests

In the case of the wear tests, given that at 50 °C the specific film thickness (Λ (–)) value, which represents the relationship between the lubricant minimum film thickness and the surface roughness, only reached 0.5 above 400 rpm, these tests were run at a rotational speed of 200 rpm. Table 3.4 shows the operating conditions of the wear tests.

Table 3.4 Operating conditions of the wear tests

Load	Speed	Temperature	Time
5 kN	200 rpm	50 °C	120 h

After the test, a grease sample was collected for wear particle analysis by means of the ferrometry and ferrography techniques. More details regarding this wear particle analysis procedure can be found elsewhere [10].

3.2.1.3.3. Grease volume

In order to fill part of the chamber of the rolling bearing house while also assuring that all the rolling elements were wet up to half of their diameter, 10 mL of grease was used; 2 mL was spread across the rolling bearings raceways and the holes between the cage and the rolling elements, while the other 8 mL was put in the rolling bearing house. Figure 3.4 shows the grease spread on the different parts of the rolling bearing assembly.

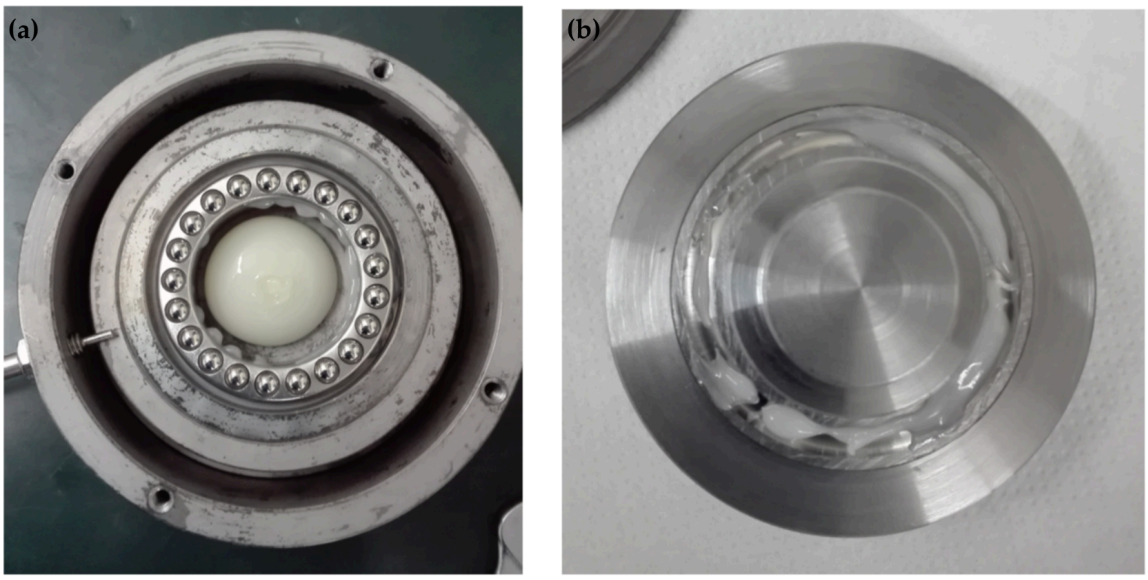

Figure 3.4 Grease spread on (a) the rolling bearing house, lower raceway, and cage, and (b) on the upper raceway shaft

3.2.2. Rheological tests

Rheological properties of all model greases were studied by using a controlled-stress rheometer MCR-302 (Anton Paar GmbH, Graz, Austria). To characterize the internal friction behaviour by quantifying the energy density, rotational transient flow tests were performed at different temperatures. On the other hand, rotational transient flow tests and oscillation amplitude sweep tests were carried out in order to investigate the relationship between the activation energy and the extent of the structural degradation that occurs under different shearing conditions.

3.2.2.1. Rotational transient flow tests

The rotational transient flow measurements of complete biogenic grease samples (1-9 and S1-S4) and two reference grease samples (R1 and R2) were carried out on a MCR-302 rheometer (Anton Paar GmbH, Graz, Austria). In this study, the model and reference greases were tested using a 25 mm plate–plate system with a gap of 1 mm. All tests were performed by applying a constant shear rate of 1 s^{-1} at different temperatures (25 °C, 40 °C and 80 °C). The measuring time was set at 3600 s and the selected greases were left to rest for 15 min after setting the gap and the temperature. Every measurement for each grease was repeated three times at each temperature.

In addition, to quantify the activation energy, six traditional lubricating greases were characterized in the same rheometer and measuring geometry by applying a constant shear rate of 1000 s^{-1} at different temperatures (25 °C, 40 °C, 55 °C, and 70 °C). The measuring time was set at 1800 s, which was sufficient to reach steady-state values of the stress for all of the grease samples studied.

3.2.2.2. Oscillatory shear tests - Amplitude sweeps tests

Amplitude sweep tests were carried out, at 25 °C, on the six traditional lubricating greases by applying deformation ramps from 0.01% to 100% at a constant angular frequency of 10 rad/s (as recommended in DIN 51810–2) and the evolution of G' and G'' monitored. Samples were left to rest for 15 min after setting the gap and temperature. All the rheological measurements were repeated three times and averaged before analysis to ensure reproducibility.

3.3. References

1. Borrero-López, A.M.; Valencia, C.; Franco, J.M. Rheology of lignin-based chemical oleogels prepared using diisocyanate crosslinkers: Effect of the diisocyanate and curing kinetics. *European Polymer Journal*, 2017, 89, 311–323.
2. Cortes-Triviño, E.; Valencia, C.; Franco, J.M. Influence of epoxidation conditions on the rheological properties of gel-like dispersions of epoxidized kraft lignin in castor oil. *Holzforschung*, 2017, 71, 777–784.
3. Cortes-Triviño, E.; Valencia, C.; Delgado, M.A.; Franco, J.M. Modification of alkali lignin with poly (ethylene glycol) diglycidyl ether to be used as a thickener in bio-lubricant formulations. *Polymers*, 2018, 10, 670.
4. Litters, T.; Koch, B. Untersuchungen zum Kälte-Fließverhalten von Schmierfetten mit modernen Rotationsviskosimetern-Einfluss von Verdicker und Basisöl auf die viskoelastischen Eigenschaften bei -40°C. 47. *German Tribology Conference*, Göttingen, Germany, 2006. b
5. Kuhn, E. Zur Tribologie der Schmierfette: Eine Energetische Betrachtungsweise des Reibungs-und Verschleißprozesses. *Expert Verlag*, Renningen, Germany, 2017.
6. Cousseau, T.; Graça, B.; Campos, A.; Seabra, J. Experimental measuring procedure for the friction torque in rolling bearings. *Lubrication Science*, 2010, 22, 133–147.
7. Cousseau, T.; Graça, B.; Campos, A.; Seabra, J. Friction torque in grease lubricated thrust ball bearings. *Tribology International*, 2011, 44, 523–531.
8. Gonçalves, D.; Cousseau, T.; Gama, A.; Campos, A.V.; Seabra, J.H.O. Friction torque in thrust roller bearings lubricated with greases, their base oils and bleed-oils. *Tribology International*, 2017, 107, 306–319.
9. Gonçalves, D.; Pinho, S.; Graça, B.; Campos, A.V.; Seabra, J.H.O. Friction torque in thrust ball bearings lubricated with polymer greases of different thickener content. *Tribology International*, 2016, 96, 87–96.
10. Available online: www.tricocorp.com/product/direct-reading-ferrograph/ (accessed on 31.05.2018).

Chapter 4

Results & Discussion

4.1. Tribological and rheological characterization of completely biogenic lubricating greases

4.1.1. Friction results

Averaged friction coefficients of the examined model greases from *Fuchs* (1-6, R1 and R2) and *Pro²TecS* (S1-S4) obtained in the nanotribometer set-up by applying two different relative speeds are shown in Figure 4.1. The average standard deviation is described by the error bars in the diagram. Model greases 7, 8, and 9 could not be tested on the nanotribometer due to their coarse structure. In the experiments with these model greases, the rotational movement causes the coarse particles in the grease to contact the ball socket in the cantilever. Consequently, the fiber-optic sensors deflect, even though there was actually no friction load. This results in high initial values of the friction coefficient or suddenly high values of friction coefficient during the test.

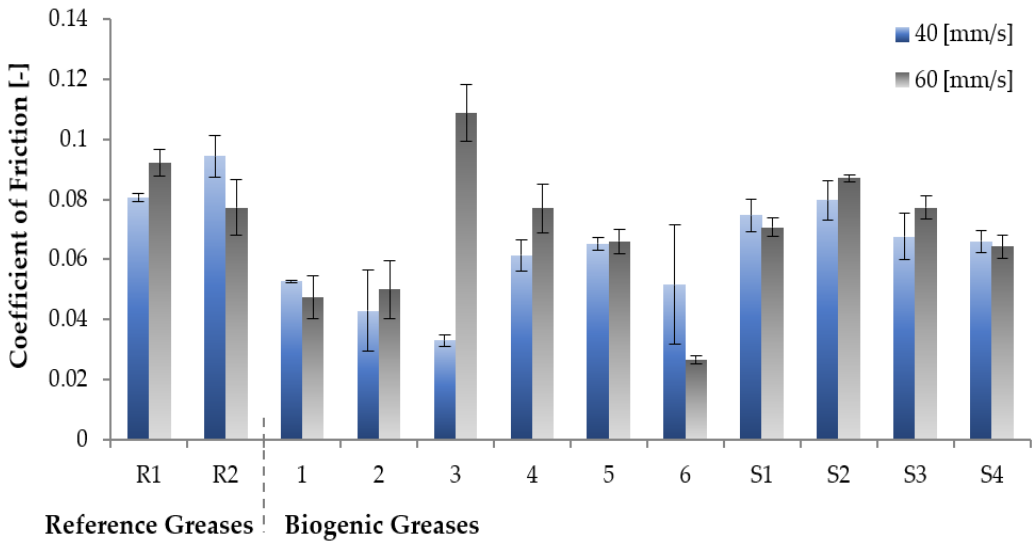

Figure 4.1 Friction coefficients determined in a steel ball-on-steel disc configuration (wear path s_R= 80 m)

As can be seen in Figure 4.1, the reference greases, R1, based on synthetic ester and Li/Ca-Soap, and R2, based on Li-12-Hydroxystearate and HOSO, generally show higher frictional values than biogenic grease samples in the present steel ball on steel plate frictional contact situation.

The use of biogrease S2, based on castor oil and lignin/PEGDGE as a thickener, provides similar or lower values of the friction coefficient than the two reference lubricating greases, R1 and R2. Moreover, the biogenic grease sample S4, containing lignin/HMDI as a thickener agent, stands out because of its lowest friction coefficient in comparison with the reference greases R1 and R2 and the other model greases from *Pro²TecS*: S1, S2, and S3. Another interesting point is that the biogenic grease samples produced by *Pro²TecS* by applying a relative speed of 40 $mm \cdot s^{-1}$ exhibit higher frictional values than the other model greases from *Fuchs*.

As can be seen in Figure 4.1, the model biogenic grease 3, based on HOSO, glycerol, and cellulose ether, has the lowest frictional coefficient at a relative speed of 40 $mm \cdot s^{-1}$; nevertheless, this model grease provides higher frictional value at a relative speed of 60 $mm \cdot s^{-1}$ than all of the other examined model greases. In addition, this grease exhibits an adhesive behaviour, which could lead to a negative influence on the friction behaviour at the nanotribometer. This directly shows the influences of the model grease components on frictional behaviour.

Moreover, model greases 1 and 2, based on a mixture of castor oil and HOSO as base oil, as well as model grease 6, provide lower values of the friction coefficient than the reference greases and the other model biogenic greases. These model greases 1 and 2 also contain glyceryl monostearate and/or sorbitan monostearate, such as biodegradable thickener agents. This optimum frictional behaviour can be attributed to both the presence of castor oil with much higher viscosity than HOSO, and the much lower molecular weight of sorbitan and glyceryl monostearates in comparison with the rest of bio-thickeners, that is, biopolymers. In addition, this type of grease exhibits very poor mechanical stability, though this could provide an advantage from a tribological point of view. This means that the microstructure of the grease is easily destroyed inside the tribological contact, turning into a more fluid material, significantly decreasing the consistency, and being able to lubricate contact more effectively [1].

Looking at the detail, the friction coefficients of the greases 1, 5, S1, and S4, remain stable in almost all test series. It shows that the friction coefficients of these grease samples are not highly influenced by relative speed differences.

According to the data in Figure 4.1, the friction coefficients of some examined greases, especially R1, 2, 3, 4, S2, and S3, increase with increasing relative speed. This is not the expected relative speed influence on the frictional behaviour, because the friction coefficient decreases with increasing relative speed in the mixed-friction lubrication regime. This frictional behaviour could be explained by taking into account the beginning of the transition to the

hydrodynamic lubrication regime. This approach is supported by wear data shown in Figure 4.3 and discussed below, in which the wear volume obtained in the contact lubricated with R1, 2, 4, S2, and S3 decreases with increasing relative speed.

4.1.2. Wear results

In this series of experiments, the wear marks on the steel discs, obtained after performing the frictional tests with the normal load of 200 mN and a relative speed of 40 $mm \cdot s^{-1}$ in the nanotribometer, were investigated using the white light interferometry (the optical 3D surface profilometer) as displayed in Figure 4.2. These pictures provide a perspective view of the main contacting area on the steel plate. The wear scars on the steel surface appear quite clearly in the perspective view. As can be seen in Figure 4.2, while the reference grease R2 and the biogenic greases 3, 4, and 6 produced very wide and strong abrasive wear on the steel plate, the reference grease R1 and the biogenic grease 1 caused the narrowest wear tracks but pronounced abrasive wear. Moreover, the biogenic greases S1, S2, and S3 show wide but less pronounced wear scars on the steel plate. These wear results can be explained by the different components in grease formulations and resulting rheological behaviours.

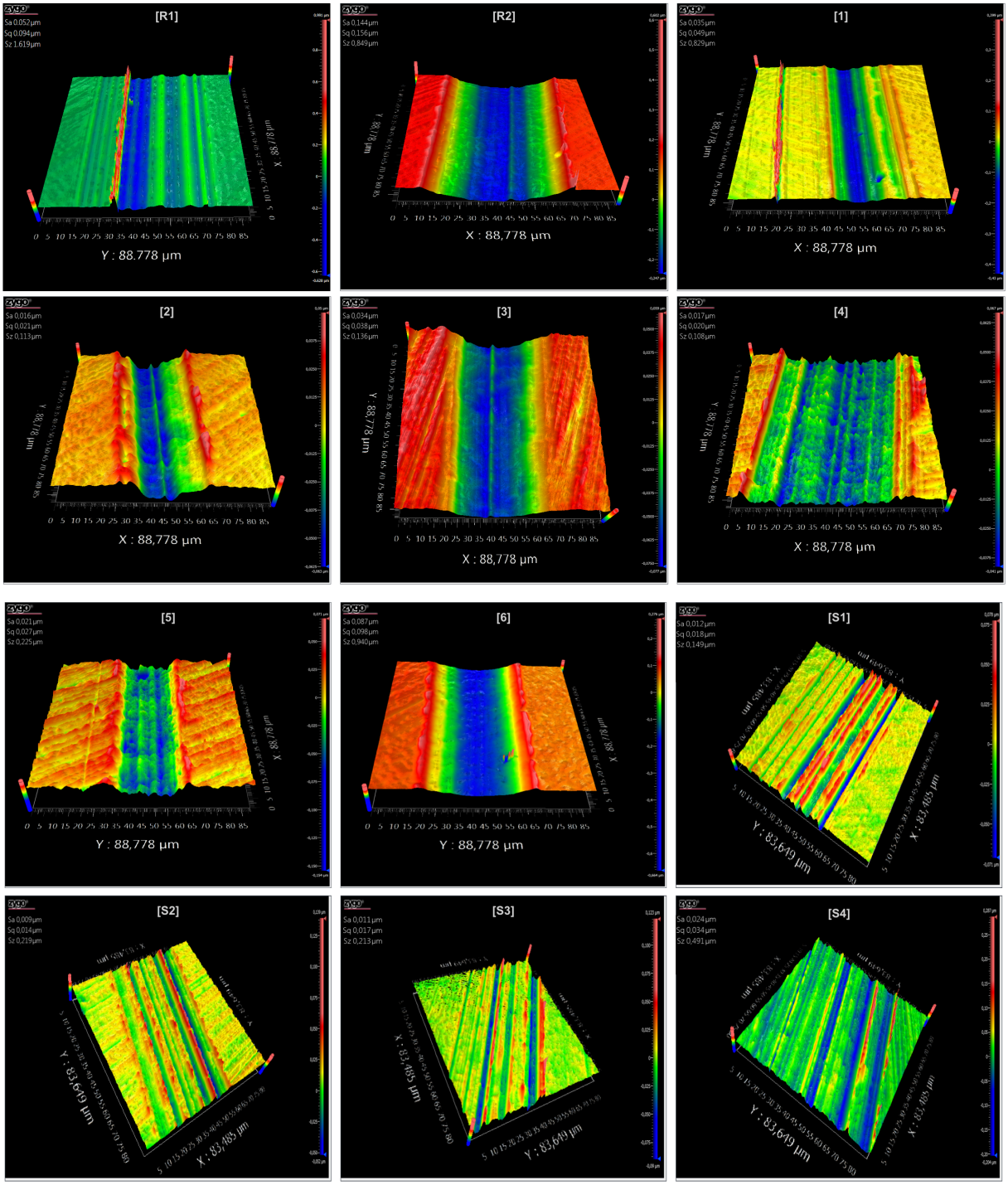

Figure 4.2 Profilometric pictures obtained from the steel discs as a function of the grease used as lubricants (window sizes of 88.778 µm × 88.778 µm and 83.485 µm × 83.649 µm)

The average volumes of the wear tracks on the steel plate, which were obtained after performing the frictional tests in the nanotribometer, are displayed as a function of the two different imposed relative speeds in Figure 4.3. The average standard deviation is described by the error bars in the diagram.

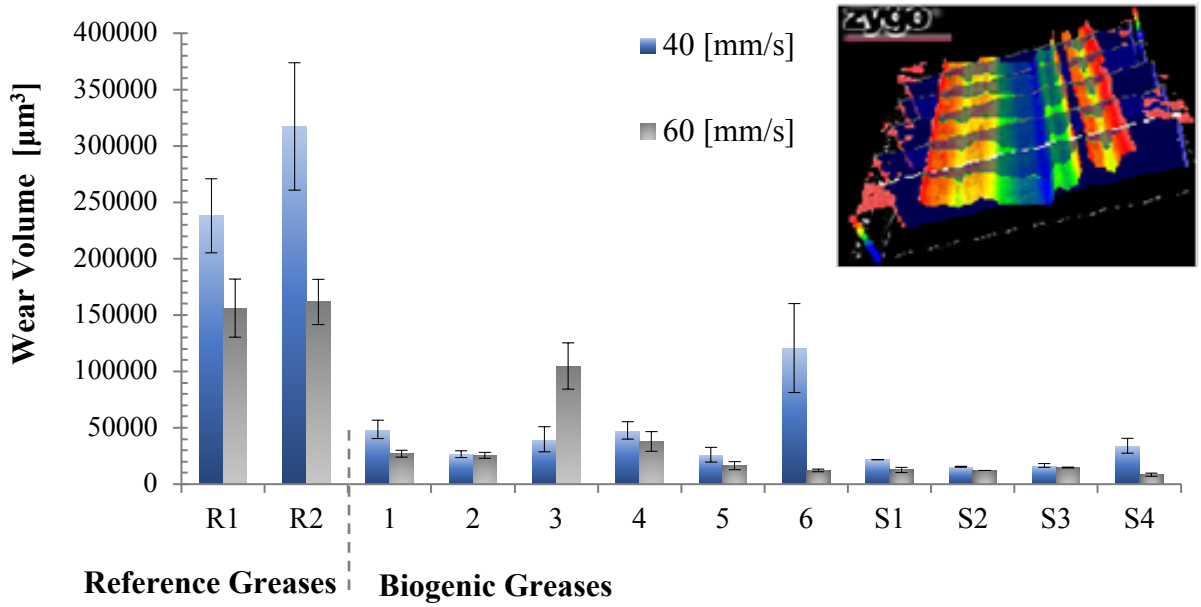

Figure 4.3 Wear volume in steel disc (wear path $s_R = 80$ m)

As can be observed in Figure 4.1, the friction coefficients of the reference greases are only slightly higher than those of the biogenic greases, despite the significantly higher wear volume values, which were at least three times the wear marks obtained with the biogenic greases.

Moreover, although biogenic grease 6, prepared with natural cellulose fiber of length of 18 µm, exhibits the lowest frictional value, it produces the highest wear volume at the lower relative speed of 40 mm·s^{-1} compared with all of the other biogenic greases, but the least wear at a relative speed of 60 mm·s^{-1}.

Another interesting point is that biogenic grease 3 produces a higher value of the friction coefficient at a relative speed of 60 mm·s^{-1}, which is reflected in the wear volumes. In addition to this, wear volume obtained in the contact lubricated with biogenic grease 3 increases by increasing relative speed, and decreases when using the other biogenic greases.

The biogenic grease samples containing castor oil and lignin/PEDGE or lignin/HMDI-thickener present higher values of the friction coefficient than the other biogenic greases, but the least wear on the steel plates. Under an assumption, these results could be explained by the better mechanical stability of these biogenic greases. This means that grease microstructures achieved by chemically cross-linking castor oil and lignin are not easily broken inside the tribological contact. This property of the grease microstructures could favor the grease not being easily ejected from the contact and therefore increases the efficiency of the grease in the lubricating contact.

4.1.3. Rotational transient flow tests

Figure 4.4 shows different transient flow curves for selected biogenic (1-9 and S1-S4) and reference grease samples (R1 and R2), at 25 °C. The rheological energy densities were determined by integration of shear stress over time at 25 °C, 40 °C, and 80 °C, according to Equations (2.16) and (2.17).

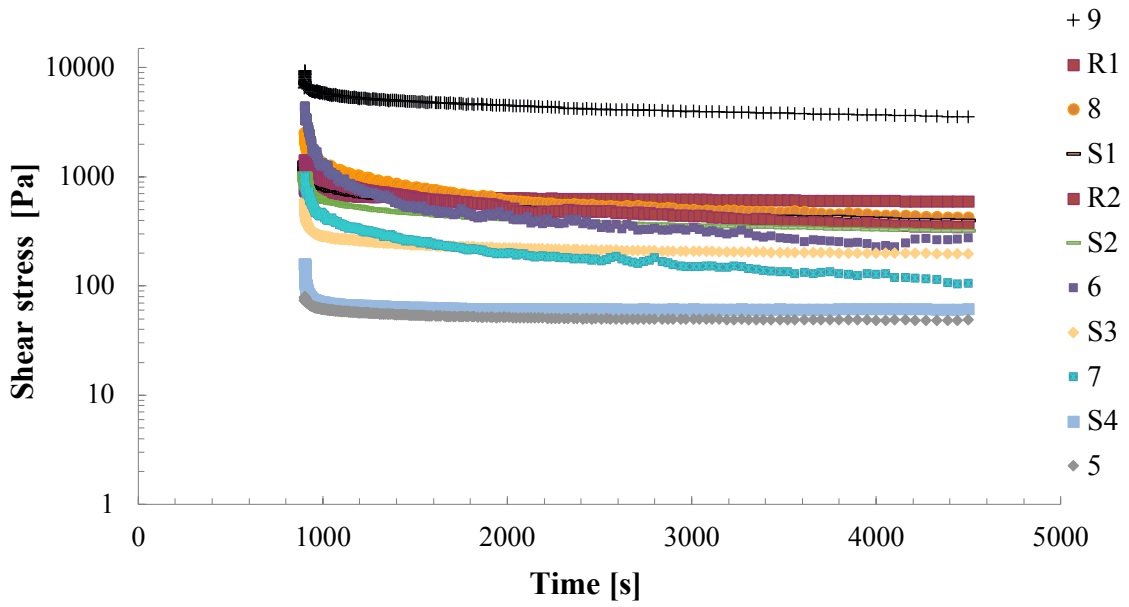

Figure 4.4 Transient flow curves for selected model grease samples at 25 °C

The values of e_{rheo} for the investigated biogenic greases (R1, R2, 1-9 and S1-S4) are displayed in Figure 4.5. Model greases 1 and 2 could not be tested at 80 °C on the rheometer, because sorbitan and glyceryl monostearates melted below this temperature [2].

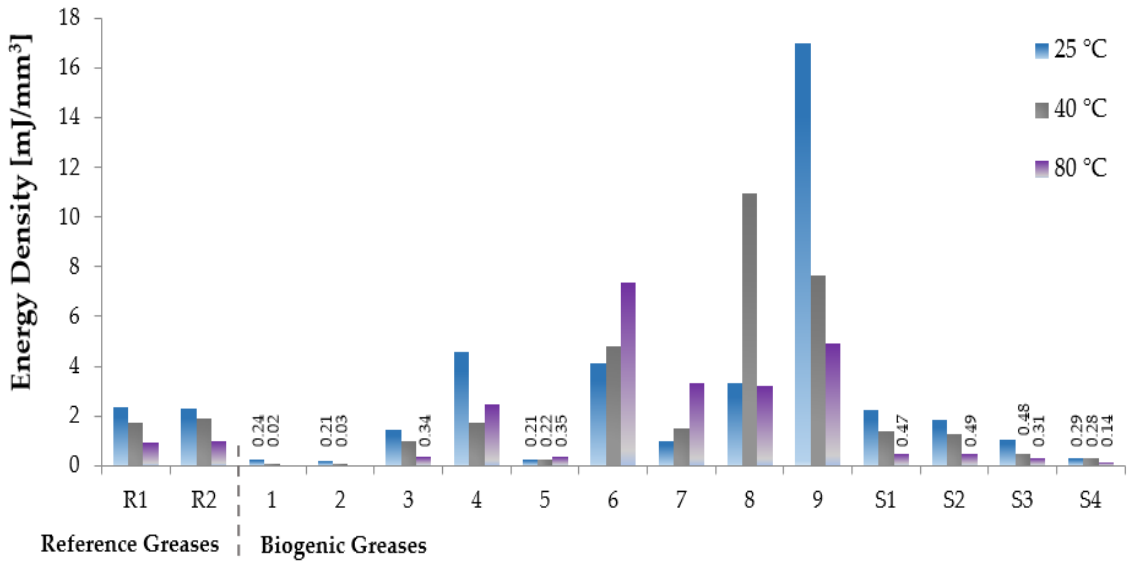

Figure 4.5 Energy densities (e_{rheo}) determined by integration of the shear stress vs. time plots at 25 °C, 40 °C, and 80 °C

These results show that the energy expenditure depends strongly on the temperature applied during the shearing of model greases at a constant shear rate. As can be seen in Figure 4.5, high test temperatures generally lead to less energy expenditure than is needed to stress the thickener structure. This indicates that shear-induced structural modifications of the model greases are significantly influenced by the temperature. Unexpectedly, however, the energy density values of the grease samples 5, 6, 7, and 8 (excluding the energy density value of sample 8 at 80 °C) increase with increasing temperature. The unusual temperature-influenced flow behaviour of these biogenic greases can be explained by the weak interactions between the base oil and cellulosic thickeners, based on hydrogen bonding, which significantly decrease with temperature. This favors oil separation (oil bleeding) at high temperatures, thus increasing viscosity as a result of the higher effective thickener concentration.

Another interesting point is that the biogenic grease samples 6, 8, and 9, consisting of HOSO as a base oil and natural cellulose fiber of length of 18 µm and 20–40 µm and natural wood pulp from softwood 70–150 µm as thickener agents, exhibit the highest values of energy density in all test series, probably because these formulations need higher thickener concentrations to be physically stabilized. Moreover, model grease samples 1 and 2, based on a mixture of castor oil and HOSO as base oil, and model grease sample 5, stand out because of their low values of the energy density in comparison with the reference greases and the other model biogenic greases. Looking at the detail, biogenic greases S3 and S4, based on lignin/HMDI as a

thickener, provide less energy expenditure compared with biogenic grease samples S1 and S2, based on lignin/PEGDGE as a thickener. This shows that the energy expenditure due to the shearing process is also influenced by the kind of lignin chemical modification.

From the analysis of the results discussed above, it seems obvious that grease microstructure plays an important role in the friction process. For a better understanding of the influence of the grease structure on the tribological behaviour, it is necessary to investigate the relationship between the rheological energy density and grease structure. Therefore, the microstructure of some biogenic greases was examined by means of transmitted light microscopy.

The microstructures of selected biogenic greases are shown in Figure 4.6. As can be observed, the geometry and the distribution of the thickener particles are clearly different. The biogenic grease samples 1, 3, and 5 display rather homogeneous structures. This is especially relevant in samples 3 and 5, where the thickener and base oil cannot be clearly distinguished from each other. By contrast, the thickeners in the biogenic grease samples 6, 8, 9, S1, S2, and S3 are conspicuous. At first consideration, from the thickener structures and the rheological energy density point of view, one detects that the homogeneous structure of grease sample 5 provides the lowest values of energy density at 25 °C and 40 °C (see Figure 4.5), compared with samples 6, 8, 9, S1, S2, and S3, which show thickener agglomerates in the form of platelets or granules. On the other hand, the model grease sample 1, based on glyceryl monostearate as thickener agent, exhibits less energy expenditure than model grease sample 3, based on cellulose ether as thickener agent, which provides higher values of the rheological energy density (see Figure 4.5). Overall, these results reflect the fact that the characteristics and type of the thickener microstructure influence the friction behaviour of the grease in the tribological process. In general, the more homogenous the structure and the smaller the particle size, the lower the resulting energy density.

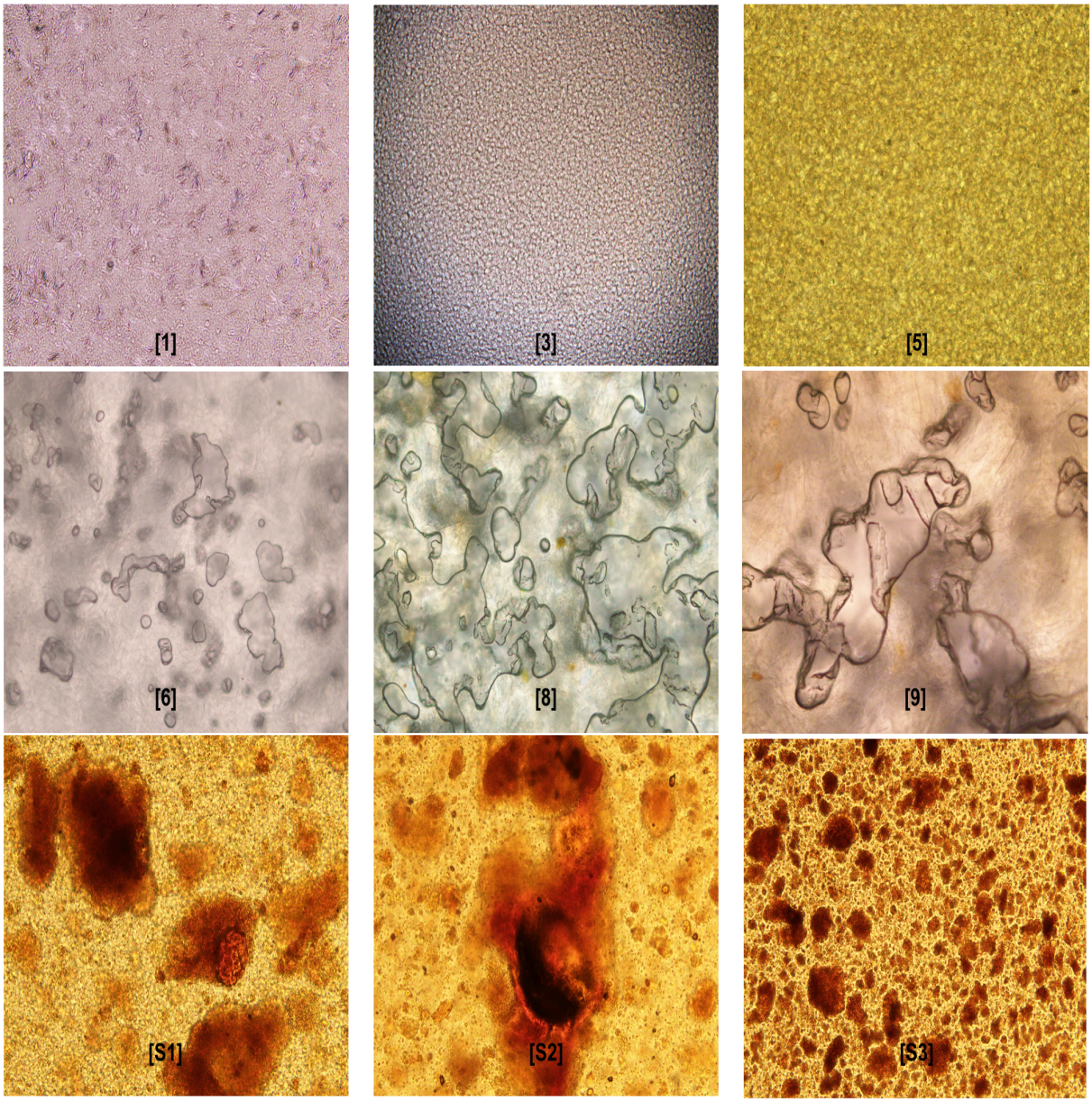

Figure 4.6 Transmitted Light Microscope micrographs for examined biogenic grease samples (window sizes of 683.5 μm × 536 μm) [3]

4.2. Analysis of the friction and wear behaviours of biogenic lubricating greases in steel–steel contacts

4.2.1. Apparent friction energy density determined from tribological tests on the ball-on-disc tribometer

The average friction coefficient and the average volume of the wear tracks on the steel plate were obtained after performing the frictional tests in the ball-on disc tribometer; results from all the examined biogenic model greases are shown in Figure 4.7.

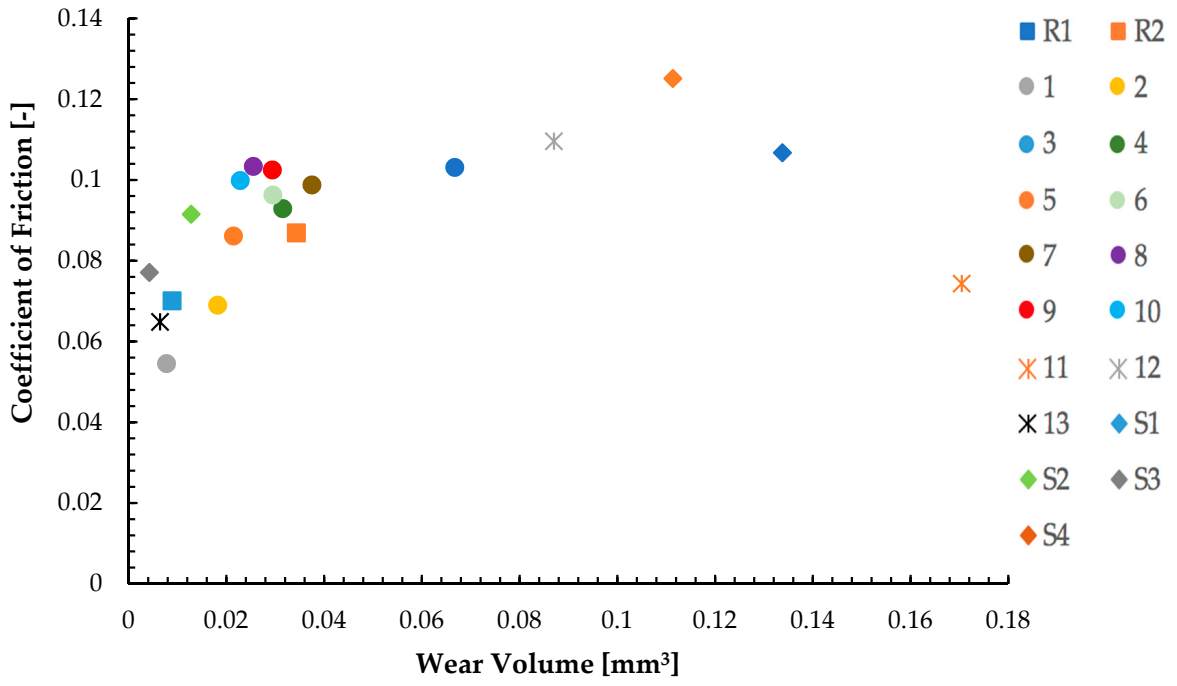

Figure 4.7 Friction coefficients versus wear volume on a steel plate for all model greases (wear path s_R= 387 m)

According to the data in Figure 4.7, a linear correlation was found between the friction coefficient and the wear data for most of the examined model grease samples. In this sense, the biogenic grease samples that exhibited low friction coefficient values, such as grease samples R1, 1, 2, 5, 13, and S3, produced less wear on the steel plate. On the other hand, the use of some biogenic grease samples, such as 3, 12, S1, and S4, provided high friction coefficient values, which were reflected in the wear volume.

Moreover, biogenic grease sample 11, which was based on a mixture of castor oil and HOSO as the base oil, stood out because of its low friction coefficient but exhibited the highest wear volume in comparison with model greases 1 and 2, which also contained castor oil and HOSO. Under appropriate assumptions, the microstructure and physical and chemical properties of the thickeners of biogenic grease 11 could lead to a negative influence in the present steel ball on the steel disc frictional contact. Biogenic grease 11, which was based on ethyl cellulose and carnauba wax as the thickener, which was a different composition to biogenic grease samples 1 and 2, presented a coarse and fragile structural appearance, probably due to its poor mechanical stability and low resistance to structural breakdown. This property can cause the grease microstructure to be easily destroyed upon tribological contact. Therefore, the grease can be gradually ejected from the contact, eventually yielding lubricant starvation.

The effects of the different thickeners were also illustrated when comparing the results provided by biogenic greases 6, 8, and 10. Biogenic grease 10, which was prepared with a natural cellulose fiber of 120 μm in length as the thickener, exhibited the least wear on the steel plate compared with model grease 6, which was based on a natural cellulose fiber 18 μm in length, and grease 8, which was based on a natural cellulose fiber 20–40 μm in length. This result indicated that the longer the natural cellulose fiber of the thickener was, the lower the wear volume on the steel plate (i.e., 22% lower for sample 10 compared to sample 6).

These results showed that the different behaviours of different grease lubricant formulations were more explicitly observed in the wear results than in the frictional results in the tribological process.

To illustrate the wear on the steel plates produced from the ten repetitions of the measurements on the same track in the ball-on disc tribometer, the wear marks were investigated using an optical 3D surface profilometer, as shown in Figure 4.8. The pictures allowed for the contacting surface on the steel plate to be observed. As seen in Figure 4.8, while the use of biogenic grease 3 and reference grease R2 caused wide and strong abrasive wear, biogenic grease 2 and reference grease R1 produced wide but less pronounced wear on the steel disc. Looking at the detail, the use of biogenic grease 3 and reference grease R2 caused higher wear depth values, which are described as “Mean [μm]” in Figure 4.8, compared with biogenic grease 2 and reference grease R1. These data support the wear data shown in Figure 4.7.

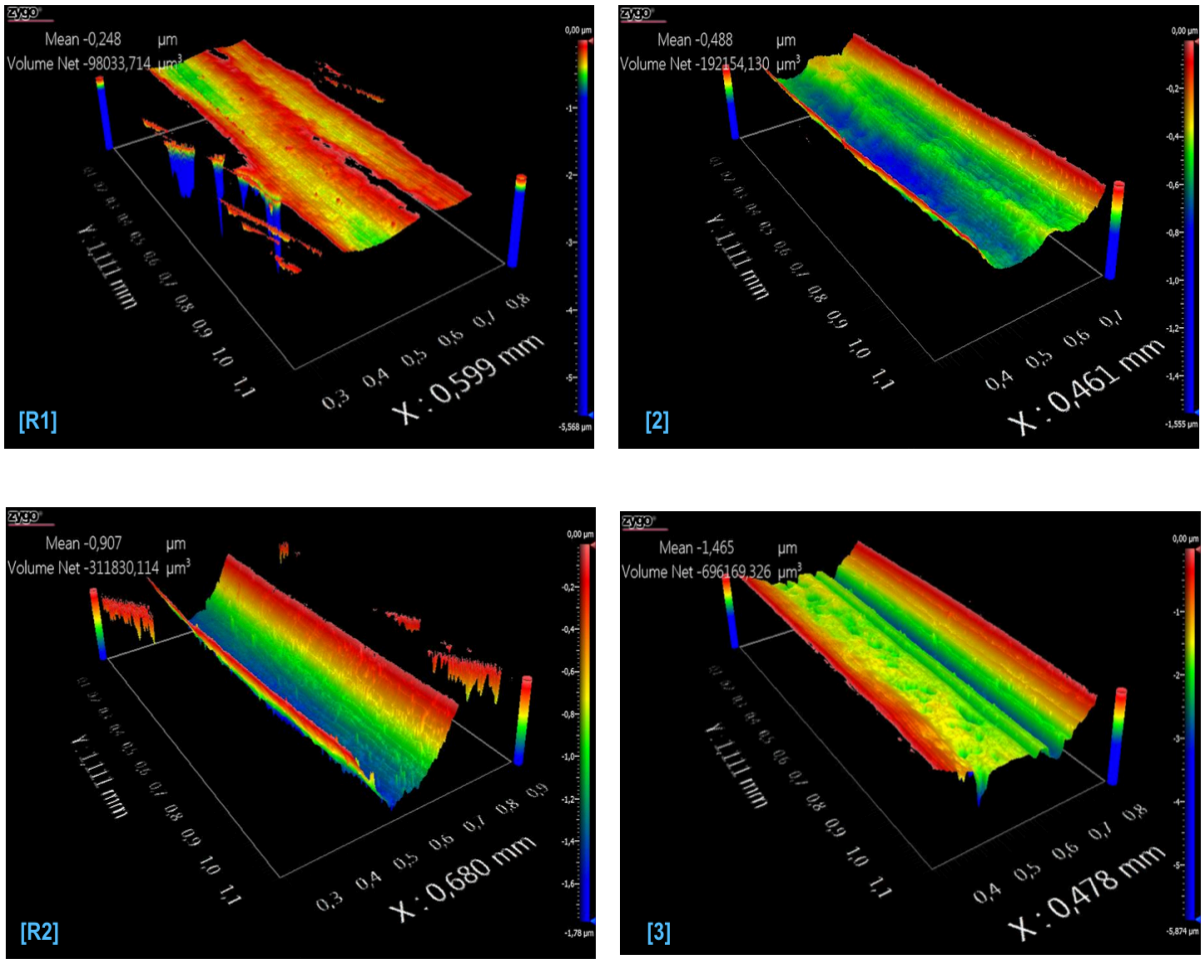

Figure 4.8 Profilometric pictures obtained from the steel plates as a function of the lubricant grease (window sizes of 0.599 mm × 1.111 mm, 0.461 mm × 1.111 mm, 0.680 mm × 1.111 mm, and 0.478 mm × 1.111 mm)

Figure 4.9 shows the apparent friction energy densities (e_R^*) plotted as a function of the wear intensities (I_h) for all the model greases. In this study, Fleischer's wear model was experimentally used to investigate the relationship between friction and wear in a state of mixed friction, where only the wear on the steel plate was taken into consideration. In this sense, the apparent friction energy densities (e_R^*), which describe the amount of friction work required for the separation of the friction-exposed material, and the wear intensities (I_h), which are expressed by the wear depth (h_v) divided by the wear path (i.e., friction distance, s_R), were determined according to Equation (2.11). As in Figure 4.9, there was an inverse relationship between the e_R^* and I_h, indicating that the greases that exhibited the highest friction energy densities caused the lowest wear intensities on the steel plate. For example, reference grease sample R1 showed the highest value of e_R^* and the lowest intensity of wear on the steel plate.

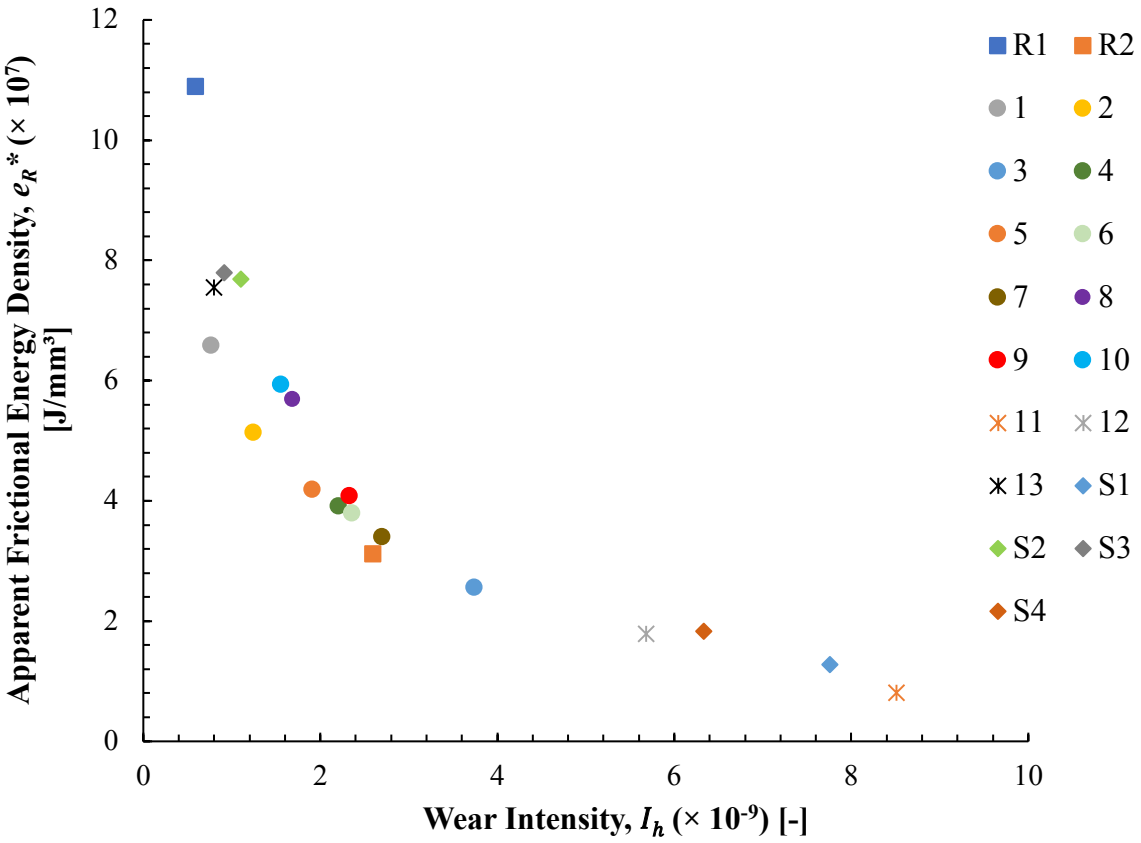

Figure 4.9 Apparent friction energy density (e_R^*) vs. wear intensity (I_h) for all the model greases

For further comprehension, the values of the three associated tribological parameters e_R^*, I_h, and τ_R were plotted on a graph depicting the basic energy equation of wear for the model greases (Figure 4.10). As observed, all the model greases were in the range of 1, indicating that all the lubricating grease experiments in the tribometer were conducted in the quasi-fluid-friction/mixed-friction state, thereby leading to deformation on the steel plates.

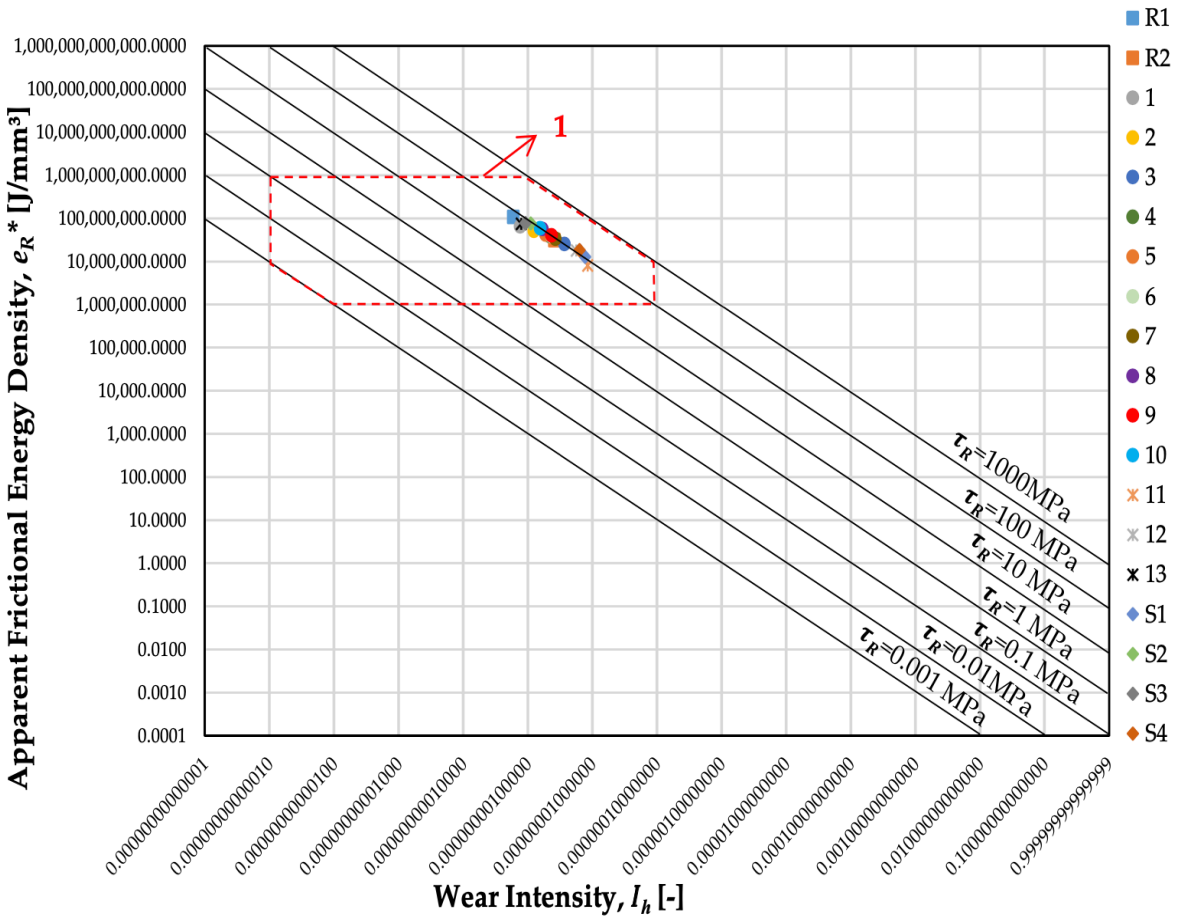

Figure 4.10 Graph of the basic energy equation of wear for all the model greases

Finally, the results of the measured tribological parameters, i.e., e_R^*, I_h, and τ_R, showed that all the model grease samples applied some friction pairings, such as the toothed wheel or rolling bearing, according to a large number of studies looking at different machine elements [4].

4.2.2. Rolling bearings test results

4.2.2.1. Power loss tests

Figure 4.11 shows the value of the rolling bearing friction torque (Mt), which was the average of five replicates for each of the biogenic greases selected. For the rolling bearing tests, model grease samples 1 and 2 were selected since they produced lower friction coefficient values and the smallest wear marks from the ball on the disc tribometer.

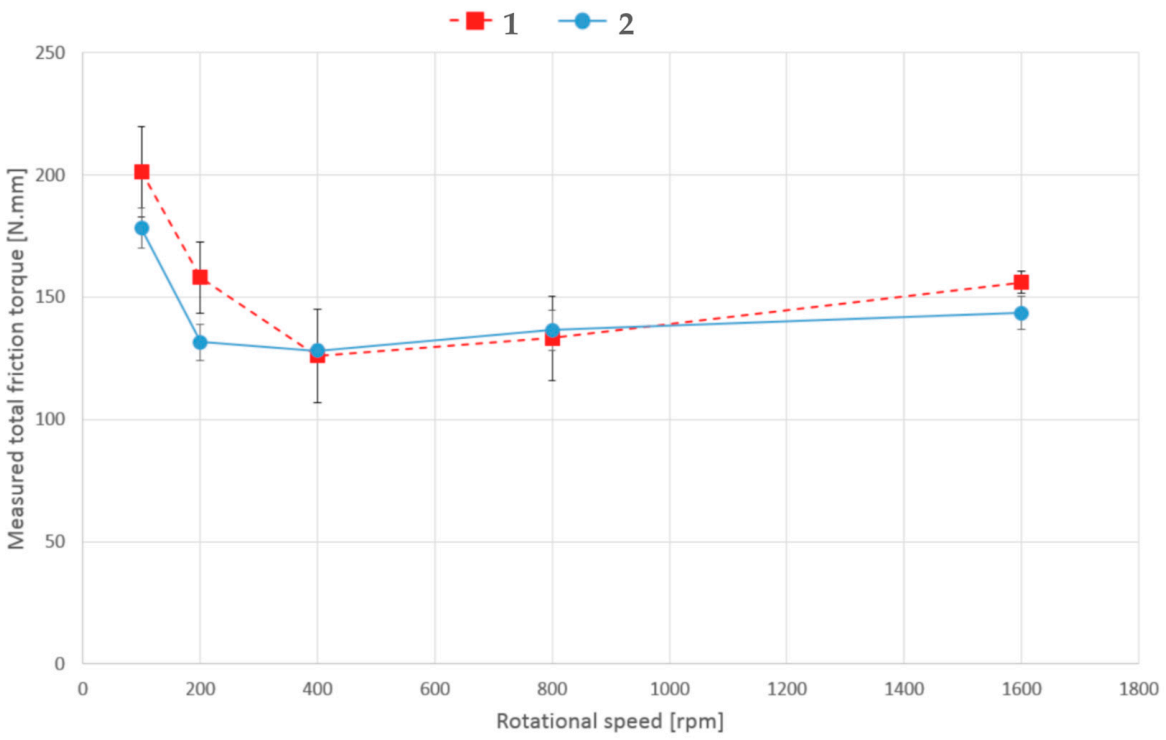

Figure 4.11 TBB friction torque results as a function of the entrainment speed for greases 1 and 2

As expected, the friction torque at very low speeds was high and decreased rapidly as the speed increased and the lubricant film built up. In this low-speed region, the sliding friction torque was dominant due to more frequent interactions of the surface asperities [5,6]. The friction torque then reached a minimum value around 400 rpm for both greases; above that speed, the friction torque started to increase again, albeit only slightly. This increase was due to greater drag losses and increased rolling friction torque [5,7-10].

Moreover, grease 1 showed higher friction torque than grease 2, both at low and high speeds. The differences found at low speeds can be related to the thickener type and oil-bleeding rate, while at high speeds, the differences should mainly be related to the higher base-oil viscosity of grease 1. This approach was supported by data regarding base-oil viscosity and oil-bleeding tests. The base-oil viscosity of each grease was determined at 40 °C and 100 °C according to the ASTM (American Society for Testing and Materials) D341 test (Standard Practice for Viscosity-Temperature Charts for Liquid Petroleum Products). The results showed that although model grease samples 1 and 2 contained the same type of base oil, i.e., a combination of castor oil and HOSO, grease sample 1 had a higher value of base-oil viscosity at 40 °C and 100 °C than model grease 2. In addition to this analysis, the bleed-oil of each grease was extracted using a non-standard dynamic bleeding process, similar to the ASTM D4425 standard

method. The bleed-oil obtained through this non-standard dynamic method showed the same viscosity as the bleed-oil obtained using the static ASTM D6184 method. This dynamic method was used to calculate the oil-bleeding rate of each grease sample. The results showed that the amount was very similar between the two greases, although slightly higher for model grease 2 due to having a lower base-oil viscosity. Finally, grease 2 showed a better wear performance from a power loss perspective.

4.2.2.2. Wear tests

As previously stated, the wear tests were performed under 5 kN, 200 rpm, and at 50 °C over 120 h. During this time, the friction torque was measured 2 h after the start of the test and then at 5, 8, 26, and 120 h, after which the machine was stopped.

The friction torque measured over time is shown in Figure 4.12. In the first hours of operation at 200 rpm, the friction torque was higher due to the grease churning. After approximately 5 h, the friction torque reduced substantially for the rest of the test. The exception was grease 1, which showed a very steep friction torque increase between 26 and 120 h. Either way, grease 1 generally showed a higher friction torque than grease 2.

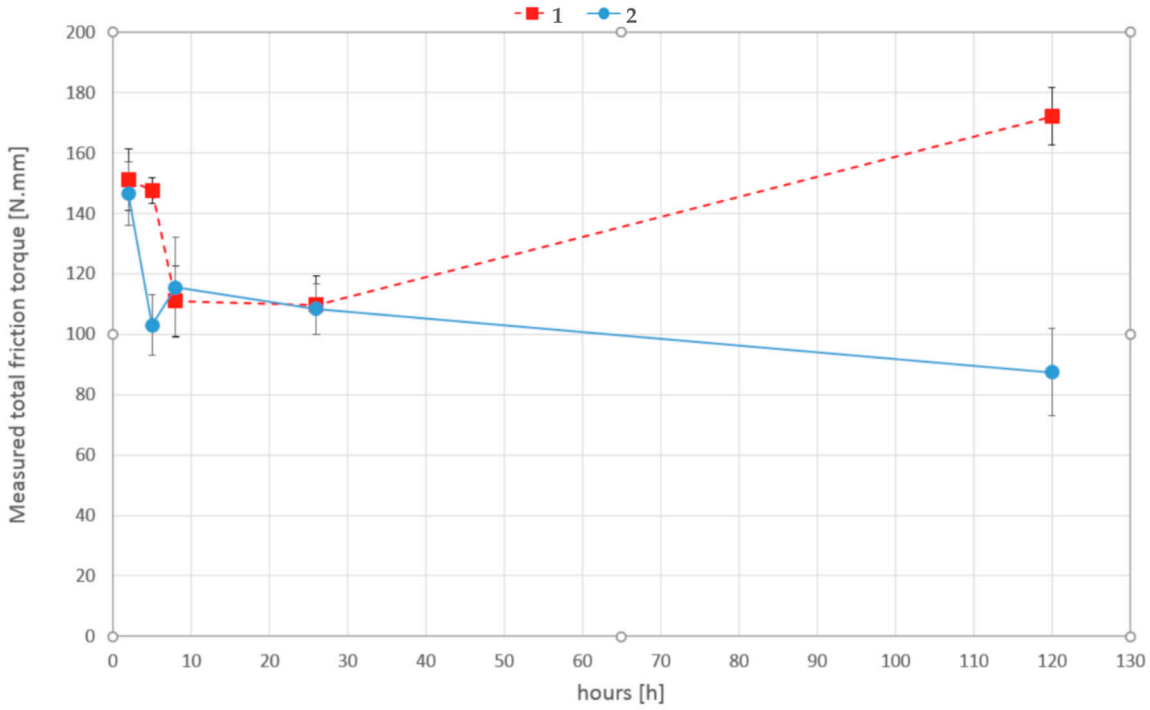

Figure 4.12 TBB friction torque results as a function of the test time for greases 1 and 2

After 120 h, both greases displayed a very dark coloration, particularly between the rolling elements and the raceway, as shown in Figure 4.13. This dark coloration was probably related to the presence of metallic particles originating from the wear process, but also due to some temperature-induced oxidation.

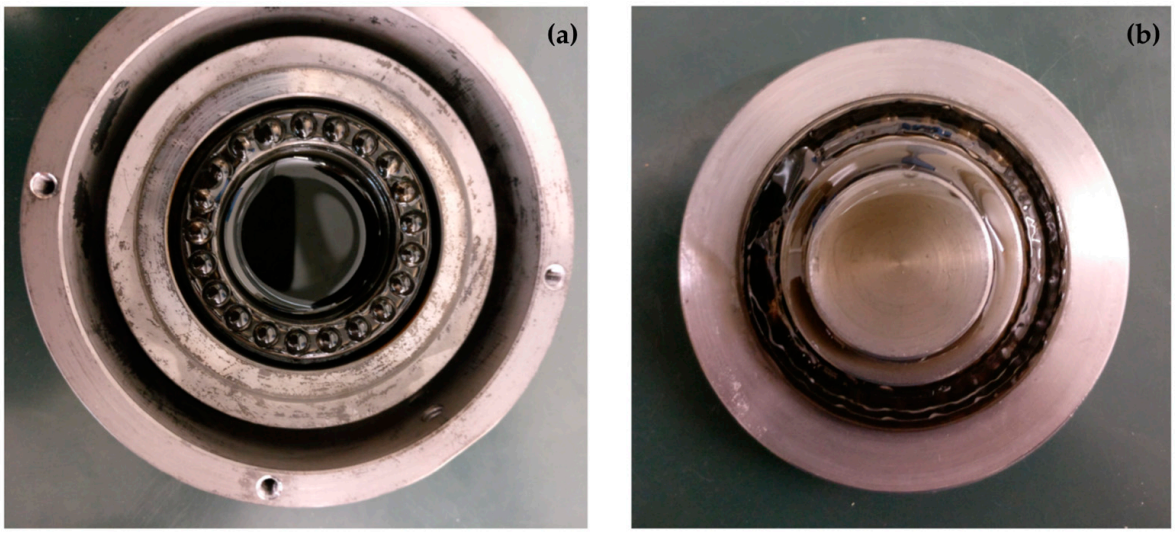

Figure 4.13 Remaining grease on (a) the rolling bearing house, lower raceway, and cage, and (b) the upper raceway shaft

Finally, a sample of each grease was collected at the end of the power loss tests and wear tests for particle analysis. The ferrometry and ferrography analysis results are shown in Table 4.1. The indexes of small (DS, smaller than 1–2 μm) and large particles (DL, larger than 5 μm) refer to the concentration and size of particles found in a given sample of grease (100 mg diluted with 20 mL of an adequate solvent), collected after the power loss and wear tests. The particle concentration index (CPUC) and the severity of wear index (ISUC) can be estimated from DS and DL follows:

$$\text{Particle Concentration Index (CPUC)} = DS + DL \tag{4.1}$$

$$\text{Severity of Wear Index (ISUC)} = DL^2 - DS^2 \tag{4.2}$$

Table 4.1 Ferrometry and ferrography results of the power loss and wear tests

Identification	**Power Loss Tests**		**Wear Tests**	
Sample	1	2	1	2
Bearing Load (kN)	5	5	5	5
Number of cycles	250–300k	250–300k	1440k	1440k
Ferrometry				
Large Particles Index (DL)	67.7	17.7	86.0	57.1
Small Particles Index (DS)	17.7	5.1	30.7	17.7
Particle Concentration Index (CPUC)	85.4	22.8	116.7	74.8
Severity of Wear Index (ISUC)	4270.0	287.3	6453.5	2947.1
Ferrography				
Normal Wear	Strong	Medium	Strong	Strong
Severe Wear	Strong	Strong	Medium	Medium
Fatigue Wear Particles	Medium	Medium	Medium	Medium
Adhesion Wear Particles	Fair	Fair	Fair	Fair
Friction Polymers	Fair	Fair	Fair	Fair
Black Oxides	Medium	Fair	Strong	Strong

Based on these indexes and the ferrography analysis, a classification may be established according to wear severity, presence of fatigue or adhesion wear particles, and the presence of friction polymers and black oxides. More details regarding these procedures can be found elsewhere [11-13]. According to the results of the power loss tests, grease 1 showed more severe wear with a higher particle concentration index (CPUC) and severity of wear index (ISUC), suggesting once again that grease 2 performed better. Moreover, as seen in this table, the results of the wear tests were considerably higher than the results obtained for the power loss tests.

4.3. Study on the shear-induced structural degradation of lubricating greases and associated activation energy

4.3.1. Frictional energy density and activation energy determined from rotational transient flow tests

Figure 4.14 shows selected transient flow curves obtained at 25 °C for six traditional grease samples. As can be seen, the shear stress decreases continuously with the time at a constant shear rate of 1000 s^{-1}, reflecting the shear-induced structural degradation of the greases discussed in sections 2.4.5 and 2.6 of chapter 2. The rheological energy densities (e_{rheo}) were determined by integrating the shear stress over time between t_{max} and t_{lim} according to Equation (2.16), for all of the examined grease samples and testing temperatures (25 °C, 40 °C, 55 °C, and 70 °C). The calculated values of e_{rheo} for the investigated greases are listed in Table 4.2.

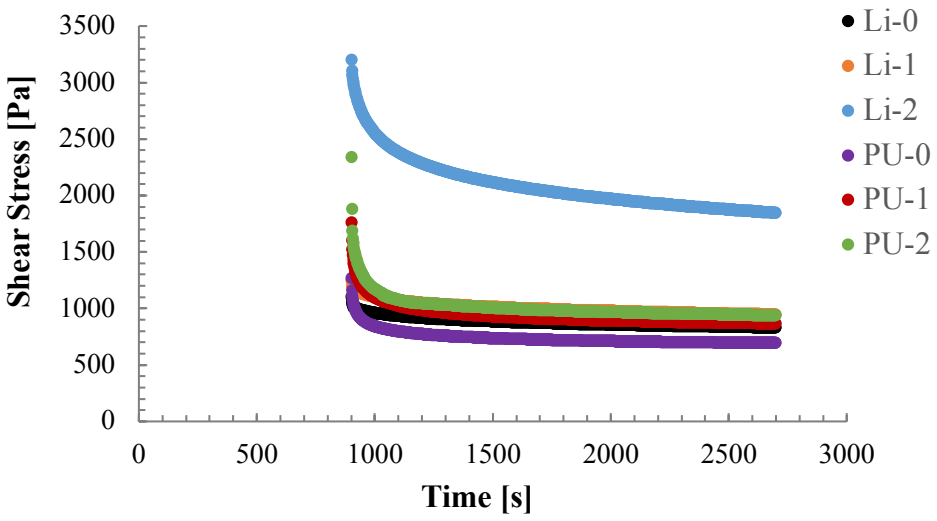

Figure 4.14 Transient flow curves for the model grease samples at 25 °C (applied shear rate: 1000 s^{-1})

Table 4.2 Energy density (e_{rheo}) values determined by integration of the shear stress over time at 25 °C, 40 °C, 55 °C, and 70 °C

Temperature	Energy density (e_{rheo}) [J/m³]					
[°C]	Li-0	Li-1	Li-2	PU-0	PU-1	PU-2
25	1.60E+09	1.83E+09	3.87E+09	1.38E+09	1.75E+09	1.88E+09
40	1.02E+09	1.15E+09	2.75E+09	7.47E+08	9.34E+08	1.45E+09
55	6.81E+08	7.97E+08	2.11E+09	4.24E+08	5.48E+08	8.43E+08
70	3.93E+08	4.78E+08	1.58E+09	2.74E+08	3.48E+08	5.47E+08

These results show that the energy expenditure during the fluid frictional process strongly depends on the nature and concentration of the thickener and the temperature applied during the transient flow tests. As expected, the energy density (e_{rheo}), i.e. the energy expenditure per stressed grease volume, increased with increasing thickener content at any applied temperature. This is a result of the higher viscosity, i.e. higher internal fluid friction, that occurs with a higher concentration of thickener particles. On the other hand, the lithium greases always had higher e_{rheo} values than the polyurea greases for the same NLGI degree; this is especially dramatic in the case of sample Li-2, despite the lower thickener concentration required. This result indicates that the grease microstructure plays an important role in the friction process. For a better understanding of the influence of the grease structure on the tribological behaviour, the microstructure of Li-2 and PU-2 grease was examined using AFM as can be seen in Figure 4.15. Figure 4.15 shows the microstructures of samples Li-2 and PU-2, revealing that the shape of the thickener particles is clearly different in the two samples. Lithium grease, which is composed of long and twisted fibres and fibre agglomerates, provides a higher energy density compared to polyurea grease, which contains smaller and more uniform thickener agglomerates in the form of small fibrils and/or platelets. This means that the thickener microstructure noticeably influences the energy expenditure, i.e. the rheological behaviour of the lubricating greases [14] during the transient flow test.

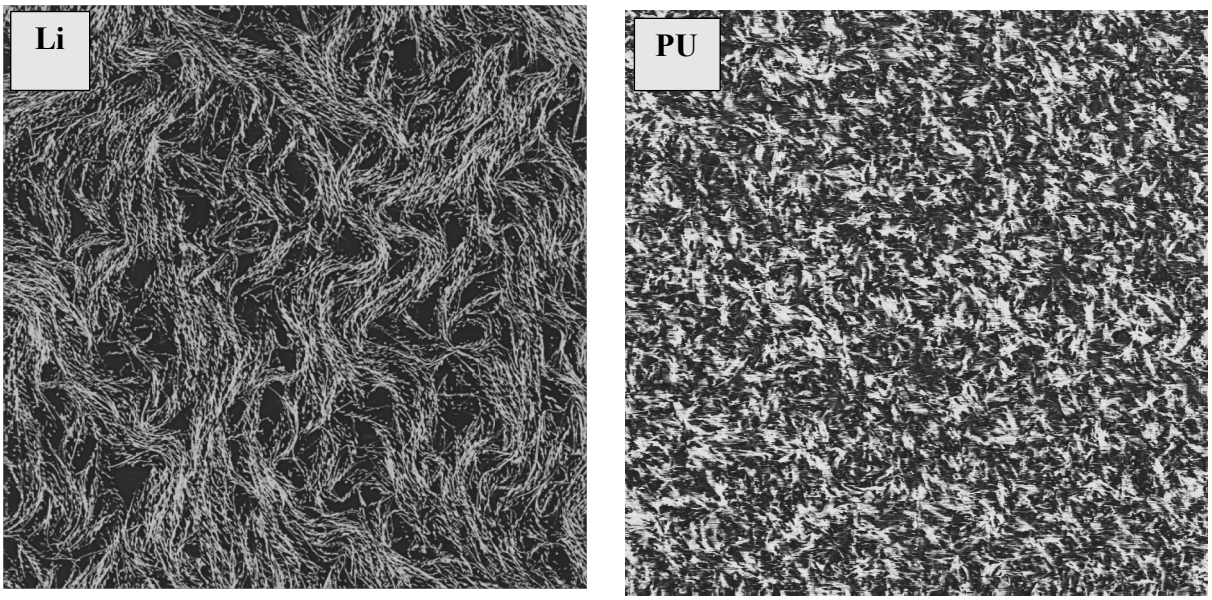

Figure 4.15 Atomic Force Microscopy (AFM) micrographs of Li-2 and PU-2 samples (window size: 20 μm x 20 μm)

The energy density (e_{rheo}) also decreased with increasing temperature, which reflects the softening of the greases due to the decrease in inter-particle interactions. This temperature-dependent behaviour of the energy density can be described fairly well by the Arrhenius equation (Eq. (2.18)), as shown by the plot of the logarithm of the rheological energy density versus the reciprocal of the temperature in Figure 4.16. Figure 4.16 shows that the slope of the lines, viz. E_a/R, decreases as the amount of thickener in the grease structure increases, following the same tendency previously observed Arrhenius plots of the viscosity vs. temperature [15].

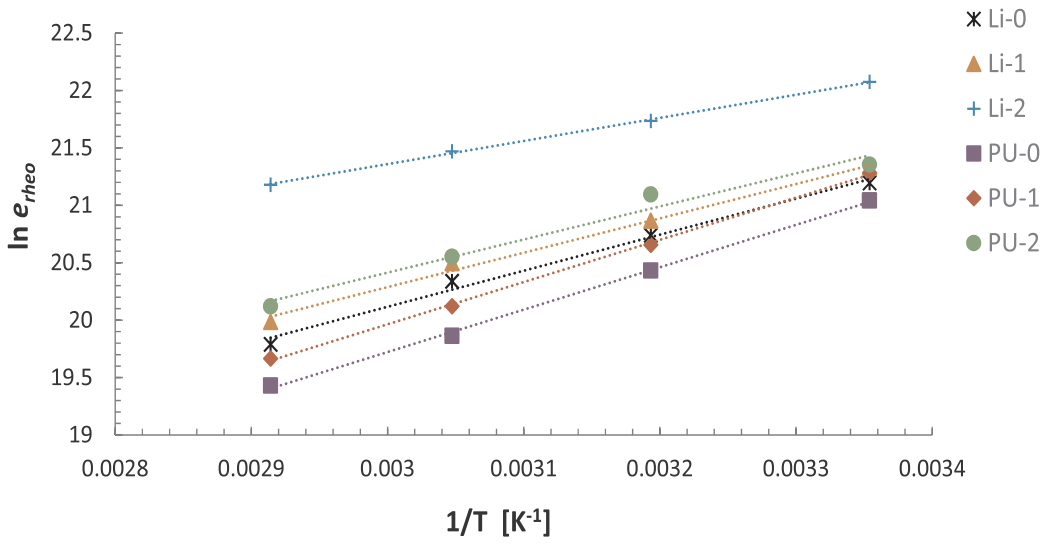

Figure 4.16 Evolution of the energy densities with temperature for all model greases; the Arrhenius fitting is indicated by the dashed lines

Figure 4.17. shows the values of E_a obtained from fitting Equation (2.18) for all of the model grease samples. The value of E_a is characteristic for each grease sample, and represents the energy required to achieve a certain shear-induced structural degradation (frictional degradation). As can be seen in Figure 4.17, the values of E_a decrease with increasing thickener concentration, which can be explained by considering the effect of inter-particle interactions (i.e. van der Waals forces). These physical interactions are responsible for the connection between the structural units that determines the architecture of the grease structural skeleton, and thus need to be overcome for any structural degradation to occur. Logically, there will be more interactions among particles with increasing thickener concentration; however, the resulting network is also more sensitive to shear. Bauer et al. [15] explained this effect by considering that van der Waals forces at the fibre contacts, which provide the main barrier to flow, should be weaker than those acting between oil molecules; hence, it is to be expected that higher thickener concentrations will lead to lower activation energies. Overall, this reflects the

sensitivity of the energy density to temperature. In other words, if the E_a of a grease sample is high for a given temperature range, e_{rheo} will be highly sensitive to changes in temperature, which generally occurs in more concentrated greases. For a better understanding of this phenomenon, E_a was plotted versus Δe_{rheo}, which is the percentage change in the energy density from 25 °C to 70 °C, as shown in Figure 4.17 for the model grease samples.

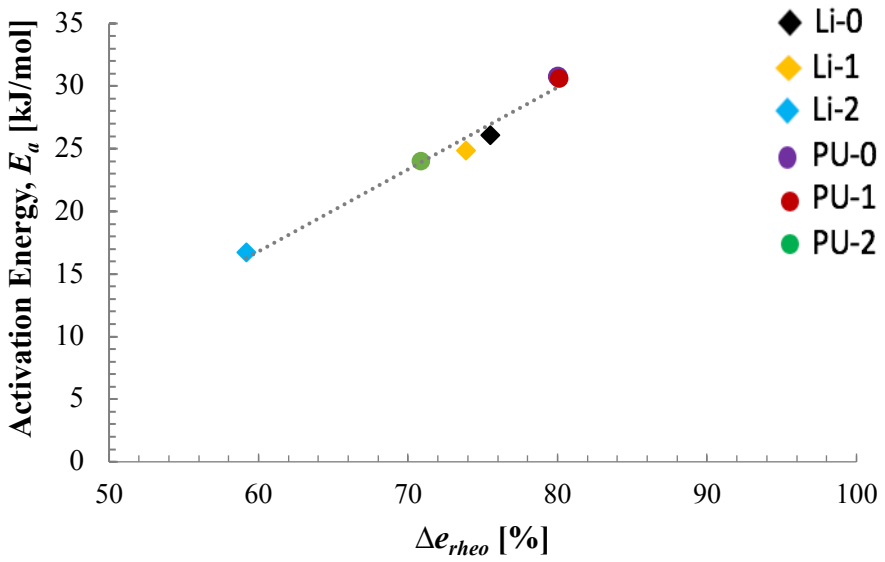

Figure 4.17 Activation energy (E_a) vs. the percentage change in the energy density (Δe_{rheo}) from 25 °C to 70 °C for the model grease samples

4.3.2. Relationship between the activation energy and structural degradation of greases in amplitude sweep tests

It has been established that the grease microstructure remains almost unperturbed in the LVE [16,17], and structural degradation occurs once the critical deformation at the limit of the LVE has been reached. Therefore, this critical point (see Figure 2.13) can be considered the onset point for quantifying any significant structural degradation in a given grease sample. In this sense, it is interesting to evaluate any possible correlation between the activation energy and the rheological response of greases at or just beyond the limit of the LVE regime. The values of the critical deformation, $\gamma_{critical}$ (%), at this critical point were determined for Li- and PU-grease samples by a change in G' or G'' of more than 10% from the LVE-plateau values, as recommended in DIN 51810-2 [18]. In addition, the values of the critical deformation, $\gamma_{critical}$ (%), can be estimated from $\tau - \gamma$ plots as the last point following a linear trend between both magnitudes. The slope in the $\tau - \gamma$ diagram corresponds to the complex viscoelastic modulus, G^*, which can be decomposed into elastic and viscous components (G' and G'', respectively),

and remains constant within the LVE, identically to those viscoelastic moduli (see Figure 2.13). As long as the ratio of the shear stress, τ, to the deformation, γ, is constant, the slope of the $\tau-\gamma$ diagram can be used to determine the limit of the LVE range, at which the grease sample is deformed without undergoing significant structural changes [19]. Once the $\tau-\gamma$ plot deviates from linearity, significant changes in the material structure of the grease begin to occur [19].

According to the experimental critical deformation values presented in Figure 4.18, the Li-grease samples reached the LVE limit at lower deformation values than the PU-grease samples. This indicates that the structural degradation occurs earlier, i.e. at lower deformations, in the Li-grease samples, which generally also had lower activation energies compared to the PU-greases. In addition, $\gamma_{critical}$ decreases with increasing thickener content. Figure 4.19 illustrates how the activation energy and critical deformation, $\gamma_{critical}$, follow a roughly linear trend. Thus, in general terms, the greases with low activation energies exhibited lower critical deformation values, although the chemical nature of the thickener and the type of structural network may influence this relationship. In this sense, further experimental work should be carried out with a wider spectrum of greases containing thickeners of different natures. However, in general, assuming that the activation energy is the required energy that must be overcome to produce shear-induced structural degradation, it would be expected that the degradation process for a grease with a low activation energy will begin earlier than that of a grease with a high activation energy. For example, the structural degradation of Li-2 grease due to the shearing process begins at a much lower deformation value than that of PU-0 grease as a result of the significantly lower activation energy of the Li-2 grease.

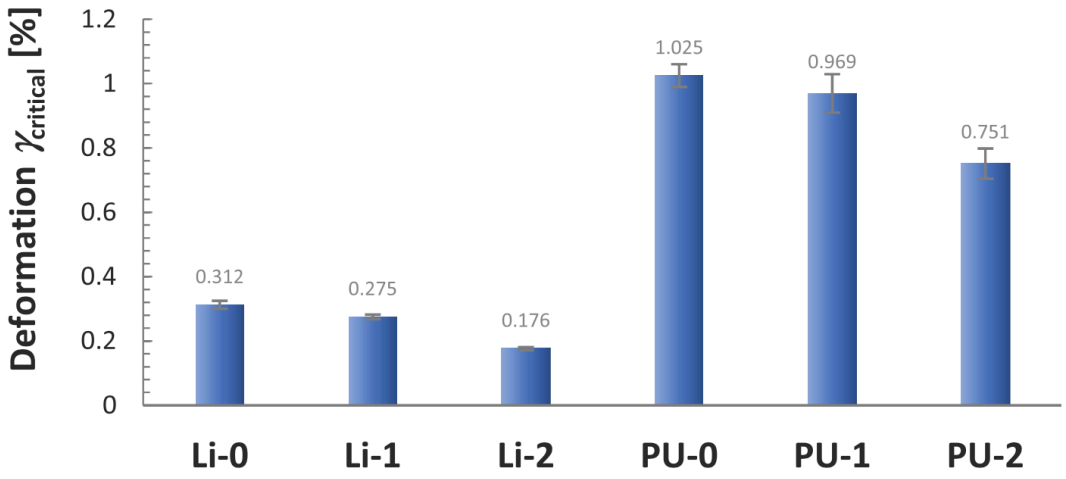

Figure 4.18 Deformation ($\gamma_{critical}$, %) for the model greases; the values were determined at the critical point

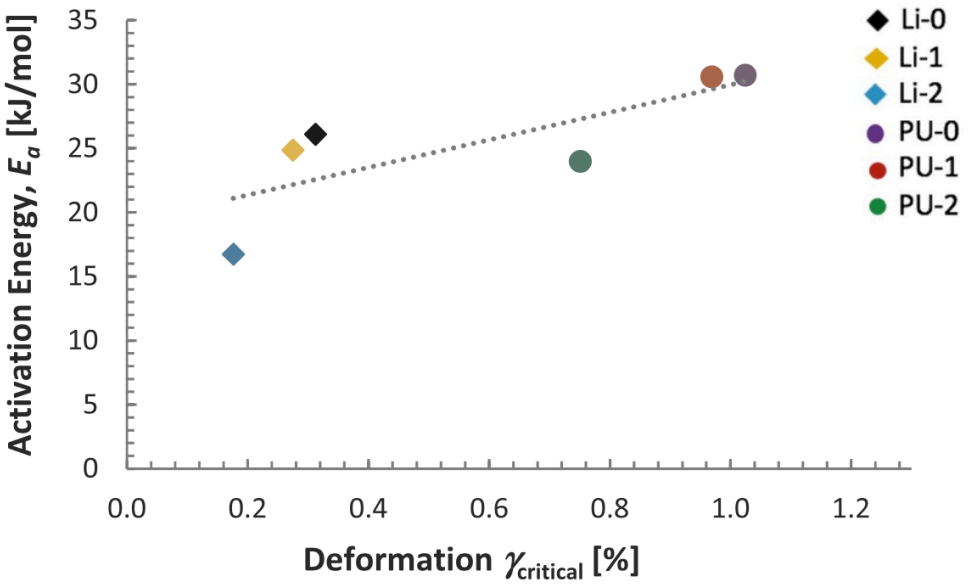

Figure 4.19 Critical deformation ($\gamma_{critical}$, %) vs. activation energy for the model greases

As previously mentioned, beyond the LVE range, the crossover point between G' and G'' is assumed to be the point at which greases begin to flow. In fact, the yield stress of greases has been frequently estimated from oscillatory amplitude sweep tests at this point [20]. The associated energy expenditure due to the internal friction in this early stage of structural degradation can be calculated in terms of the energy density using Equation (2.6). The calculated energy density values for the model greases are shown in Figure 4.20. As Figure 4.20 shows, there is an inverse linear relationship between E_a and $e_{rheo\text{-}cross}$.

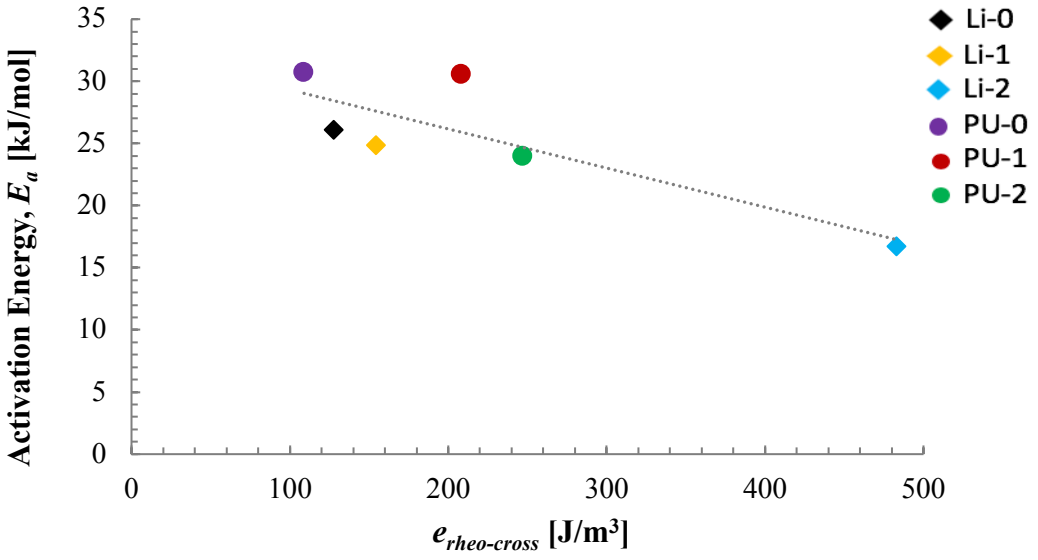

Figure 4.20 Activation energies (E_a) versus rheological energy densities ($e_{rheo\text{-}cross}$) at the crossover point from the amplitude sweep tests

Other important parameters in this early stage of shear-induced structural degradation are the values of G' and G'' both at the limit of the LVE range, i.e. at the critical point, and at the crossover point. These values are listed in Table 4.3. For example, in Figure 2.13, the G' values are greater than the G'' values in the LVE regime for all of the model greases, reflecting a typical solid-like viscoelastic response. Moreover, it is well-known that an increase in thickener concentration, which produces a more compact and/or entangled microstructural network, will lead to an increase in the values of both viscoelastic moduli in the LVE regime, and also at the crossover point [21,22]. The initial structural degradation beyond the LVE range results in a change in both moduli, and this change is more dramatic for G'. Figure 4.21 shows the activation energies plotted as a function of the increment in the storage modulus ($\Delta G'$, %) from the critical point to the crossover point for the model greases. It can be seen that similar to Figure 4.20, there is an inverse linear correlation between the activation energy and $\Delta G'$. This indicates that the change observed in G' from the critical point to the crossover point increases with decreasing activation energy. Again, if the activation energy is interpreted as the energy level that must be overcome to produce structural degradation in the grease, it is reasonable to expect that the degradation process at the crossover point would be more important for greases with low activation energies. In addition, if a gradual breakdown of grease structure leads to decreasing G' values beyond the LVE region [23], higher increments in G' would indicate more shear-sensitive structural networks under these conditions.

Table 4.3 Values of the storage modulus (G') and loss modulus (G") at the critical point and values of $G' = G''$ at the crossover point for the model greases

Grease Sample	G' [Pa]	G'' [Pa]	$G' = G''$ [Pa]
Li-0	4104.6	663.42	308.75
Li-1	4949	770.15	350.17
Li-2	24781	3656.9	891.77
PU-0	3851.1	515.42	309.51
PU-1	6194.1	747.39	437.53
PU-2	11762	1463.4	752.54

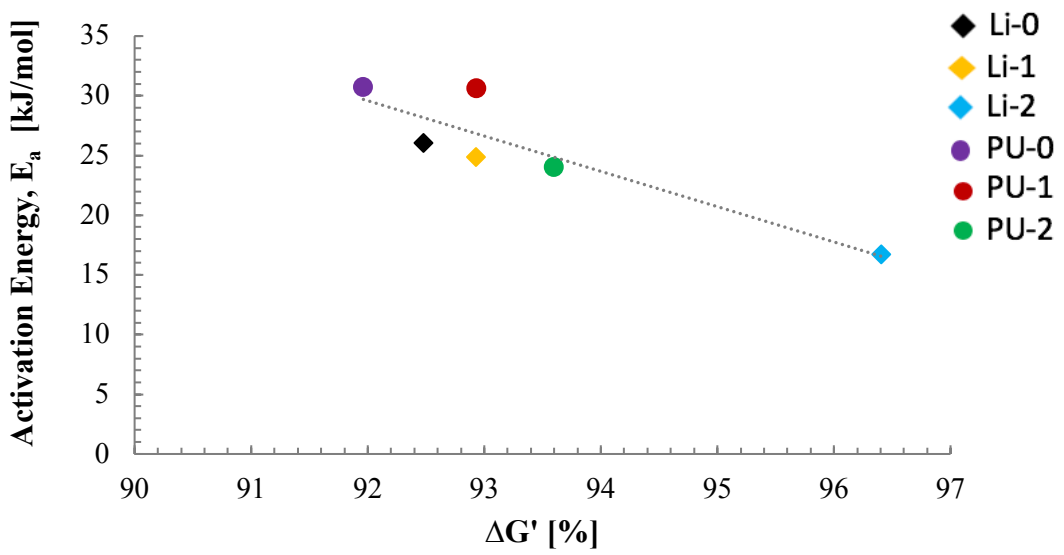

Figure 4.21 Activation energy versus the increment in the storage modulus (ΔG') from the critical point to the crossover point for all model greases

4.4. References

1. Sánchez, R.; Franco, J.M.; Kuhn, E.; Fiedler, M. Tribological characterization of green lubricating greases formulated with castor oil and different biogenic thickener agents: a comparative experimental study. *Industrial Lubrication and Tribology*, 2011, 63, 446–452.
2. Sánchez, R.; Franco, J.M.; Delgado, M.A.; Valencia, C.; Gallegos, C. Effect of thermo-mechanical processing on the rheology of oleogels potentially applicable as biodegradable lubricating greases. *Chemical Engineering Research and Design*, 2008, 86, 1073–1082.
3. Slabka, I. Rheologische Charakterisierung biogener Modellfette. *Master Thesis*, Hamburg University of Applied Sciences, Hamburg, Germany, 2017.
4. Fleischer, G.; Gröger, H.; Thum, H. Verschleiß und Zuverlässigkeit. *VEB Verlag Technik*, Berlin, Germany, 1980.
5. SKF. Evolution online and G Morales-Espejel. Using a friction model as an engineering tool. *Evolution Technology Magazine from SKF*, 2006, 2, 27–30.
6. SKF. SKF General Catalogue; *SKF*: Schweinfurt, Germany, 2003.
7. Cousseau, T.; Graça, B.; Campos, A.; Seabra, J. Experimental measuring procedure for the friction torque in rolling bearings. *Lubrication Science*, 2010, 22, 133–147.
8. Cousseau, T.; Graça, B.; Campos, A.; Seabra, J. Friction torque in grease lubricated thrust ball bearings. *Tribology International*, 2011, 44, 523–531.
9. Gonçalves, D.; Cousseau, T.; Gama, A.; Campos, A.V.; Seabra, J.H.O. Friction torque in thrust roller bearings lubricated with greases, their base oils and bleed-oils. *Tribology International*, 2017, 107, 306–319.
10. Gonçalves, D.; Pinho, S.; Graça, B.; Campos, A.V.; Seabra, J.H.O. Friction torque in thrust ball bearings lubricated with polymer greases of different thickener content. *Tribology International*, 2016, 96, 87–96.
11. Available online: http://www.plus-sci.co.kr/image/ana/predict-dli/pdf/ferrography_overview.pdf (accessed on 20.12.2019).
12. Available online: https://pdfs.semanticscholar.org/17d4/b8224be1a7df01929af300874e6f5017f18c.pdf (accessed on 20.12.2019).
13. Available online: https://wearcheck.com/virtual_directories/Literature/Techdoc/WCA001.htm (accessed on 20.12.2019).

14. Delgado, M.A.; Secouard, S.; Valencia, C.; Franco, J.M. On the steady-state flow and yielding behaviour of lubricating greases. *Fluid*, 2019, 4, 6.

15. Bauer, W.H.; Finkelstein, A.P.; Wiberley, S.E. Flow properties of lithium stearate-oil model greases as functions of soap concentration and temperature. *ASLE Trans*, 1960, 3, 215–224.

16. Delgado, M.A.; Franco, J.M.; Kuhn, E. Effect of rheological behaviour of lithium greases on the friction process. *Industrial Lubrication and Tribology*, 2008, 60, 37–45.

17. Balan, C.; Franco, J.M. Influence of the geometry on the transient and steady flow of lubricating greases. *Tribology Transactions*, 2001, 44, 53–58.

18. DIN 51810-2. Testing of lubricants - testing rheological properties of lubricating greases – part2: determination of flow point using an oscillatory rheometer with a parallel-plate measuring system. 2011, 04.

19. Sorgatz, C. Physikalische charakterisierung von überzugsmaterialien in der lebensmittelindustrie. *PhD Thesis*. Germany Technische Universität München, 2011.

20. Cyriac, F.; Lugt, P.M.; Bosman, R. On a new method to determine the yield stress in lubricating grease. *Tribology Transactions*, 2015, 58, 1021–1030.

21. Martin-Alfonso, J.E.; Valencia, C.; Sánchez, M.C.; Franco, J.M.; Gallegos, C. Development of new lubricating grease formulations using recycled LDPE as rheology modifier additive. *European Polymer Journal*, 2007, 43, 139 – 149.

22. Delgado, M.; Valencia, C.; Sánchez, M.; Franco, J.; Gallegos, C. Influence of soap concentration and oil viscosity on the rheology and microstructure of lubricating greases. *Industrial and Engineering Chemistry Research*, 2006, 45, 1902–1910.

23. Kuhn, E. Energetic investigations of the structural degradation of lubricating greases caused by friction. *5th World Tribology Congress*, Turin, Italy, 2013.

Chapter 5

Conclusions

5.1. Conclusions

The experimental research comprising this PhD has allowed to investigate the tribological and rheological behaviour of a variety of traditional and biogenic model lubricating greases.

Several bio-sourced materials were used as thickener agents to formulate complete biogenic lubricating greases. These samples were tribologically investigated in a nanotribometer and in a rheometer, and compared with traditional lithium-12-hydroxystearate/HOSO and lithium-calcium soap/synthetic ester greases. In addition, the structural degradation six traditional greases of different NLGI grade based on lithium soap and polyurea thickeners were investigated from an energetic point view. The following general conclusions can be derived from this work:

- Results obtained from nanotribometer tests showed a distinctive influence of the components of completely biogenic model greases on the frictional and wear behaviour. In almost all cases, the use of biodegradable model greases produced lower values of the friction coefficient than the reference greases. The model greases containing glyceryl and sorbitan monostearates as thickener agents, and the combination of HOSO and castor oil as base oil, generally yielded the lowest values of the friction coefficient no matter the test conditions. The reference greases produced much higher values of the wear volume on the steel plate despite exhibiting only slightly higher friction coefficient values than the model greases. Moreover, the use of biogenic greases based on only castor oil as the base oil exhibited the lowest wear volume on the steel plate; however, these biogenic greases provided higher frictional coefficients (especially at relative speed of 40 $mm \cdot s^{-1}$), compared with biogenic greases consisting of HOSO or a combination of HOSO and castor oil.
- To investigate the fluid friction behaviour of the biodegradable model greases and to quantify the rheological energy density upon shearing the grease, transient flow tests were performed at different temperatures. The estimation of the energy density from the shear stress versus time curve revealed that the amount of energy expenditure per stressed volume (e_{rheo}) strongly depends on the test temperature. In this sense, the rheological energy density (e_{rheo}) generally decreased by increasing the test temperature. However, the opposite tendency was found for some model biogenic greases. These results can be explained by the thickener microstructure and the thickener/base oil interactions. Weak physical interactions like those expected between the base oil and cellulosic thickeners may also favor oil separation (oil bleeding) at high temperatures, resulting in higher viscosity and therefore higher energy density. The biogenic grease samples consisting of a combination

of HOSO and castor oil as the base oil and glyceryl and/or sorbitan monostearates as thickener yielded the lowest energy expenditure at 25 °C and 40 °C. Moreover, biogenic model greases based on lignosulfonate or chemically-modified lignin as thickener agents provided less energy expenditure than biogenic model greases based on isoprene derivatives, natural cellulose fibers, or natural wood pulp from softwood, the latter also provided higher values of the energy expenditure by friction process compared with the reference greases.

- A correlation between the rheological energy density (e_{rheo}) and the friction coefficient can be inferred for some model greases. Biogenic greases with less energy expenditure during the flow process, such as grease samples 1, 2, and S4 showed low values of the friction coefficient. In addition to this, semi-biogenic greases (reference greases), which showed the highest values of the friction coefficient, exhibited high energy density values compared with most of the biogenic greases studied.
- According to results obtained from the ball-on disc tribometer, a linear relationship was observed between the friction coefficient and the wear data for most of the examined model grease samples. This result revealed that the lower the friction coefficient was, the lower the wear volume that occurred on the steel plate due to the friction process. Moreover, the composition of model greases highly influenced the frictional and wear behaviours. Using Fleischer's energetic wear model, the apparent friction energy density (e_R^*), the intensity of wear (I_h), and the friction shear stress (τ_R) for all the model greases were experimentally estimated and the relationship between these tribological parameters was elucidated. Plotting these three associated tribological parameters on the Fleischer's graph of the basic energy equation of wear for the model greases allowed for the determination of the friction and wear states the experiments were conducted in, which was a combination of fluid friction and mixed friction for all the grease samples. In addition, the estimation of the apparent friction energy density revealed that the grease-lubricated contacts with high friction energy densities led to lower wear intensities on the steel plate.
- In order to assess the tribological behaviour of the biogenic greases in real machine elements, rolling bearing power loss and rolling bearing wear tests were carried out using two selected biogenic grease samples. Results from the power loss tests showed that model grease 2, which had a lower base-oil viscosity, provided smaller friction torque values than model grease 1 under the operating conditions of the experiment. Comparing the tested greases, model grease 2 showed a better overall performance, a slightly lower internal

torque loss, and less wear particle generation even though both model greases were similar in composition, with sample 2 containing sorbitan monostearate instead of beeswax in the thickener blend. Regarding the wear tests, similar conclusions were found, i.e., higher friction torque was associated with greater wear. Model grease 1 exhibited higher wear indexes and showed worse performance than model grease 2. Moreover, both grease samples showed very dark coloration after the test, and a considerable number of wear particles were found, some of them with large dimensions.

- The rheological energy density of six traditional grease samples was experimentally estimated through transient flow tests conducted at a constant shear rate of 1000 s^{-1} and varying temperatures. The rheological energy density decreased linearly with increasing temperature as a result of the softening of the grease microstructure, following an Arrhenius-type evolution. The fitting of the energy density data to the Arrhenius equation allowed the activation energy to be calculated; the activation energy was interpreted as the required energy level that needs to be overcome to produce shear-induced structural degradation in the grease. This characteristic activation energy for each lubricating grease depends on the nature and concentration of the thickener used. For a particular thickener, the higher the thickener concentration, the lower the activation energy. This phenomenon can be explained by considering a more shear-sensitive structural network with increasing thickener concentration. Therefore, the activation energy decreases as the amount of fibre contacts increases. Moreover, for the same grease consistency (NLGI degree), the activation energy of lithium greases is lower than that of polyurea greases.

- The activation energy was correlated with some rheological parameters of the greases at or just beyond the limit of the LVE regime, i.e. at the early stages of shear-induced structural degradation, as determined by small-amplitude oscillatory shear tests. The value of critical deformation ($\gamma_{critical}$) is proportional to the activation energy. This result reveals that the lower the activation energy, the earlier the structural degradation of greases due to the shearing process. The activation energy was also correlated with some rheological parameters at the crossover point between G' and G'' beyond the LVE range, which is assumed to be the point at which greases start to flow. An inverse linear relationship was observed between the activation energy and the energy density associated with the internal friction at this crossover point. Moreover, the same inverse linear relationship was observed between the activation energy and the decrease in the storage modulus ($\Delta G'$) from the critical point delimiting the LVE range to the crossover point. This suggests that greases with lower activation energies are more sensitive to structural degradation under low

deformation conditions, i.e. just beyond the LVE range, resulting in higher frictional energy expenditure.

5.2. Conclusiones

El trabajo experimental que se recoge en esta Tesis Doctoral ha permitido investigar el comportamiento tribológico y reológico de una variedad de grasas lubricantes modelo, tradicionales y biogénicas.

Se utilizaron diferentes compuestos de origen natural como agentes espesantes para formular completamente grasas lubricantes biogénicas. Estas muestras se investigaron tribológicamente en un nanotribómetro y en un reómetro, y se compararon con grasas tradicionales de litio-12-hidroxiestearato/HOSO y de jabón de litio-calcio/éster sintético. Además, se investigó la degradación estructural de seis grasas tradicionales de diferente grado NLGI espesadas con jabón de litio y poliurea, desde un punto de vista energético. De este trabajo se derivan las siguientes conclusiones generales:

- Los resultados obtenidos en el nanotribómetro mostraron una influencia diferenciada de los componentes de las grasas modelo biogénicas sobre el comportamiento de fricción y desgaste. En casi todos los casos, el uso de grasas modelo biogénicas produjo valores más bajos del coeficiente de fricción que las grasas de referencia. Las grasas modelo que contenían monoestearatos de glicerilo y sorbitano como agentes espesantes, y la combinación de HOSO y aceite de ricino como aceite base, produjeron en general los valores más bajos del coeficiente de fricción, independientemente de las condiciones de ensayo. Las grasas de referencia produjeron valores mucho más altos del volumen de desgaste en las placas de acero, a pesar de presentar valores del coeficiente de fricción sólo ligeramente superiores a los de las grasas biogénicas. Además, el uso de grasas biogénicas basadas únicamente en aceite de ricino como aceite base mostró el menor volumen de desgaste en las placa de acero. Sin embargo, estas grasas biogénicas proporcionaron coeficientes de fricción más altos (especialmente a una velocidad relativa de 40 $mm \cdot s^{-1}$), en comparación con las grasas biogénicas compuestas por HOSO o una combinación de HOSO y aceite de ricino.
- Para investigar el comportamiento de fricción de las grasas modelo biodegradables y para cuantificar la densidad de energía reológica al cizallar la grasa, se realizaron ensayos de flujo transitorio a diferentes temperaturas. La estimación de la densidad de energía a partir

de la curva del esfuerzo frente al tiempo de cizalla reveló que la cantidad de energía disipada por unidad de volumen estresado (e_{rheo}) depende en gran medida de la temperatura. En este sentido, la densidad de energía reológica (e_{rheo}) disminuye generalmente al aumentar la temperatura de ensayo. Sin embargo, en el caso de algunas grasas biogénicas se observó la tendencia contraria. Estos resultados pueden explicarse atendiendo a la microestructura del espesante y a las interacciones espesante/aceite base. Las interacciones físicas débiles, como las esperadas entre el aceite base y los espesantes celulósicos, también favorecen la separación del aceite (sangrado del aceite) a altas temperaturas, lo que da lugar a una mayor viscosidad y, por tanto, a una mayor densidad de energía. Las muestras de grasa biogénica consistentes en una combinación de HOSO y aceite de ricino como aceite base y monoestearatos de glicerilo y/o sorbitán como espesantes, produjeron el menor gasto energético a 25 °C y 40 °C. Además, las grasas biogénicas modelo basadas en lignosulfonato o lignina modificada químicamente como agentes espesantes proporcionaron un menor gasto energético que las grasas biogénicas modelo basadas en derivados de isopreno, fibras naturales de celulosa o pulpa de celulosa procedente de madera blanda. Estas últimas también proporcionaron valores más altos del gasto energético por fricción en comparación con las grasas de referencia.

- Se ha podido deducir una correlación entre la densidad de energía reológica (e_{rheo}) y el coeficiente de fricción para algunas grasas modelo. Las grasas biogénicas con menor gasto de energía durante el flujo en cizalla, como las muestras de grasa 1, 2 y S4, mostraron valores bajos del coeficiente de fricción. Además, las grasas semi-biogénicas (grasas de referencia), que mostraron los valores más altos del coeficiente de fricción, presentaron valores elevados de e_{rheo} en comparación con la mayoría de las grasas biogénicas estudiadas.
- Según los resultados obtenidos en el tribómetro de bola-disco, existe una relación lineal entre el coeficiente de fricción y el desgaste para la mayoría de las grasas modelo examinadas. Este resultado revela que cuanto menor es el coeficiente de fricción, menor es el volumen de desgaste que se produce en la placa de acero debido al proceso de fricción. Además, la composición de las grasas modelo influye en gran medida en los comportamientos de fricción y desgaste. Utilizando el modelo de desgaste energético de Fleischer, se ha dilucidado una relación entre la densidad de energía de fricción aparente (e_R^*), la intensidad del desgaste (I_h) y el esfuerzo de cizallamiento por fricción (τ_R) para todas las grasas modelo estudiadas. La representación de estos tres parámetros tribológicos en el gráfico de Fleischer de energía básica de desgaste ha permitido determinar los estados de fricción y de desgaste en los que se realizaron los experimentos, que fue una combinación

de fricción fluida y fricción mixta para todas las muestras de grasa. Además, la estimación de la densidad de energía de fricción aparente reveló que los contactos lubricados con grasas con altas densidades de energía proporcionan una menor intensidad de desgaste en la placa de acero.

- Para evaluar el comportamiento tribológico de las grasas biogénicas en elementos de máquinas reales, se realizaron ensayos de pérdida de potencia en rodamientos y de desgaste de rodamientos con dos muestras de grasa biogénica seleccionadas. Los resultados de las pruebas de pérdida de potencia mostraron que la grasa modelo 2, que contenía un aceite base de menor viscosidad, proporciona valores del par de fricción menores que la grasa modelo 1, en las mismas condiciones de funcionamiento. Comparando las grasas ensayadas, la grasa modelo 2 mostró un mejor rendimiento general, una reducción del torque ligeramente menor y una menor generación de partículas de desgaste, a pesar de que ambas grasas modelo tenían una composición similar, conteniendo la muestra 2 monoestearato de sorbitano en lugar de cera de abeja en la mezcla de espesantes. En cuanto a las pruebas de desgaste, se obtuvieron conclusiones similares, es decir, un par de fricción más elevado se asocia a un mayor desgaste. La grasa modelo 1 proporciona mayores índices de desgaste y muestra un peor rendimiento que la grasa modelo 2. Además, ambas grasas mostraron una coloración oscura después de los ensayos, y se encontró un número considerable de partículas de desgaste, algunas de ellas de gran tamaño.

- La densidad de energía reológica (e_{rheo}) de seis muestras de grasa tradicional se estimó experimentalmente mediante ensayos de flujo transitorio realizados a una velocidad de cizalla constante de 1000 s^{-1} y temperaturas variables. e_{rheo} disminuye linealmente con el aumento de la temperatura, como resultado del ablandamiento de la microestructura de la grasa, siguiendo una evolución de tipo Arrhenius. El ajuste de los datos de e_{rheo} a la ecuación de Arrhenius permitió calcular la energía de activación; que se interpreta como el nivel de energía necesario que hay que superar para producir una degradación estructural inducida por cizalla en la grasa. Esta energía de activación característica de cada grasa lubricante depende de la naturaleza y de la concentración del espesante utilizado. Para un espesante concreto, cuanto mayor es la concentración de espesante, menor es la energía de activación. Este fenómeno puede explicarse considerando que se forma una red estructural más sensible a la cizalla al aumentar la concentración de espesante. Por lo tanto, la energía de activación disminuye a medida que aumenta la cantidad de contactos físicos entre las fibras. Además, para la misma consistencia de la grasa (grado NLGI), la energía de activación de las grasas de litio es menor que la de las grasas de poliurea.

- La energía de activación se correlacionó con algunos parámetros reológicos de las grasas en el límite del régimen viscoelástico lineal (LVE) o justo después de superarlo, es decir, en las primeras etapas de la degradación estructural inducida por cizalla, determinados mediante ensayos de cizalla oscilatoria de pequeña amplitud. El valor de la deformación crítica ($\gamma_{critical}$) es proporcional a la energía de activación. Este resultado revela que cuanto más baja es la energía de activación, más temprana es la degradación estructural de las grasas debido al proceso de cizallamiento. La energía de activación también se correlacionó con algunos parámetros reológicos en el punto de cruce entre G' y G'' más allá del rango LVE, asumiendo que es el punto en el que las grasas comienzan a fluir. Se dedujo una relación lineal inversa entre la energía de activación y la densidad de energía asociada a la fricción interna en este punto de cruce. Además, se observó la misma relación lineal inversa entre la energía de activación y la disminución del módulo de almacenamiento ($\Delta G'$) desde el punto crítico que delimita el rango LVE hasta ese punto de cruce. Esto sugiere que las grasas con energías de activación más bajas son más sensibles a la degradación estructural en condiciones de baja deformación, es decir, justo por encima del rango LVE, lo que da lugar a un mayor gasto de energía de fricción.

List of Tables

Chapter 1: Introduction

Chapter 2: State of the Art

Chapter 3: Materials & Experimental Methods

Chapter 4: Results & Discussion

List of Figures

Chapter 1: Introduction

Chapter 2: State of the Art

Chapter 3: Materials & Experimental Methods

Chapter 4: Results & Discussion

Annexe - Published Articles

The following journal publications resulted from the scientific research of this work with their content presented in chapter 4:

1. Acar, N.; Kuhn, E.; Franco, J.M. Tribological and rheological characterization of new completely biogenic lubricating greases: a comparative experimental investigation. *Lubricants* 2018, 6, 45, https://www.mdpi.com/2075-4442/6/2/45.

2. Acar, N.; Franco, J.M.; Kuhn, E.; Gonçalves, D.E.P.; Seabra, J.H.O. Tribological investigation on the friction and wear behaviors of biogenic lubricating greases in steel-steel contact. *Applied sciences*, 2020, 10, 1477, doi:10.3390/app10041477.

3. Acar, N.; Franco, J.M.; Kuhn, E. On the shear-induced structural degradation of lubricating greases and associated activation energy: An experimental rheological study. *Tribology International*, 2020, 144, 106105, https://doi.org/10.1016/j.triboint.2019.106105.

Tribological and Rheological Characterization of New Completely Biogenic Lubricating Greases: A Comparative Experimental Investigation

Nazli Acar[1], Erik Juhn[1] and José M. Franco[2]

[1] Laboratory of Machine Elements and Tribology, Department of Mechanical Engineering and Production Management, Faculty of Engineering Technology and Computer Science, Hamburg University of Applied Sciences (HAW-Hamburg), Berliner Tor 21, 20099 Hamburg, Germany

[2] Pro2TecS-Chemical Product and Process Technology Research Centre, Complex Fluid Engineering Laboratory, Department of Chemical Engineering, University of Huelva, 21071 Huelva, Spain

Published in: ***Lubricants***

Publishing company: Multidisciplinary Digital Publishing Institute (MDPI)

Editor-in-Chief: Prof. Dr. Homer Rahnejat

Volume 6, Issue 2, pp: 45

Year: 2018

DOI: 10.3390/lubricants6020045

E-ISSN:2075-4442

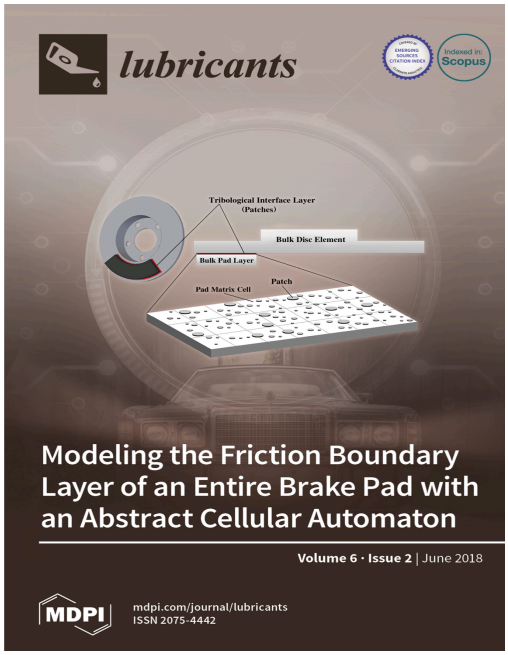

CiteScore (2018): 2.0

CiteScore Category	Rank
Engineering (Mechanical Engineering)	263/587
Materials Science (Surfaces, Coatings and Films)	63/118

Lubricants was indexed in the Science Citation Index Expanded (SCIE) in the Journal Citation Reports 2020 (Journal Citation Indicator 0.56).

lubricants

MDPI

Article

Tribological and Rheological Characterization of New Completely Biogenic Lubricating Greases: A Comparative Experimental Investigation

Nazli Acar [1,*], Erik Kuhn [1] and José M. Franco [2]

[1] Laboratory of Machine Elements and Tribology, Department of Mechanical Engineering and Production, Faculty of Engineering Technology and Computer Science, Hamburg University of Applied Sciences (HAW-Hamburg), Berliner Tor 21, 20099 Hamburg, Germany; erik.kuhn@haw-hamburg.de

[2] Pro2TecS-Chemical Product and Process Technology Research Centre, Complex Fluid Engineering Laboratory, Department of Chemical Engineering, University of Huelva, 21071 Huelva, Spain; franco@uhu.es

* Correspondence: nazli.acar@haw-hamburg.de; Tel.: +49-4042-8758-744

Received: 22 March 2018; Accepted: 2 May 2018; Published: 5 May 2018

check for updates

Abstract: Against the background of raw material shortage and the ever-expanding environmental consciousness, the use of biodegradable greases becomes more and more important. The aim of this experimental work is to investigate the tribological response of completely biodegradable greases. Complete biodegradable lubricating greases were formulated with high-oleic sunflower oil (HOSO) and/or castor oil, and different biodegradable thickener agents such as natural cellulose fibers of different lengths and some derivatives, as well as glyceryl and sorbitan stearates. To investigate the friction process, the model greases were tribologically examined with a nanotribometer at a normal force of 200 mN using a material combination of a steel ball on a steel disc. All frictional results, along with the volumes of wear tracks and micrographs of the main contacting area on the steel plate, are presented and discussed. In addition to this, rotational transient flow measurements were carried out on a rheometer at different temperatures to monitor the evolution of the shear stress with time at a constant shear rate, and to characterize the internal friction behavior by quantifying the energy density. All results were also analyzed from an energetic point of view.

Keywords: biogenic lubricating greases; tribology; rheology; friction; transient flow

1. Introduction

Lubricating greases have a wide range of applications and a long history. A consequence of intensive research and development in the past is the number of the so-called bio-grease formulations reported in the literature or even industrially produced. These lubricants consist of a vegetable-derived oil like castor oil or sunflower oil and traditional thickeners like metal soaps [1–6].

More recently, a further development from biodegradable lubricants to completely biogenic or bio-sourced lubricants has been initiated. It means that both the base oil and the thickener consist of biogenic material. First research works on completely biogenic lubricating greases were done by Sánchez, Franco, and co-workers [7–13], where castor oil or soybean oil was used as biodegradable lubrication oil and traditional thickener agents were replaced by natural thickeners like cellulose derivatives, chitin, chitosan, glyceryl stearates or sorbitan stearates. These comparative studies of bio-based greases with other traditional greases like lithium-12-hydroxysteate lubricating grease show that some of the bio-based greases provided comparable thermal, mechanical, and rheological properties for potential lubricating applications. Moreover, in one study [9], the evolution of the friction coefficient in several tribological tests performed using several ball-on-disc configurations and

coupling materials was investigated for the different biodegradable lubricating greases. The model greases, containing sorbitan monostearate, glyceryl monostearate, or acylated chitosan as thickener agents and castor oil as base oil, generally provided lower values of the friction coefficient than some traditional lithium greases in all tribological tests.

The main aim of the application of a lubricant is the prevention of the direct contact of the two solid rubbing bodies. That means for a friction balance that the friction behavior (the so-called fluid friction) of the lubricant plays an important role for the friction of a whole tribo-system. In addition, the loss of material as one type of wear will be reduced. In most practical situations, grease-lubricated contacts work in a state of mixed friction. This means the friction energy consists of a part of fluid friction and a part of solid friction. Mixed-friction was also observed for the tribometer tests reported in this paper. Using a ball-on-plate configuration with a grease-lubricated steel–steel contact that measured friction force, the friction coefficient can represent the mixed friction under these conditions. In addition, rheometer tests were performed to investigate the fluid friction inside the grease film as the second part of mixed friction. The energy density concept was used to quantify the energy expenditure for a shearing process. In this paper, grease samples containing newly developed biogenic thickeners and HOSO and/or castor oil as base oils were investigated. The aim of the paper is to present comparative results on the frictional response of a number of new completely biogenic model greases.

2. Experimental Section

2.1. Materials

A series of completely biogenic lubricating greases was produced by Fuchs Europe Schmierstoffe (Mannheim, Germany) and Fuchs Lubritech (Kaiserslautern, Germany). To compare the tribological behavior of the greases, two reference grease samples (R1 and R2) were added for the investigation. The compositions of the grease samples are listed in Table 1.

Table 1. Compositions of greases provided by Fuchs.

Grease Sample (Code)	Base Oil	Substance of Content
R1	Synthetic Ester	Lithium/Calcium Soap
R2	HOSO [1]	Lithium-12-hydroxystearate
1	HOSO and Castor oil	Beeswax, glyceryl monostearate and cetyl alcohol
2	HOSO and Castor oil	Glyceryl monostearate, cetyl alcohol and sorbitan monostearate
3	HOSO	Cellulose ether and glycerin
4	HOSO	Isoprene derivative
5	HOSO	Lignosulfonate
6	HOSO	Natural cellulose fibers 18 µm
7	HOSO	Corncob grits 80–120 µm
8	HOSO	Natural cellulose 20–40 µm
9	HOSO	Natural wood pulp from softwood 70–150 µm

[1] HOSO: high-oleic sunflower oil.

To extend the experimental work, four completely biogenic grease samples from Pro2TecS (University of Huelva, Huelva, Spain) were used and investigated. These four samples are listed in Table 2.

Table 2. Compositions of greases provided by Pro2TecS.

Grease Sample (Code)	Oil	Thickener
S1	Castor Oil	Lignin/PEGDGE [1] (weight ratio of 1/0.25)
S2	Castor Oil	Lignin/PEGDGE (weight ratio of 1/1)
S3	Castor Oil	Lignin/HMDI [2] (weight ratio of 1/2)
S4	Castor Oil	Lignin/HMDI (weight ratio of 1/1)

[1] PEGDGE: polyethylene glycol diglycidyl ether; [2] HMDI: hexamethylene diisocyanate.

The base oil for all Fuchs samples is high-oleic sunflower oil (HOSO) or a combination of HOSO and castor oil. Many efforts were made to create effective and efficient biogenic thickeners by testing different natural products, for example, beeswax, natural cellulose, glyceryl- and sorbitan monostearate, in different combinations and proportions. Unfortunately, here we are not able to present the percentage of each thickener.

The second group of grease samples used castor oil as the base oil and lignin as the thickener agent, once chemically modified with an epoxy compound (polyethylene glycol diglycidyl ether (PEGDGE)) or hexamethylene diisocyanate (HMDI) to promote the chemical interaction with the base oil [14,15].

2.2. Tribological Tests

A nanotribometer from CSM Instruments (Peseux, Switzerland) is used to determine the friction values of tribologically stressed material combinations. The test set-up consists of a static ball, which is fixed to a cantilever to avoid rolling, and a rotating disc. In the nanotribometer, the disc is stressed by pressure caused by applying a normal force. The ball-on-disc apparatus works in rotational mode. The fiber-optic sensors measure the deflection of the cantilever in radial (frictional force) and normal (normal force) directions, and by the precise calibration of the spring constant of the cantilever in both directions determined into frictional and normal forces.

In the Laboratory for Machine Elements and Tribology (MuT) of HAW-Hamburg, all tests were performed using material combinations of a steel ball (100Cr6) with 1 mm diameter on a steel disc (115CrV3, hardness 60–62 HRC, Zentrale Laborwerkstatt at the HAW-Hamburg, Hamburg, Germany) in rotational mode. All the steel discs were metallographically grinded and polished with a soft finish diamond paste of particle size 3 µm in the last polishing step. Normal load was kept constant at 200 mN with resulting Hertzian stress values of 1.2 GPa, and relative speed was varied with values of 40 mm·s^{-1} and 60 mm·s^{-1}. Under these conditions, a mixed-friction lubricated contact was achieved. The evolution of the friction coefficient with time was followed during 34 min (with relative speed 40 mm·s^{-1}) and 22 min (with relative speed 60 mm·s^{-1}). Each test was performed with each of the model grease samples and repeated three times at an ambient temperature of 22 ± 1 °C to calculate a quite accurate average friction coefficient. The friction and wear behaviors of the model greases were investigated under these conditions because they are optimal/ideal parameters of the nanotribometer.

The wear marks, which were produced from the three-time repetition of measurement in the same track at the nanotribometer, were analyzed by means of white light Interferometry (by Zygo Nexview, Middlefield, OH, USA). In this investigation, biogenic grease samples were examined to quantify the wear in the solids.

2.3. Rheological (Rotational Transient Flow) Tests

As previously described, a grease-lubricated contact works in a number of applications in the mixed-friction regime. It means that two subprocesses of the friction energy influence the whole system. Those are solid friction (e.g., deformation of asperities) and fluid friction (that arises inside the grease film).

To get an impression of the internal fluid friction behavior, rheometer tests were performed on the different grease samples studied. Figure 1 shows an example of the typical curve for a rotational transient test at a constant shear rate ($\dot{\gamma}$ = const.).

A previously reported model [16] was used to characterize the described friction behavior in a rotational transient test from an energy point of view. It defines a rheological energy density, (e_{rheo}), which represents energy expenditure per stressed grease volume. The rheological energy density can be calculated by the integration of the second part of the τ vs. t curve at a constant shear rate ($\dot{\gamma}$) as follows [17]:

$$e_{\mathrm{rheo}} = \dot{\gamma} \cdot \int_{t_{\mathrm{max}}}^{t} \tau(t)\mathrm{d}t \quad (1)$$

where t_{max} is the time necessary to reach the maximum shear stress (τ_{max}) and t is the shearing time. Moreover, the following empirical model was introduced for the shear stress as a function of time [18]:

$$\tau(t) = \tau_{lim} \cdot \left(\frac{t}{t_{lim}}\right)^{-n} \quad (2)$$

where t_{lim} is the time necessary to reach the steady-state shear stress (τ_{lim}), and n is the dimensionless exponent which describes the intensity of the structure degradation and can be determined with the help of a potential regression. An important explanation here is that τ_{lim} and t_{lim} represent the stationary state of the grease. Using Equations (1) and (2), the energy expenditure per stressed volume can be estimated for a defined stress period.

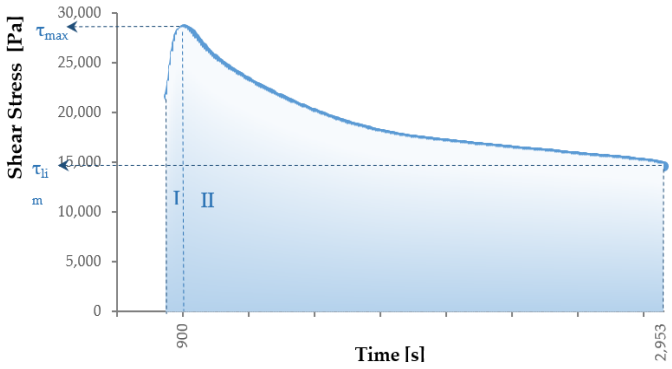

Figure 1. Example of a stress vs. time curve obtained in rotational transient flow tests.

The energetic interpretation of the two distinct regions of the shear stress versus time curve can play an important role in providing some information about the rheological and tribological behavior of the lubricating greases in the flow process. In this work, the energetic study was focused on the second part of the $\tau(t)$ curve—that is, after reaching the maximum stress value—evaluated at different temperatures.

The rotational transient flow measurements of complete biogenic greases were carried out on a MCR-302 rheometer (Anton Paar GmbH, Graz, Austria) in the Laboratory for Machine Elements and Tribology (MuT) of HAW-Hamburg. In this study, the model and reference greases were tested using a plate–plate system with a gap of 1 mm due to their coarse structure. All tests were performed by applying a constant shear rate of 1 s^{-1} at different temperatures (25 °C, 40 °C and 80 °C). The measuring time was set at 3600 s and the selected greases were left to rest for 15 min after setting the gap and the temperature. Every measurement for each grease was repeated three times at each temperature. These temperature parameters were selected from our investigation point of view and were determined to monitor the temperature-influenced flow behavior of the biogenic model greases.

3. Results and Discussion

3.1. Frictional Behavior

Averaged coefficients of friction of all the examined model greases from Fuchs and Pro2TecS obtained in the nanotribometer set-up by applying two different relative speeds are shown in Figure 2. The average standard deviation is described by the error bars in the diagram. Model greases 7, 8, and 9 could not be tested on the nanotribometer due to their coarse structure. In the experiments with these model greases, the rotational movement causes the coarse particles in the grease to contact the ball socket in the cantilever. Consequently, the fiber-optic sensors deflect, even though there was actually

no friction load. This results in high initial values of the friction coefficient or suddenly high values of friction coefficient during the test.

As can be seen in Figure 2, the reference greases, R1, based on synthetic Ester and Li/Ca-Soap, and R2, based on Li-12-Hydroxystearate and HOSO, generally show higher frictional values than biogenic grease samples in the present steel ball on steel plate frictional contact situation.

The use of biogrease S2, based on castor oil and lignin/PEGDGE as a thickener, provides similar or lower values of the friction coefficient than the two reference lubricating greases, R1 and R2. Moreover, the biogenic grease sample S4, containing lignin/HMDI as a thickener agent, stands out because of its lowest friction coefficient in comparison with the reference greases R1 and R2 and the other model greases from Pro2TecS: S1, S2, and S3. Another interesting point is that the biogenic grease samples produced by Pro2TecS by applying a relative speed of 40 mm·s^{-1} exhibit higher frictional values than the other model greases from Fuchs.

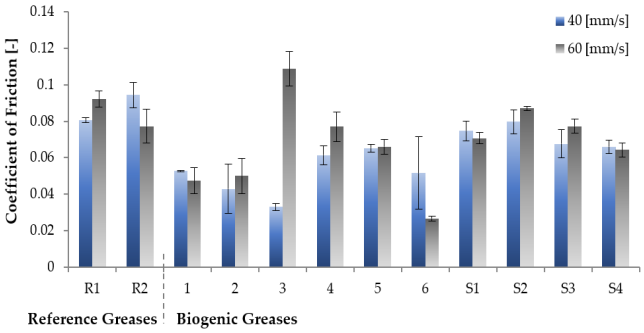

Figure 2. Friction coefficients determined in a steel ball-on-steel disc configuration (wear path s_R = 80 m).

As can be seen in Figure 2, the model biogenic grease 3, based on HOSO, Glycerin, and cellulose ether, has the lowest frictional coefficient at a relative speed of 40 mm·s^{-1}; nevertheless, this model grease provides the highest frictional value at a relative speed of 60 mm·s^{-1} than all of the other examined model greases. In addition, this grease exhibits an adhesive behavior, which could lead to a negative influence on the friction behavior at the nanotribometer. This directly shows the influences of the model grease components on frictional behavior.

Moreover, model greases 1 and 2, based on a mixture of castor oil and HOSO as base oil, as well as model grease 6, provide lower values of the friction coefficient than the reference greases and the other model biogenic greases. These model greases 1 and 2 also contain glyceryl monostearate and/or sorbitan monostearate, such as biodegradable thickener agents. This optimum frictional behavior can be attributed to both the presence of castor oil with much higher viscosity than HOSO, and the much lower molecular weight of sorbitan and glyceryl monostearates in comparison with the rest of bio-thickeners, that is, biopolymers. In addition, this type of grease exhibits very poor mechanical stability, though this could provide an advantage from a tribological point of view. This means that the microstructure of the grease is easily destroyed inside the tribological contact, turning into a more fluid material, significantly decreasing the consistency, and being able to lubricate contact more effectively [9].

Looking at the detail, the friction coefficients of the greases 1, 5, S1, and S4, remain stable in almost all test series. It shows that the friction coefficients of these grease samples are not highly influenced by relative speed differences.

According to the data in Figure 2, the friction coefficients of some examined greases, especially R1, 2, 3, 4, S2, and S3, increase with increasing relative speed. This is not the expected relative speed

influence on the frictional behavior, because the friction coefficient decreases with increasing relative speed in the mixed-friction lubrication regime. This frictional behavior could be explained by taking into account the beginning of the transition to the hydrodynamic lubrication regime. This approach is supported by wear data shown in Figure 4 and discussed below, in which the wear volume obtained in the contact lubricated with R1, 2, 4, S2, and S3 decreases with increasing relative speed.

3.2. Wear Results

In this series of experiments, the wear marks on the steel discs, obtained after performing the frictional tests with the normal load of 200 mN and a relative speed of 40 mm·s^{-1} in the nanotribometer, were investigated using the white light interferometry (the optical 3D surface profilometer) as displayed in Figure 3. These pictures provide a perspective view of the main contacting area on the steel plate. The wear scars on the steel surface appear quite clearly in the perspective view. As can be seen in Figure 3, while the reference grease R2 and the biogenic greases 3, 4, and 6 produced very wide and strong abrasive wear on the steel plate, the reference grease R1 and the biogenic grease 1 caused the narrowest wear tracks but pronounced abrasive wear. Moreover, the biogenic greases S1, S2, and S3 show wide but less pronounced wear scars on the steel plate. These wear results can be explained by the different components in grease formulations and resulting rheological behaviors.

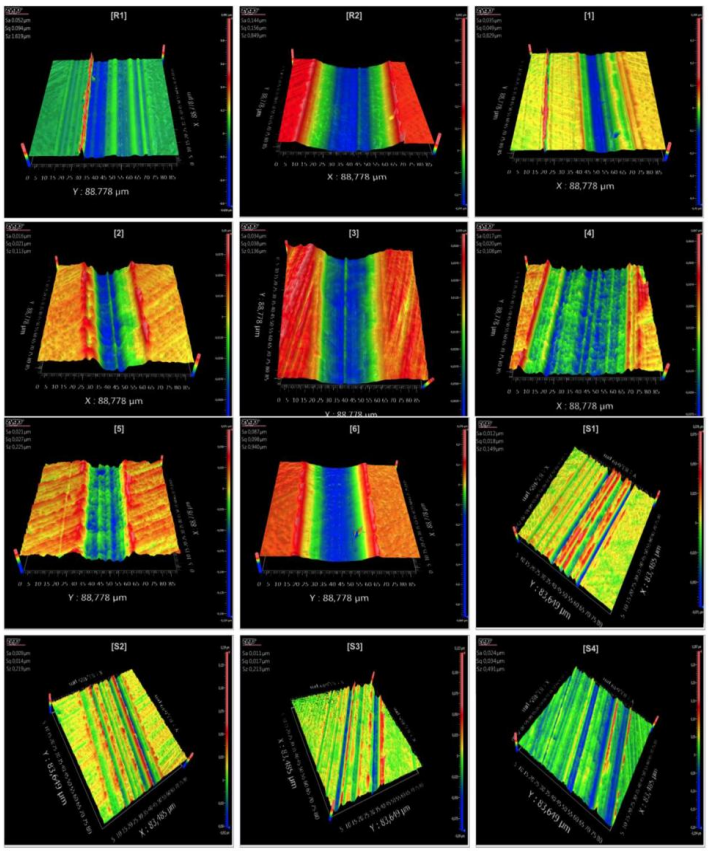

Figure 3. Profilometric pictures obtained from the steel discs as a function of the grease used as lubricants (window sizes of 88,778 µm × 88,778 µm and 83,485 µm × 83,649 µm).

The average volumes of the wear tracks on the steel plate, which were obtained after performing the frictional tests in the nanotribometer, are displayed as a function of the two different imposed relative speeds in Figure 4. The average standard deviation is described by the error bars in the diagram.

As can be observed in Figure 2, the friction coefficients of the reference greases are only slightly higher than those of the biogenic greases, despite the significantly higher wear volume values, which were at least three times the wear marks obtained with the biogenic greases.

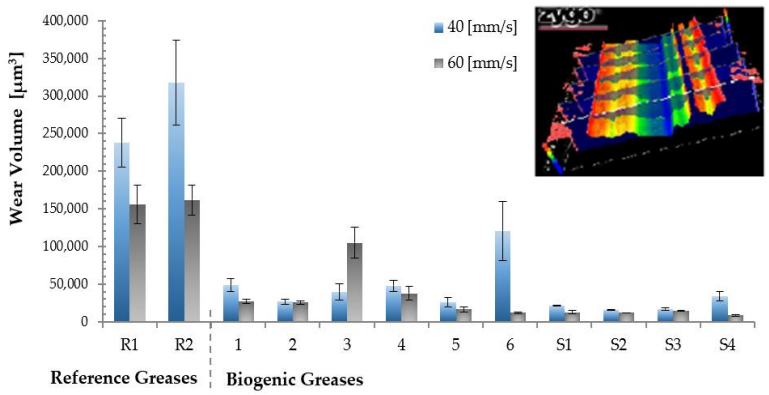

Figure 4. Wear volume in steel disc (Wear path s_R = 80 m).

Moreover, although biogenic grease 6, prepared with natural cellulose fiber of length of 18 µm, exhibits the lowest frictional value, it produces the highest wear volume at the lower relative speed of 40 mm·s^{-1} compared with all of the other biogenic greases, but the least wear at a relative speed of 60 mm·s^{-1}.

Another interesting point is that biogenic grease 3 produces a higher value of the friction coefficient at a relative speed of 60 mm·s^{-1}, which is reflected in the wear volumes. In addition to this, wear volume obtained in the contact lubricated with biogenic grease 3 increases by increasing relative speed, and decreases when using the other biogenic greases.

The biogenic grease samples containing castor oil and lignin/PEDGE or lignin/HMDI-thickener present higher values of the friction coefficient than the other biogenic greases, but the least wear on the steel plates. Under an assumption, these results could be explained by the better mechanical stability of these biogenic greases. This means that grease microstructures achieved by chemically cross-linking castor oil and lignin are not easily broken inside the tribological contact. This property of the grease microstructures could favor the grease not being easily ejected from the contact and therefore increases the efficiency of the grease in the lubricating contact.

3.3. Rotational Transient Flow Tests

Figure 5 shows different transient flow curves for selected biogenic and reference grease samples at 25 °C. The rheological energy densities were determined by integration of shear stress over time at 25 °C, 40 °C, and 80 °C, according to Equations (1) and (2).

The values of e_{rheo} for the investigated biogenic greases are displayed in Figure 6. Model greases 1 and 2 could not be tested at 80 °C on the rheometer, because sorbitan and glyceryl monostearates melted below this temperature [7].

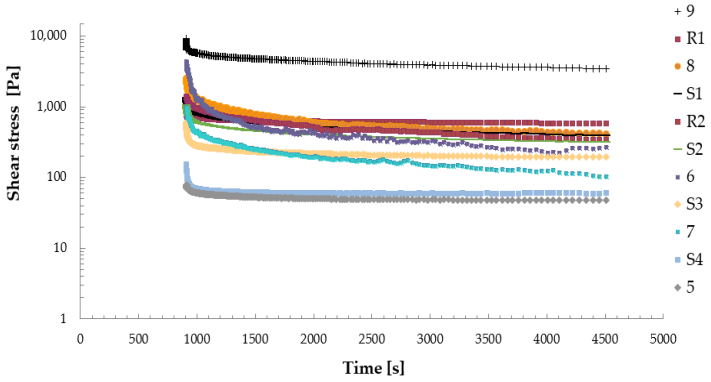

Figure 5. Transient flow curves for selected model grease samples at 25 °C.

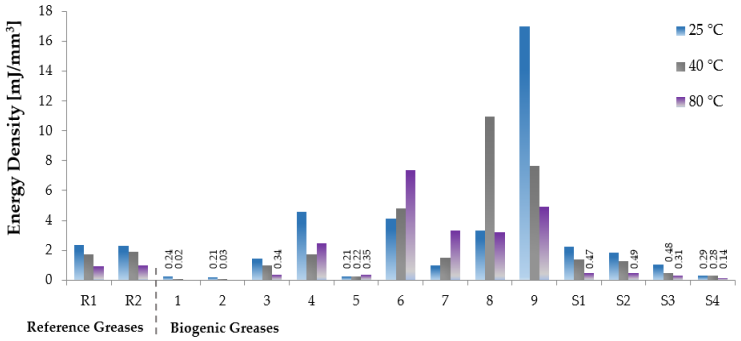

Figure 6. Energy densities (e_{rheo}) determined by integration of the shear stress vs. time plots at 25 °C, 40 °C, and 80 °C.

These results show that the energy expenditure depends strongly on the temperature applied during the shearing of model greases at a constant shear rate. As can be seen in Figure 6, high test temperatures generally lead to less energy expenditure than is needed to stress the thickener structure. This indicates that shear-induced structural modifications of the model greases are significantly influenced by the temperature. Unexpectedly, however, the energy density values of the grease samples 5, 6, 7, and 8 (excluding the energy density value of sample 8 at 80 °C) increase with increasing temperature. The unusual temperature-influenced flow behavior of these biogenic greases can be explained by the weak interactions between the base oil and cellulosic thickeners, based on hydrogen bonding, which significantly decrease with temperature. This favors oil separation (oil bleeding) at high temperatures, thus increasing viscosity as a result of the higher effective thickener concentration.

Another interesting point is that the biogenic grease samples 6, 8, and 9, consisting of HOSO as a base oil and natural cellulose fiber of length of 18 µm and 20–40 µm and natural wood pulp from softwood 70–150 µm as thickener agents, exhibit the highest values of energy density in all test series, probably because these formulations need higher thickener concentrations to be physically stabilized. Moreover, model grease samples 1 and 2, based on a mixture of castor oil and HOSO as base oil, and model grease sample 5, stand out because of their low values of the energy density in comparison with the reference greases and the other model biogenic greases. Looking at the detail, biogenic greases S3 and S4, based on lignin/HMDI as a thickener, provide less energy expenditure compared with

biogenic grease samples S1 and S2, based on lignin/PEGDGE as a thickener. This shows that the energy expenditure due to the shearing process is also influenced by the kind of lignin chemical modification.

From the analysis of the results discussed above, it seems obvious that grease microstructure plays an important role in the friction process. For a better understanding of the influence of the grease structure on the tribological behavior, it is necessary to investigate the relationship between the rheological energy density and grease structure. Therefore, the microstructure of some biogenic greases was examined by means of transmitted light microscopy.

The microstructures of selected biogenic greases are shown in Figure 7. As can be observed, the geometry and the distribution of the thickener particles are clearly different. The biogenic grease samples 1, 3, and 5 display rather homogeneous structures. This is especially relevant in samples 3 and 5, where the thickener and base oil cannot be clearly distinguished from each other. By contrast, the thickeners in the biogenic grease samples 6, 8, 9, S1, S2, and S3 are conspicuous. At first consideration, from the thickener structures and the rheological energy density point of view, one detects that the homogeneous structure of grease sample 5 provides the lowest values of energy density at 25 °C and 40 °C (see Figure 6), compared with samples 6, 8, 9, S1, S2, and S3, which show thickener agglomerates in the form of platelets or granules. On the other hand, the model grease sample 1, based on glyceryl monostearate as thickener agent, exhibits less energy expenditure than model grease sample 3, based on cellulose ether as thickener agent, which provides higher values of the rheological energy density (see Figure 6). Overall, these results reflect the fact that the characteristics and type of the thickener microstructure influence the friction behavior of the grease in the tribological process. In general, the more homogenous the structure and the smaller the particle size, the lower the resulting energy density.

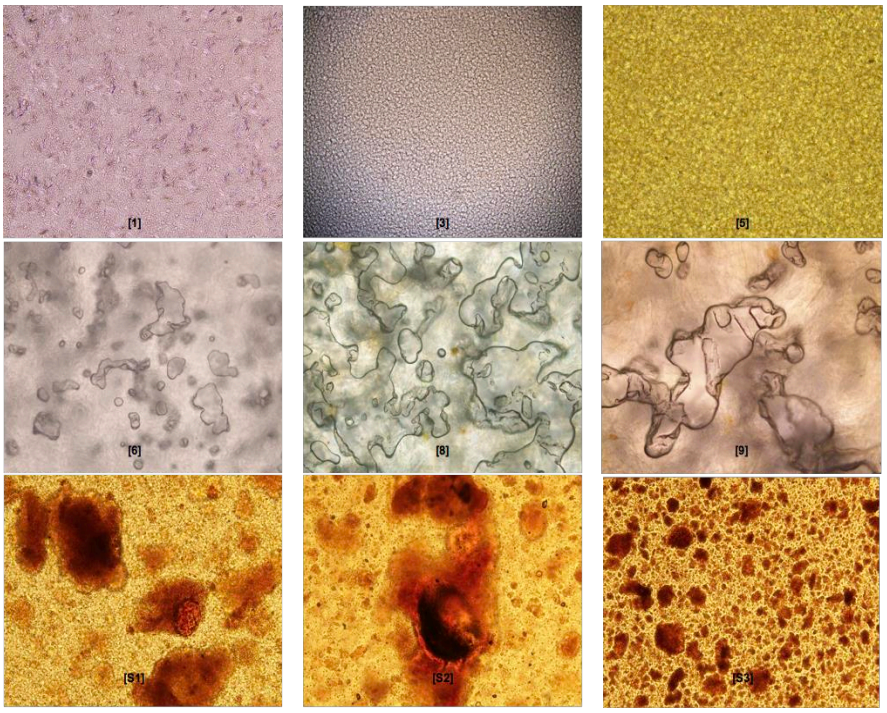

Figure 7. Transmitted Light Microscope micrographs for examined biogenic grease samples (window sizes of 683.5 µm × 536 µm) [19].

4. Conclusions

Several bio-sourced materials were used as thickener agents to formulate complete biogenic lubricating greases. These samples were tribologically investigated in a nanotribometer and in a rheometer, and compared with traditional lithium-12-hydroxystearate/HOSO and lithium-calcium soap/synthetic ester greases. Results from the nanotribometer tests showed a different influence of completely biogenic model grease components on frictional and wear behavior. In almost all cases, the use of biodegradable model greases produced lower values of the friction coefficient than the reference greases. The model greases containing glyceryl- and sorbitan monostearate as thickener agents, and the combination of HOSO and castor oil as base oil, generally yielded the lowest values of the friction coefficient no matter the test conditions. The reference greases produced higher values of the wear volume on the steel plate despite exhibiting only slightly higher friction coefficient values than the model greases. Moreover, the use of biogenic greases based on only castor oil as the base oil exhibited the lowest wear volume on the steel plate; however, these biogenic greases provided higher frictional coefficients (especially at relative speed of 40 $mm{\cdot}s^{-1}$), compared with biogenic greases consisting of HOSO or a combination of HOSO and castor oil.

To investigate the fluid friction behavior of the biodegradable model greases and to quantify the rheological energy by shearing the grease, transient flow tests were performed at different temperatures. The estimation of the energy density from the shear stress versus time curve revealed that the amount of energy expenditure per stressed volume (e_{rheo}) strongly depends on the test temperature. In this sense, the rheological energy density (e_{rheo}) generally decreased by increasing the test temperature. However, the opposite tendency was found for some model biogenic greases. These results can be explained by the thickener microstructure and the thickener/base oil interactions. Weak physical interactions like those expected between the base oil and cellulosic thickeners may also favor oil separation (oil bleeding) at high temperatures, resulting in higher viscosity and therefore higher energy density. The biogenic grease samples consisting of a combination of HOSO and castor oil as the base oil and glyceryl- and/or sorbitan monostearate as thickener yielded the lowest energy expenditure at 25 °C and 40 °C. Moreover, biogenic model greases based on lignosulfonate or chemically-modified lignin as thickener agents provided less energy expenditure than biogenic model greases based on Isoprene derivatives, natural cellulose fibers, or natural wood pulp from softwood, the latter also provided higher values of the energy expenditure by friction process compared with the reference greases.

In this paper, the fluid friction can be defined as the energy expenditure during the relative motion of the shearing process. In this sense, correspondence between the rheological energy density (e_{rheo}) and the friction coefficient can be inferred for some model greases. Biogenic greases with less energy expenditure during the flow process, such as grease samples 1, 2, and S4 showed low values of the friction coefficient. In addition to this, semi-biogenic greases (reference greases), which showed the highest values of the friction coefficient, exhibited high energy density values compared with most of the biogenic greases studied.

Author Contributions: The paper was created by Nazli Acar. Erik Kuhn und José M. Franco contributed by supervising the experimental works and amending text passages.

Funding: This research was funded by German Ministry of Education and Research grant number FKZ13FH018IX4.

Acknowledgments: This work, which is part of the research Project "Tribiogen", was supported by German Ministry of Education and Research. The authors gratefully acknowledge the financial support. Authors also acknowledge Fuchs Europe Schmierstoffe (Germany), Fuchs Lubritech (Germany), and Pro2TecS (University of Huelva (Spain)) for kindly providing model samples.

Conflicts of Interest: The authors declare no conflict of interest.

References

1. Sukirno, R.F.; Setijo, B.; Mohammad, N. Biogrease based on palm oil and lithium soap thickener: Evaluation of antiwear property. *World Appl. Sci. J.* **2009**, *6*, 401–407.

2. Fajar, R. Nasikin. Anti-wear properties of bio-grease from modified palm oil and calcium soap thickener. *CIGR J.* **2010**, *12*, 64–69.
3. Abdulbari, H.A.; Rosli, M.Y.; Abdurrahman, H.N.; Nizam, M.K. Lubricating grease from spent bleaching earth and waste cooking oil: Tribology properties. *Inter. J. Phys. Sci.* **2011**, *6*, 4695–4699.
4. El-Adly, R.A.; Ahmed, H.B.; Modather, F.H. Jojoba and Castor Oils as Fluids for the preparation of bio greases: A Comparative Study. *Inter. J. Sci. Eng. Res.* **2014**, *5*, 2229–5518.
5. Panchal, T.; Chauhan, D.; Thomas, M.; Patel, J. Bio based grease a value added product from renewable resources. *Ind. Crop. Prod.* **2015**, *63*, 48–52. [CrossRef]
6. Nagendramma, P.; Kumar, P. Eco-Friendly Multipurpose Lubricating Greases from Vegetable Residual Oils. *Lubricants* **2015**, *3*, 628–636. [CrossRef]
7. Sánchez, R.; Franco, J.M.; Delgado, M.A.; Valencia, C.; Gallegos, C. Effect of thermo-mechanical processing on the rheology of oleogels potentially applicable as biodegradable lubricating greases. *Chem. Eng. Res. Des.* **2008**, *86*, 1073–1082. [CrossRef]
8. Sánchez, R.; Franco, J.M.; Delgado, M.A.; Valencia, C.; Gallegos, C. Development of new green lubricating greases formulations based on cellulosic derivatives and castor oil. *Green. Chem.* **2009**, *11*, 686–693. [CrossRef]
9. Sánchez, R.; Franco, J.M.; Kuhn, E.; Fiedler, M. Tribological characterization of green lubricating greases formulated with castor oil and different biogenic thickener agents: a comparative experimental study. *Ind. Lubr. Tribol.* **2011**, *63*, 446–452. [CrossRef]
10. Sánchez, R.; Franco, J.M.; Delgado, M.A.; Valencia, C.; Gallegos, C. Thermal and mechanical characterization of cellulosic derivatives-based oleogels potentially applicable as bio-lubricating greases: Influence of ethyl cellulose molecular weight. *Carbohydr. Polym.* **2011**, *83*, 151–158. [CrossRef]
11. Sánchez, R.; Stringari, G.B.; Franco, J.M.; Valencia, C.; Gallegos, C. Use of chitin, chitosan and acylated derivatives as thickener agents of vegetable oils for bio lubricant applications. *Carbohydr. Polym.* **2011**, *85*, 705–714. [CrossRef]
12. Alfonso, J.E.M.; Yañez, R.; Valencia, C.; Franco, J.M.; Díaz, M.J. Optimization of the Methylation Conditions of Kraft Cellulose Pulp for Its Use As a Thickener Agent in Biodegradable Lubricating Greases. *Ind. Eng. Chem. Res.* **2009**, *48*, 6765–6771. [CrossRef]
13. Núñez, N.; Alfonso, J.E.M.; Valencia, C.; Sánchez, M.C.; Franco, J.M. Rheology of new green lubricating grease formulations containing cellulose pulp and its methylated derivative as thickener agents. *Ind. Crop. Prod.* **2012**, *37*, 500–507. [CrossRef]
14. Borrero-López, A.M.; Valencia, C.; Franco, J.M. Rheology of lignin-based chemical oleogels prepared using diisocyanate crosslinkers: Effect of the diisocyanate and curing kinetics. *Europ. Polym. J.* **2017**, *89*, 311–323. [CrossRef]
15. Triviño, E.C.; Valencia, C.; Franco, J.M. Influence of epoxidation conditions on the rheological properties of gel-like dispersions of epoxidized kraft lignin in castor oil. *Holzforschung* **2017**, *71*, 777–784.
16. Kuhn, E. *Zur Tribologie der Schmierfette: Eine energetische Betrachtungsweise des Reibungs- und Verschleißprozesses*; Expert Verlag: Renningen, Germany, 2017.
17. Delgado, M.A.; Franco, J.M.; Kuhn, E. Effect of rheological behaviour of lithium greases on the friction process. *Ind. Lubr. Tribol.* **2008**, *60*, 37–45. [CrossRef]
18. Kuhn, E. Experimental grease investigations from an energy point of view. *Ind. Lubr. Tribol.* **1999**, *51*, 246–251. [CrossRef]
19. Slabka, I. Rheologische Charakterisierung Biogener Modellfette. Master's Thesis, Hamburg University of Applied Sciences, Hamburg, Germany, 2017.
20. Kuhn, E. An algorithm to estimate the friction energy of a grease lubricated contact. *Ind. Lubr. Tribol.* **2000**, *52*, 174–177. [CrossRef]
21. Delgado, M.A.; Franco, J.M.; Valencia, C.; Kuhn, E.; Gallegos, C. Transient shear flow of model lithium lubricating greases. *Mech. Time-Depend. Mater.* **2009**, *13*, 63–80. [CrossRef]
22. Mohr, H. Tribologische Untersuchungen Komplett Biogener Schmierfette. Master's Thesis, Hamburg University of Applied Sciences, Hamburg, Germany, 2017.

Tribological Investigation on the Friction and Wear Behaviors of Biogenic Lubricating Greases in Steel–Steel Contact

Nazli Acar[1,2], José M. Franco[2,3], Erik Kuhn[1], David E. P. Gonçalves[4], Jorge H. O. Seabra[5].

[1] Laboratory of Machine Elements and Tribology, Department of Mechanical Engineering and Production Management, Faculty of Engineering Technology and Computer Science, Hamburg University of Applied Sciences (HAW-Hamburg), 20099 Hamburg, Germany
[2] Department of Chemical Engineering, University of Huelva, 21071, Huelva, Spain
[3] Pro2TecS-Chemical Product and Process Technology Research Centre, Complex Fluid Engineering Laboratory, University of Huelva, 21071, Huelva, Spain

[4] INEGI, Universidade do Porto, Rua Roberto Frias s/n, 4200-465 Porto, Portugal

[5] FEUP, Faculdade de Engenharia da Universidade do Porto, Rua Roberto Frias s/n, 4200-465 Porto, Portugal

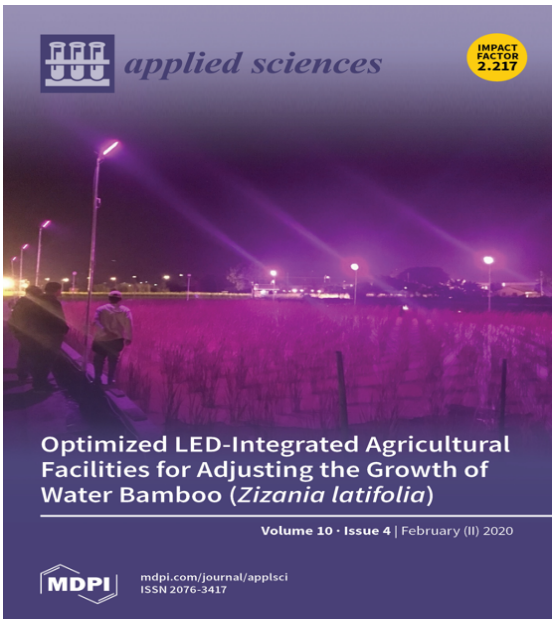

Published in: ***Applied Sciences***

Publishing company: Multidisciplinary Digital Publishing Institute (MDPI)

Volume 10, Issue 4, pp 1477

Year: 2020

DOI: 10.3390/app10041477

ISSN: 2076-3417

Impact Factor (2020): 2.679

CiteScore (2020): 3.0

JCR Category	Rank
Engineering, Multidisciplinary	38/90
Material Science, Multidisciplinary	201/334
Chemistry, Multidisciplinary	101/17
Physics, Applied	73/160

applied sciences

MDPI

Article

Tribological Investigation on the Friction and Wear Behaviors of Biogenic Lubricating Greases in Steel–Steel Contact

Nazli Acar [1,2,*], José M. Franco [2,3], Erik Kuhn [1], David E. P. Gonçalves [4] and Jorge H. O. Seabra [5]

1 Laboratory of Machine Elements and Tribology, Department of Mechanical Engineering and Production, Faculty of Engineering Technology and Computer Science, Hamburg University of Applied Sciences (HAW-Hamburg), 20099 Hamburg, Germany; erik.kuhn@haw-hamburg.de
2 Department of Chemical Engineering, University of Huelva, 21071 Huelva, Spain; franco@uhu.es
3 Pro2TecS-Chemical Product and Process Technology Research Centre, Complex Fluid Engineering Laboratory, University of Huelva, 21071 Huelva, Spain
4 INEGI, Universidade do Porto, Rua Roberto Frias s/n, 4200-465 Porto, Portugal; degoncalves@inegi.up.pt
5 FEUP, Faculdade de Engenharia da Universidade do Porto, Rua Roberto Frias s/n, 4200-465 Porto, Portugal; jseabra@fe.up.pt
* Correspondence: nazli.acar@haw-hamburg.de

Received: 23 January 2020; Accepted: 17 February 2020; Published: 21 February 2020

Abstract: The applications of biogenic lubricating greases to machine elements play important roles in the reduction of friction energy and minimizing wear in a tribological contact, as well as the prevention of environmental pollution. The aim of this work was to investigate completely biogenic lubricating greases from a tribological point of view. Model greases were examined using a ball on a disc tribometer at a constant normal force to investigate the friction and wear process according to Fleischer's energetic wear model. Using the energy-based wear model, the friction and wear process could be interpreted as a cause–effect sequence. Moreover, the influence of the model grease composition on the friction and wear process was analyzed. In addition, rolling bearing tests were performed to investigate the tribological behaviors of some selected biogenic greases during real machine element contact. These tests allowed for the quantification of the friction torque behavior of the full bearing and the evaluation of the wear obtained through lubricant analysis procedures. This experimental work provides useful information regarding the influence that the composition of biogenic model greases has on friction and wear behaviors in a tribological contact.

Keywords: biogenic lubricating greases; friction; wear; rolling bearing friction torque; tribology

1. Introduction

The use of biodegradable greases for different industrial applications is remarkably important for avoiding direct and indirect environmental pollution [1–3]. In this sense, some lubricant industries focus on developing their products from renewable resources in order to minimize adverse impacts on the environment. As discussed and reported in previous works [4–7], the use of vegetable oil instead of mineral oil as a liquid lubricant shows some advantages, such as good lubricity, the ability to adhere to metal surfaces, non-toxicity, and low volatility, as well as some disadvantages, such as poor oxidative stability and low temperature flow properties. However, these negative features can be overcome or minimized by using additives or inducing chemical modifications [5,6,8–11]. Completely biogenic lubricating greases can be obtained by replacing the mineral base oil with a

vegetable oil, as well as by substituting traditionally used thickener agents (metallic soaps or polyurea compounds) with biogenic thickeners. In some research [12–19], some formulations, such as those based on castor or soybean oil used as a biodegradable base oil, and natural thickeners like cellulose derivatives, chitin, glyceryl stearates, or sorbitan stearates, were rheologically and tribologically investigated and compared with some traditional greases, such as lithium-12-hydroxysteate lubricating grease. The results of these works showed that some formulations provided similar or better thermal, rheological, and mechanical properties than traditional lubricating greases for potential lubricating applications. Moreover, bio-grease formulations, based on castor oil as the base oil and sorbitan and glyceryl monostearate or acylated chitosan as the thickener agents, generally yielded lower friction coefficient values than the reference lithium greases in several tribological tests [14].

The friction process leads to irreversible effects, namely wear, inside a tribological system; therefore, irreversible effects are the results of friction energy input into a tribological system [20]. This approach indicates that the friction and wear process is a cause–effect sequence [21]. One of the models that describes the relationship between friction and wear is Fleischer's energy-based wear model, which is based on the energy accumulation hypothesis [22,23]. Most of the friction energy dissipates as heat into a tribological contact, while the rest accumulates in the surface layer. If the accumulated energy reaches a critical energy level, particle separation from the contacting surface occurs and the stored energy dissipates. The basic parameter in Fleischer's wear model is the apparent friction energy density (e_R^*), which presents a relationship between the friction work (W_R) and the wear volume (V_V). Fleischer's energy-based wear model plays an important role in evaluating the service life and reliability of tribological contacts. In some previous studies [24–28], Fleischer's wear model, or a modified version of it, was used to describe wear processes and predict wear in various types of tribosystems, such as piston–cylinder contacts or journal bearings. Moreover, some studies [29,30] attempted to assess the selected materials in terms of wear resistance, as well as in terms of energy using Fleischer's wear model in pin–disk test devices. In addition, the influence of entropy transport on the ability of a system to resist tribological stress [31,32] relates to the apparent friction energy density.

In this experimental study, a series of biogenic lubricating greases were tested in a tribometer using a material combination of a steel ball on a steel plate to investigate the friction and wear process according to Fleischer's energetic wear model. In addition, rolling bearing tests were carried out to assess the lubrication performance of some selected biogenic lubricating greases. These tests included both power loss and wear tests in real applications. These real application tests allowed for the quantification of the friction torque behavior of the full bearing at different operating conditions and the wear produced through lubricant analysis procedures, i.e., ferrometry and ferrography.

2. Energy-Based Wear Model and Apparent Friction Energy Density

Friction energy causes wear effects on a tribocontact (on the contacting surfaces). In the energy-based wear model, Fleischer [22] defined the term "apparent friction energy density, e_R^*" in order to describe the relationship between friction and wear. The apparent friction energy density (e_R^*) represents the amount of friction work (W_R) in relation to the wear volume (V_V):

$$e_R^* = \frac{W_R}{V_V}. \quad (1)$$

Assuming that the friction shear stress (τ_R) can be determined from the friction coefficient (f) and the nominal contact pressure (P_a):

$$\tau_R = f \cdot P_a, \quad (2)$$

the linear wear intensity (I_h) [33] according to Fleischer's fundamental equation of wear can be obtained using:

$$I_h = \frac{\tau_R}{e_R^*}. \quad (3)$$

In general, the expended energy consists of several components; therefore, there are also several components of wear [22]. Therefore, the apparent energy density can be extended to:

$$\frac{1}{e_R^*} = \frac{\alpha_1}{e_{R1}^*} + \frac{\alpha_2}{e_{R2}^*} + \frac{\alpha_3}{e_{R3}^*} \tag{4}$$

by considering the applied lubricant as a friction body. The parameters α_1, α_2, and α_3 represent the energy proportion factors, which represent the distribution of the friction energy to the respective friction bodies in a tribological system [34].

If the apparent friction energy density is considered in the steady-state phase of solid-state wear, Equation (1) can be rewritten as follows:

$$e_R^* = \frac{W_R}{V_V} = \frac{F_R \cdot s_R}{A_R \cdot h_v} = \tau_R \cdot \frac{1}{I_h} = \frac{\tau_R}{I_h}, \tag{5}$$

where F_R is the fiction force, s_R is the friction distance, A_R is the frictional contact area (wear area), and h_v is the wear depth.

Fleischer's energetic wear model was based on the so-called hypothesis of energy storage [22,23]. This hypothesis considered that the formation of a wear particle would occur only after repeated contacting since the critical energy level is usually not exceeded by the energy impulse of contact [22]. According to the energy accumulation hypothesis, a part of the energy of each impulse would be stored in a tribologically stressed material [22]. When the accumulated energy reached the critical energy value, a wear particle would form, i.e., particle separation from the contacting surface would occur and the accumulated energy would dissipate, indicating that the energy of a single contact (W_{R_e}) in the friction process partly accumulates and partly dissipates [22]:

$$W_{R_e} = W_{store_e} + W_{Diss_e}. \tag{6}$$

Fleischer et al. [22] described the critical energy level required for the formation of the wear particle by identifying the average fracture energy density with the application of a critical number of contacts (n_k):

$$\overline{e_B} = \zeta_R \cdot e_{R_e} \cdot (n_k - 1) + e_{R_e}, \tag{7}$$

where ζ_R is the energy accumulation number and e_{R_e} is the energy density of a single contact.

The previously given equation of the apparent frictional energy density (Equation (1)) can be rewritten [22] as:

$$e_R^* = \frac{n_k}{v_V} \cdot \frac{\overline{e_B}}{1 + \zeta_R \cdot (n_k - 1)} \tag{8}$$

by introducing the wear number (v_V):

$$v_V = \frac{V_V}{V_R}, \tag{9}$$

where V_R is the frictional volume.

Figure 1 shows the graph of the basic energy equation of wear and allows for visualization of the relationship between the apparent energy density (e_R^*), the intensity of wear (I_h), and the friction shear stress (τ_R). Fleischer [23] divided this plot into five different friction and wear states (areas 0–4) according to the occurring mechanisms, as shown in Figure 1 and Table 1. Range 1 is hydrodynamic lubrication, which leads to negligible wear intensities and zero wear in fluid friction. The other remarkable friction state is solid friction i.e., range 4, which leads to the immediate separation of material. The middle ranges, namely quasi-fluid friction, mixed friction, and solid friction with elastic and/or plastic deformation mechanisms, are also considered.

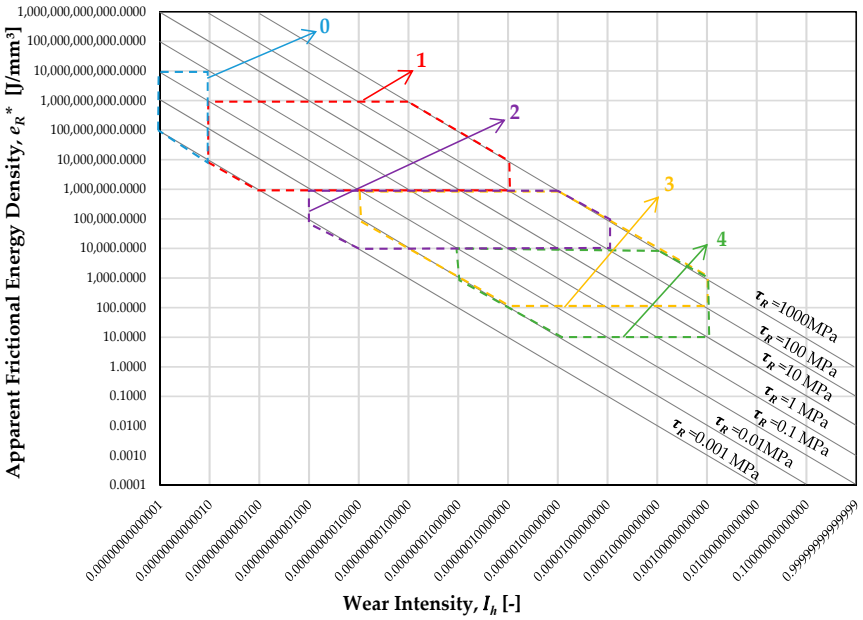

Figure 1. Graph of the basic energy equation of wear (adapted from G. Fleischer [23]).

Table 1. Friction and wear conditions with associated tribological process parameters (adapted from G. Fleischer [23]).

Range	Friction State	Wear State	Process Parameter		
			e_R^* (J/mm³)	τ_R (MPa)	I_h (–)
0	Fluid friction (rheological deformation and shear)	Zero wear	10^{10}–10^{7}	10^{0}–10^{-3}	$<10^{-13}$
1	Fluid friction/mixed friction (rheological and elastic deformation and shear)	Solid body wear level 1	10^{9}–10^{6}	10^{3}–10^{-3}	10^{-13}–10^{-7}
2	Mixed friction (rheological and plastic deformation and shear)	Solid body wear level 2	10^{6}–10^{4}	10^{3}–10^{-3}	10^{-11}–10^{-5}
3	Solid friction (elastic and plastic deformation and shear)	Solid body wear level 3	10^{6}–10^{2}	10^{3}–10^{-2}	10^{-10}–10^{-3}
4	Solid friction (separating deformation and shear)	Solid body wear level 4	10^{4}–10^{1}	10^{3}–10^{-2}	10^{-8}–10^{-3}

3. Experimental Section

3.1. Materials

Completely biogenic lubricating greases (1–13) and two reference semi-biogenic lubricating greases (R1, R2) were produced by Fuchs Europe Schmierstoffe (Mannheim, Germany) and Fuchs Lubritech (Kaiserslautern, Germany). Moreover, four completely biogenic lubricating greases (S1–S4) from Pro2TecS (University of Huelva, Huelva, Spain) were investigated in this study. All biogenic lubricating grease samples were formulated with different biogenic oils, e.g., high-oleic sunflower oil (HOSO), glycerol, castor oil, and a combination of HOSO and castor oil, to form the base oils. Moreover, different natural products, e.g., beeswax, corncob grits, natural cellulose, and lignin, were used as thickener agents. For confidentiality reasons, we are not able to give information on the percentage of

each thickener in Fuchs greases. More details regarding the biogenic grease samples from Pro2TecS can be found elsewhere [35,36]. The compositions of all the biogenic grease samples are depicted in Table 2.

Table 2. Compositions of greases.

Grease Sample (Code)	Base Oil	Substance of Content
R1	Synthetic ester	Lithium/calcium soap
R2	HOSO [1]	Lithium-12-hydroxystearate
1	HOSO and castor oil	Beeswax, glyceryl monostearate, and cetyl alcohol
2	HOSO and castor oil	Glyceryl monostearate, cetyl alcohol, and sorbitan monostearate
3	HOSO and glycerol	Cellulose ether
4	HOSO	Isoprene derivative
5	HOSO	Lignosulfonate
6	HOSO	Natural cellulose fibers, 18 µm
7	HOSO	Corncob grits, 80–120 µm
8	HOSO	Natural cellulose, 20–40 µm
9	HOSO	Natural wood pulp from softwood, 70–150 µm
10	HOSO	Natural cellulose fibers, 120 µm
11	HOSO and castor oil	Ethyl cellulose, carnauba wax, and cetyl alcohol
12	Castor oil, HOSO and MCT oil (triglyceride of C8/C10 fatty acids)	Polyhydroxybutyric acid and ethyl cellulose
13	Glycerol and sorbitan monooleate	Chitosan, glyceryl monostearate, and calcium phosphates
S1	Castor oil	Lignin/PEGDGE [2] (weight ratio of 1/0.25)
S2	Castor oil	Lignin/PEGDGE (weight ratio of 1/1)
S3	Castor oil	Lignin/HMDI [3] (weight ratio of 1/2)
S4	Castor oil	Lignin/HMDI (weight ratio of 1/1)

[1] HOSO: high-oleic sunflower oil; [2] PEGDGE: polyethylene glycol diglycidyl ether; [3] HMDI: hexamethylene diisocyanate.

3.2. Tribological Tests on the Ball-on-Disc Tribometer

A tribometer designed by the Laboratory for Machine Elements and Tribology (MuT) at the Hamburg University of Applied Sciences (HAW-Hamburg, Germany), as shown in Figure 2, was used to determine the friction coefficient values of tribologically stressed material combinations. The test set-up was composed of a rotatory plate and a fixed ball. In the tribometer, the steel plate was lubricated with a grease sample and stressed by applying a normal force. By means of a load cell, the friction force was measured during the test, thereby allowing the friction coefficient to be determined.

In the MuT laboratory of HAW-Hamburg, all tests were carried out in rotational mode with a relative speed of 0.129 $m \cdot s^{-1}$, using a steel ball (100Cr6) 12.7 mm in diameter and steel plates (S235JR (St37), Zentrale Laborwerkstatt at the HAW-Hamburg, Hamburg, Germany). In order to achieve comparable results, frictional and wear behaviors of the model greases were investigated under the same test parameters and conditions for the tribometer. All the steel plates were metallographically grinded and polished with a soft finish diamond paste of particle size 3 µm in order to significantly reduce surface roughness. Grease layers of the same thickness were applied to the steel plates, as shown in Figure 2. The normal load was kept constant at 12.62 N, with a resulting Hertzian stress value of 930.76 MPa and a test duration of 5 min. Each test was replicated ten times on the same track at an ambient temperature of 22 ± 1 °C in order to get a representative average friction coefficient value.

To quantify the wear of the solids, the wear marks on the steel plates created after the ten repetitions of the test on the same track of the tribometer were investigated using white light interferometry with a Zygo Nexview apparatus (Middlefield, OH, USA). Wear depths were quantified by means of the Zygo Mx software.

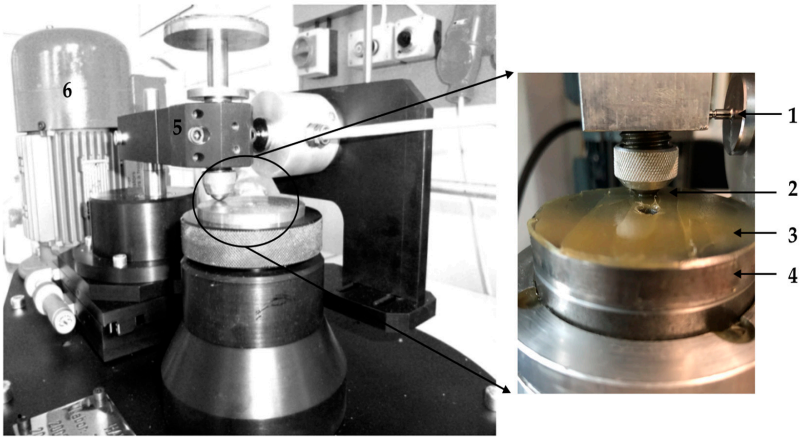

Figure 2. Tribometer designed by the Laboratory for Machine Elements and Tribology (MuT) laboratory at Hamburg University of Applied Sciences (HAW-Hamburg). Note: 1—Friction force-sensor, 2—steel ball, 3—lubricating grease, 4—steel disc, 5—swivel arm, and 6—electromotor (adapted from E. Kuhn [34]).

3.3. Rolling Bearing's Friction Torque Tests

In order to assess the tribological behavior of the biogenic greases on real machine element contacts, rolling bearing (RB) tests were performed with selected model greases 1 and 2 in a dedicated rolling bearing test rig, as seen in Figure 3. In this test rig, the rolling bearing was subjected to a constant axial load (P) applied from bottom to top; the thrust roller bearing tested in this work operated in a vertical arrangement [37–40].

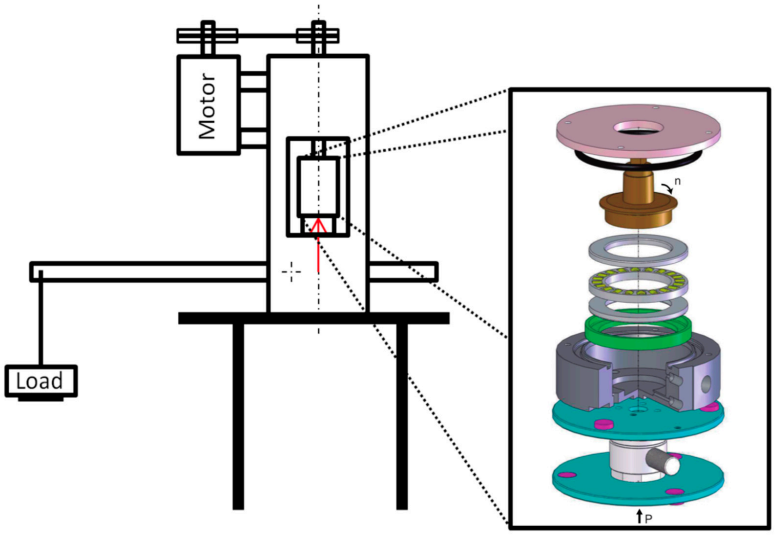

Figure 3. Rolling bearing test rig scheme.

An electrical motor provided the necessary power to overcome the power loss of the system and keep the rotational speed steady. A belt-pulley arrangement transmitted the power from the

motor to the rolling bearing shaft, forcing the upper raceway to rotate. The lower raceway was fixed to the bearing house and the torque cell, while the rolling elements' cage rotated due to the motion imposed by the upper raceway. A piezoelectric reaction torque cell KISTLER® 9339A (Kistler Group, Winterthur, Switzerland) was used to measure the friction torque. For each speed step tested, five torque measurements were performed.

The tests were performed with a thrust ball bearing (TBB) 51107 from SKF (SKF Group, Gothenburg, Sweden). The TBB had 21 rolling elements that were 6 mm in diameter and the raceways had a mean diameter of 43.5 mm. Regarding the thrust load, the tests were performed with approximately 5 kN. Given the number of rolling elements of the TBB and the radius of curvature, the maximum Hertzian pressure was around 2 GPa during the ball–raceway contact. Since the melting temperature of the thickeners was around 60 °C, we chose to control the temperature inside the TBB at 50 °C. Since the temperature did not reach 60 °C, the thickener did not melt and therefore the structure should have only been affected by the mechanical working, avoiding a premature degradation of the grease structure.

3.3.1. Power Loss Tests

The operating conditions chosen for the power loss tests are shown in Table 3. The tests performed were well above the minimum required load (0.02C) while also not exceeding the maximum dynamic load rating (P/C ≈ 25%, P: equivalent dynamic bearing load (kN), C: basic dynamic load rating (kN)).

Table 3. Operating conditions of the power loss tests. TBB: Thrust ball bearing.

Parameter	TBB 51107
Mean diameter (mm)	43.5
Number of rolling elements	21
Height (mm)	12
Composite roughness (nm)	155
Rotational speed (rpm)	100, 200, 400, 800, 1600
Axial Load (N)	5 kN (≈2.08 GPa)
Temperature (°C)	Controlled at 50 °C

The friction torque measuring procedure involved the following steps:

1. The machine was loaded with 5 kg (load on the bearing ≈1000 N) and the motor was started, with the speed increasing to 500 rpm for 5 min.
2. The load was increased to 25 kg (5 kN) and the speed was set at 100 rpm.
3. Temperature stabilization was undertaken (less than 1 °C degree variation in a time window of 10 min).
4. The friction torque was measured five times at constant operating conditions.
5. The rotational speed was increased. Steps 3 and 4 were repeated to reach the required rotational speed.
6. The test was stopped.

The total test duration was between 6 and 7 h to allow for the temperature to stabilize at 50 °C every time the speed was increased. The rolling bearing test rig was able to maintain the temperature at 50 °C with less than 1 °C deviation for all rotational speeds by using an external thermal bath.

3.3.2. Wear Tests

In the case of the wear tests, given that at 50 °C the specific film thickness (Λ (–)) value, which represents the relationship between the lubricant minimum film thickness and the surface roughness, only reached 0.5 above 400 rpm, these tests were run at a rotational speed of 200 rpm. Table 4 shows the operating conditions of the wear tests.

Table 4. Operating conditions of the wear tests.

Load	Speed	Temperature	Time
5 kN	200 rpm	50 °C	120 h

After the test, a grease sample was collected for wear particle analysis via ferrometry and ferrography. More details regarding this wear particle analysis procedure can be found elsewhere [41].

3.3.3. Grease Volume

In order to fill part of the chamber of the rolling bearing house while also assuring that all the rolling elements were wet up to half of their diameter, 10 mL of grease was used; 2 mL was spread across the rolling bearings raceways and the holes between the cage and the rolling elements, while the other 8 mL was put in the rolling bearing house. Figure 4 shows the grease spread on the different parts of the rolling bearing assembly.

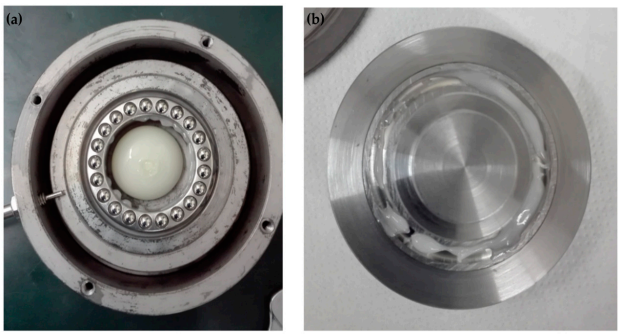

Figure 4. Grease spread on (**a**) the rolling bearing house, lower raceway, and cage, and (**b**) on the upper raceway shaft.

4. Results and Discussion

4.1. Apparent Friction Energy Density

The average friction coefficient and the average volume of the wear tracks on the steel plate were obtained after performing the frictional tests in the tribometer; results from all the examined model greases are shown in Figure 5.

According to the data in Figure 5, a linear correlation was found between the friction coefficient and the wear data for most of the examined model grease samples. In this sense, the biogenic grease samples that exhibited low friction coefficient values, such as grease samples R1, 1, 2, 5, 13, and S3, produced less wear on the steel plate. On the other hand, the use of some biogenic grease samples, such as 3, 12, S1, and S4, provided high friction coefficient values, which were reflected in the wear volume.

Moreover, biogenic grease sample 11, which was based on a mixture of castor oil and HOSO as the base oil, stood out because of its low friction coefficient but exhibited the highest wear volume in comparison with model greases 1 and 2, which also contained castor oil and HOSO. Under appropriate assumptions, the microstructure and physical and chemical properties of the thickeners of biogenic grease 11 could lead to a negative influence in the present steel ball on the steel disc frictional contact. Biogenic grease 11, which was based on ethyl cellulose and carnauba wax as the thickener, which was a different composition to biogenic grease samples 1 and 2, presented a coarse and fragile structural appearance, probably due to its poor mechanical stability and low resistance to structural breakdown. This property can cause the grease microstructure to be easily destroyed upon tribological contact. Therefore, the grease can be gradually ejected from the contact, eventually yielding lubricant starvation.

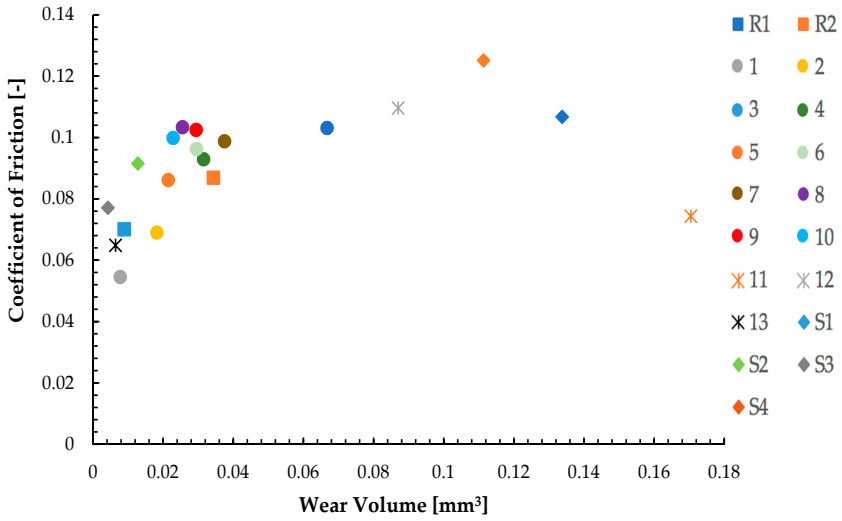

Figure 5. Friction coefficients versus wear volume on a steel plate for all model greases (wear path s_R = 387 m).

The effects of the different thickeners were also illustrated when comparing the results provided by biogenic greases 6, 8, and 10. Biogenic grease 10, which was prepared with a natural cellulose fiber of 120 µm in length as the thickener, exhibited the least wear on the steel plate compared with model grease 6, which was based on a natural cellulose fiber 18 µm in length, and grease 8, which was based on a natural cellulose fiber 20–40 µm in length. This result indicated that the longer the natural cellulose fiber of the thickener was, the lower the wear volume on the steel plate (i.e., 22% lower for sample 10 compared to sample 6).

These results showed that the different behaviors of different grease lubricant formulations were more explicitly observed in the wear results than in the frictional results in the tribological process.

To illustrate the wear on the steel plates produced from the ten repetitions of the measurements on the same track in the tribometer, the wear marks were investigated using an optical 3D surface profilometer, as shown in Figure 6. The pictures allowed for the contacting surface on the steel plate to be observed. As seen in Figure 6, while the use of biogenic grease 3 and reference grease R2 caused wide and strong abrasive wear, biogenic grease 2 and reference grease R1 produced wide but less pronounced wear on the steel disc. Looking at the detail, the use of biogenic grease 3 and reference grease R2 caused higher wear depth values, which are described as "Mean [µm]" in Figure 6, compared with biogenic grease 2 and reference grease R1. These data support the wear data shown in Figure 5.

Figure 7 shows the apparent friction energy densities (e_R^*) plotted as a function of the wear intensities (I_h) for all the model greases. In this study, Fleischer's wear model was experimentally used to investigate the relationship between friction and wear in a state of mixed friction, where only the wear on the steel plate was taken into consideration. In this sense, the apparent friction energy densities (e_R^*), which describe the amount of friction work required for the separation of the friction-exposed material, and the wear intensities (I_h), which are expressed by the wear depth (h_v) divided by the wear path (i.e., friction distance, s_R), were determined according to Equation (5). As in Figure 7, there was an inverse relationship between the e_R^* and I_h, indicating that the greases that exhibited the highest friction energy densities caused the lowest wear intensities on the steel plate. For example, reference grease sample R1 showed the highest value of e_R^* and the lowest intensity of wear on the steel plate.

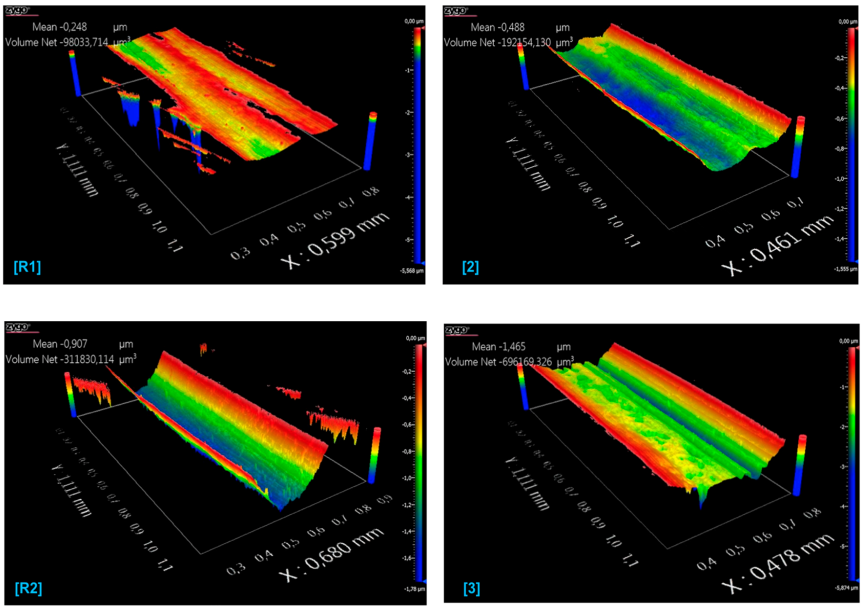

Figure 6. Profilometric pictures obtained from the steel plates as a function of the lubricant grease (window sizes of 0.599 mm × 1.111 mm, 0.461 mm × 1.111 mm, 0.680 mm × 1.111 mm, and 0.478 mm × 1.111 mm).

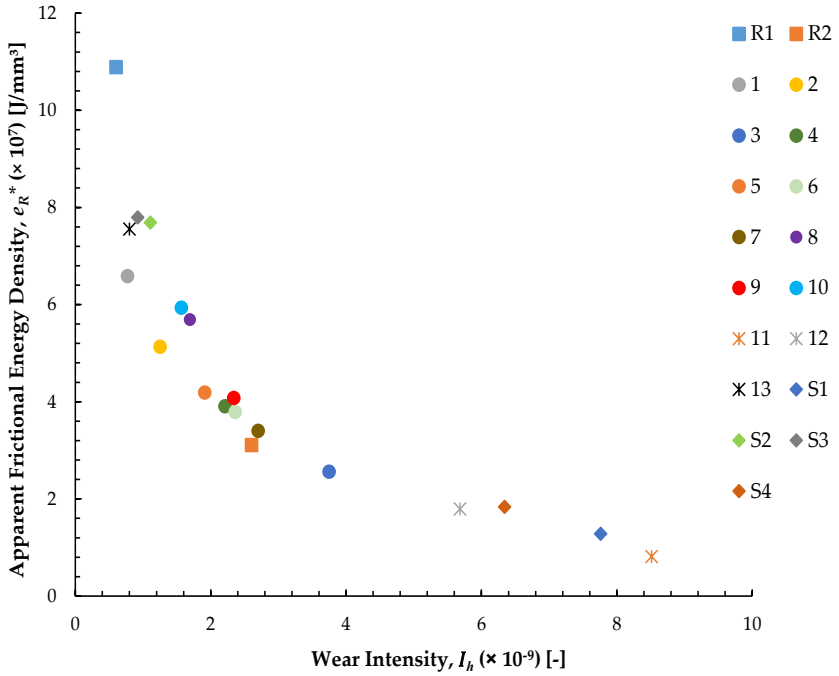

Figure 7. Apparent friction energy density (e_R^*) vs. wear intensity (I_h) for all the model greases.

For further comprehension, the values of the three associated tribological parameters e^*_R, I_h, and τ_R were plotted on a graph depicting the basic energy equation of wear for the model greases (Figure 8). As observed, all the model greases were in the range of 1, indicating that all the lubricating grease experiments in the tribometer were conducted in the quasi-fluid-friction/mixed-friction state, thereby leading to deformation on the steel plates.

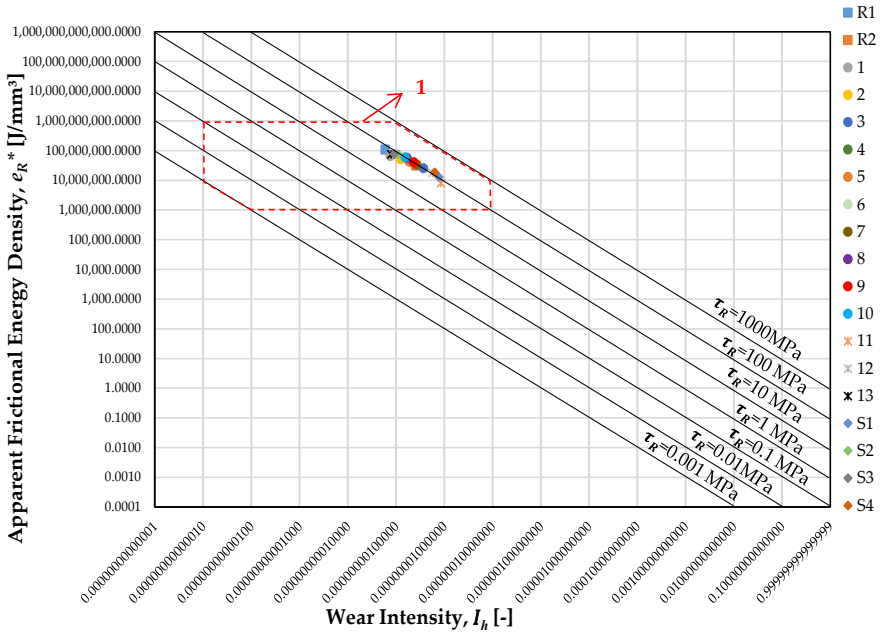

Figure 8. Graph of the basic energy equation of wear for all the model greases.

Finally, the results of the measured tribological parameters, i.e., e^*_R, I_h, and τ_R, showed that all the model grease samples applied some friction pairings, such as the toothed wheel or rolling bearing, according to a large number of studies looking at different machine elements [22].

4.2. Rolling Bearings Test Results

4.2.1. Power Loss Tests

Figure 9 shows the value of the rolling bearing friction torque (Mt), which was the average of five replicates for each of the biogenic greases selected. For the rolling bearing tests, model grease samples 1 and 2 were selected since they produced lower friction coefficient values and the smallest wear marks from the ball on the disc tribometer.

As expected, the friction torque at very low speeds was high and decreased rapidly as the speed increased and the lubricant film built up. In this low-speed region, the sliding friction torque was dominant due to more frequent interactions of the surface asperities [42,43]. The friction torque then reached a minimum value around 400 rpm for both greases; above that speed, the friction torque started to increase again, albeit only slightly. This increase was due to greater drag losses and increased rolling friction torque [37–40,42].

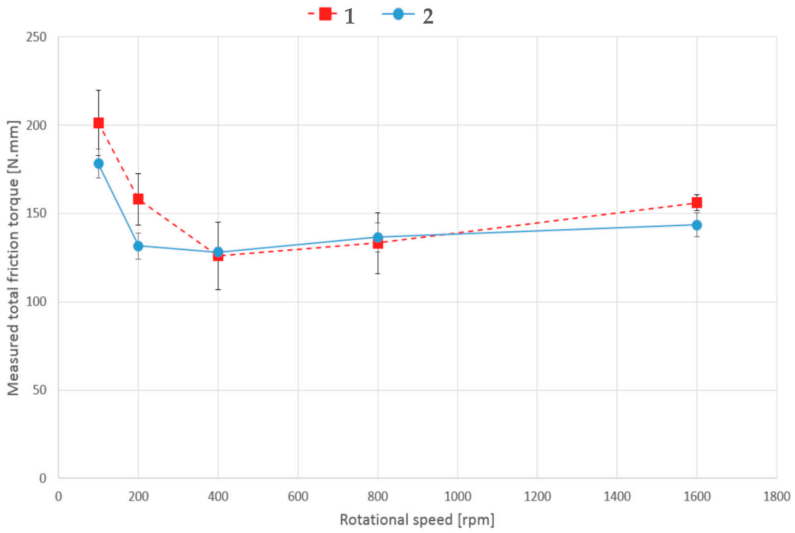

Figure 9. TBB friction torque results as a function of the entrainment speed for greases 1 and 2.

Moreover, grease 1 showed higher friction torque than grease 2, both at low and high speeds. From our understanding, the differences found at low speeds should be related to the thickener type and oil-bleeding rate, while at high speeds, the differences should mainly be related to the higher base-oil viscosity of grease 1. This approach was supported by data regarding base-oil viscosity and oil-bleeding tests. The base-oil viscosity of each grease was determined at 40 °C and 100 °C according to the ASTM (American Society for Testing and Materials) D341 test (Standard Practice for Viscosity-Temperature Charts for Liquid Petroleum Products). The results showed that although model grease samples 1 and 2 contained the same type of base oil, i.e., a combination of castor oil and HOSO, grease sample 1 had a higher value of base-oil viscosity at 40 °C and 100 °C than model grease 2. In addition to this analysis, the bleed-oil of each grease was extracted using a non-standard dynamic bleeding process, similar to the ASTM D4425 standard method. The bleed-oil obtained through this non-standard dynamic method showed the same viscosity as the bleed-oil obtained using the static ASTM D6184 method. This dynamic method was used to calculate the oil-bleeding rate of each grease sample. The results showed that the amount was very similar between the two greases, although slightly higher for model grease 2 due to having a lower base-oil viscosity. Finally, grease 2 showed a better wear performance from a power loss perspective.

4.2.2. Wear Tests

As previously stated, the wear tests were performed under 5 kN, 200 rpm, and at 50 °C over 120 h. During this time, the friction torque was measured 2 h after the start of the test and then at 5, 8, 26, and 120 h, after which the machine was stopped.

The friction torque measured over time is shown in Figure 10. In the first hours of operation at 200 rpm, the friction torque was higher due to the grease churning. After approximately 5 h, the friction torque reduced substantially for the rest of the test. The exception was grease 1, which showed a very steep friction torque increase between 26 and 120 h. Either way, grease 1 generally showed a higher friction torque than grease 2.

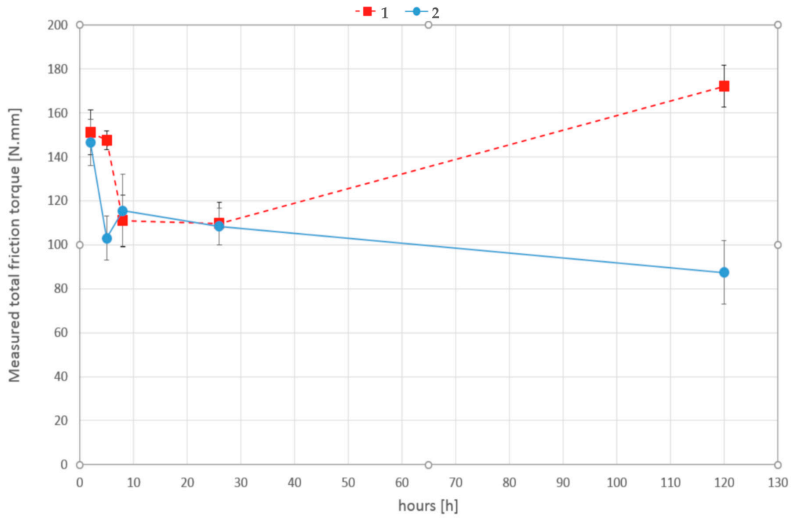

Figure 10. TBB friction torque results as a function of the test time for greases 1 and 2.

After 120 h, both greases displayed a very dark coloration, particularly between the rolling elements and the raceway, as shown in Figure 11. This dark coloration was probably related to the presence of metallic particles originating from the wear process, but also due to some temperature-induced oxidation.

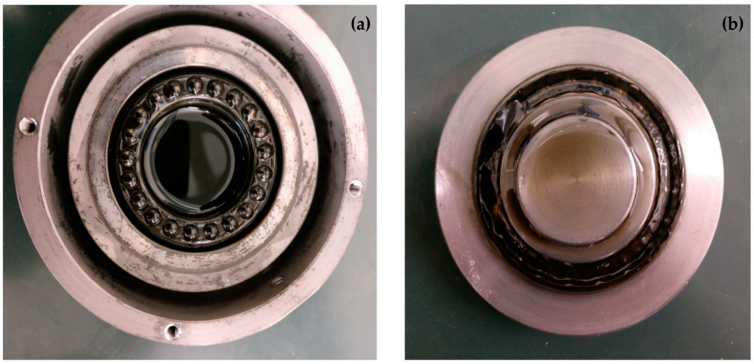

Figure 11. Remaining grease on (**a**) the rolling bearing house, lower raceway, and cage, and (**b**) the upper raceway shaft.

Finally, a sample of each grease was collected at the end of the power loss tests and wear tests for particle analysis. The ferrometry and ferrography analysis results are shown in Table 5. The indexes of small (DS, smaller than 1–2 µm) and large particles (DL, larger than 5 µm) refer to the concentration and size of particles found in a given sample of grease (100 mg diluted with 20 mL of an adequate solvent), collected after the power loss and wear tests. The particle concentration index (CPUC) and the severity of wear index (ISUC) can be estimated from DS and DL follows:

$$\text{Particle Concentration Index (CPUC)} = \text{DS} + \text{DL} \tag{10}$$

$$\text{Severity of Wear Index (ISUC)} = \text{DL}^2 - \text{DS}^2 \tag{11}$$

Table 5. Ferrometry and ferrography results of the power loss and wear tests.

Identification	Power Loss Tests		Wear Tests	
Sample	1	2	1	2
Bearing Load (kN)	5	5	5	5
Number of cycles	250–300 k	250–300 k	1440 k	1440 k
Ferrometry				
Large Particles Index (DL)	67.7	17.7	86.0	57.1
Small Particles Index (DS)	17.7	5.1	30.7	17.7
Particle Concentration Index (CPUC)	85.4	22.8	116.7	74.8
Severity of Wear Index (ISUC)	4270.0	287.3	6453.5	2947.1
Ferrography				
Normal Wear	Strong	Medium	Strong	Strong
Severe Wear	Strong	Strong	Medium	Medium
Fatigue Wear Particles	Medium	Medium	Medium	Medium
Adhesion Wear Particles	Fair	Fair	Fair	Fair
Friction Polymers	Fair	Fair	Fair	Fair
Black Oxides	Medium	Fair	Strong	Strong

Based on these indexes and the ferrography analysis, a classification may be established according to wear severity, presence of fatigue or adhesion wear particles, and the presence of friction polymers and black oxides. More details regarding these procedures can be found elsewhere [44–46]. According to the results of the power loss tests, grease 1 showed more severe wear with a higher particle concentration index (CPUC) and severity of wear index (ISUC), suggesting once again that grease 2 performed better. Moreover, as seen in this table, the results of the wear tests were considerably higher than the results obtained for the power loss tests.

5. Conclusions

In this study, completely biogenic lubricating greases were tribologically investigated using a ball-on-disc tribometer and compared with two traditional reference greases. A linear relationship was observed between the friction coefficient and the wear data for most of the examined model grease samples. This result revealed that the lower the friction coefficient was, the lower the wear volume that occurred on the steel plate due to the friction process. Moreover, the results showed how the different compositions of model greases highly influenced the frictional and wear behaviors. Using Fleischer's energetic wear model, the apparent friction energy density (e_R^*), the intensity of wear (I_h), and the friction shear stress (τ_R) for all the model greases were experimentally estimated and the relationship between these tribological parameters was calculated. Plotting these three associated tribological parameters on the Fleischer's graph of the basic energy equation of wear for the model greases allowed for the determination of the friction and wear states the experiments were conducted in, which was a combination of fluid friction and mixed friction for all the grease samples. In addition, the estimation of the apparent friction energy density revealed that the grease-lubricated contacts with high friction energy densities led to low wear intensities on the steel plate.

In order to assess the tribological behavior of the biogenic greases in real machine elements, rolling bearing power loss and rolling bearing wear tests were carried out with two selected biogenic grease samples. Results from the power loss tests showed that model grease 2, which had a lower base-oil viscosity, provided smaller friction torque values than model grease 1 under the operating conditions of the experiment. Comparing the tested greases, model grease 2 showed a better overall performance, a slightly lower internal torque loss, and less wear particle generation even though both model greases were similar in composition, with sample 2 containing sorbitan monostearate instead of beeswax in the thickener blend. Regarding the wear tests, similar conclusions were found, i.e., higher friction torque was associated with greater wear. Model grease 1 exhibited higher wear indexes and showed worse performance than model grease 2. Moreover, both grease samples showed very dark coloration after the test, and a considerable number of wear particles were found, some with large dimensions.

Author Contributions: Most of the experiments and writing were done by N.A., E.K., J.M.F., and J.H.O.S. D.E.P.G. contributed by supervising the experimental work and writing the paper. Rolling bearing tests were performed by J.H.O.S. and D.E.P.G. at INEGI (Institute of Science and Innovation in Mechanical and Industrial Engineering). J.M.F. designed and synthetized the bio-thickeners of samples S1–S4 at Pro2TecS (University of Huelva). All authors have read and agreed to the published version of the manuscript.

Funding: This research, which is part of the research Project "Tribiogen", was funded by the German Ministry of Education and Research, grant number FKZ13FH018IX4. The authors gratefully acknowledge the financial support.

Acknowledgments: The authors acknowledge Fuchs Europe Schmierstoffe (Mannheim, Germany) and Fuchs Lubritech (Kaiserslautern, Germany) for kindly providing the model samples. Finally, the authors also gratefully acknowledge Beatriz Graça for her support and help in performing the rolling bearing tests.

Conflicts of Interest: The authors declare no conflict of interest.

References

1. Bartz, J.W. Lubricants and the environment. *Tribol. Int.* **1998**, *31*, 35–47. [CrossRef]
2. Wilson, B. Lubricants and functional fluids from renewable resources. *Ind. Lubr. Tribol.* **1998**, *50*, 6–15. [CrossRef]
3. Boyde, S. Green lubricants. Environmental benefits and impacts of lubrication. *Green Chem.* **2002**, *4*, 293–307. [CrossRef]
4. Erhan, S.Z.; Asadauskas, S. Lubricant basestocks from vegetable oils. *Ind. Crops Prod.* **2000**, *11*, 277–282. [CrossRef]
5. Adhvaryu, A.; Erhan, S.Z. Epoxidized soybean oil as a potential source of high-temperature lubricants. *Ind. Crops Prod.* **2002**, *15*, 247–254. [CrossRef]
6. Adhvaryu, A.; Erhan, S.Z.; Perez, J.M. Tribological studies of thermally and chemically modified vegetable oils for use as environmentally friendly lubricants. *Wear* **2004**, *257*, 359–367. [CrossRef]
7. Erhan, S.Z.; Sharma, B.K.; Perez, J.M. Oxidation and low temperature stability of vegetable oil-based lubricants. *Ind. Crops Prod.* **2006**, *24*, 292–299. [CrossRef]
8. Adhvaryu, A.; Sung, C.; Erhan, S.Z. Fatty acids and antioxidant effects on grease microstructures. *Ind. Crops Prod.* **2005**, *21*, 285–291. [CrossRef]
9. Quinchia, L.A.; Delgado, M.A.; Valencia, C.; Franco, J.M.; Gallegos, C. Viscosity Modification of High-Oleic Sunflower Oil with Polymeric Additives for the Design of New Biolubricant Formulations. *Environ. Sci. Technol.* **2009**, *43*, 2060–2065. [CrossRef]
10. Quinchia, L.A.; Delgado, M.A.; Valencia, C.; Franco, J.M.; Gallegos, C. Viscosity modification of different vegetable oils with EVA copolymer for lubricant applications. *Ind. Crops Prod.* **2010**, *32*, 607–612. [CrossRef]
11. García-Zapateiro, L.A.; Delgado, M.A.; Franco, J.M.; Valencia, C.; Ruiz-Méndez, M.V.; Garcés, R.; Gallegos, C. Oleins as a source of estolides for biolubricant applications. *Grasas y Aceites* **2010**, *61*, 171–174.
12. Sánchez, R.; Franco, J.M.; Delgado, M.A.; Valencia, C.; Gallegos, C. Effect of thermo-mechanical processing on the rheology of oleogels potentially applicable as biodegradable lubricating greases. *Chem. Eng. Res. Des.* **2008**, *86*, 1073–1082. [CrossRef]
13. Sánchez, R.; Franco, J.M.; Delgado, M.A.; Valencia, C.; Gallegos, C. Development of new green lubricating greases formulations based on cellulosic derivatives and castor oil. *Green Chem.* **2009**, *11*, 686–693. [CrossRef]
14. Sánchez, R.; Franco, J.M.; Kuhn, E.; Fiedler, M. Tribological characterization of green lubricating greases formulated with castor oil and different biogenic thickener agents: A comparative experimental study. *Ind. Lubr. Tribol.* **2011**, *63*, 446–452. [CrossRef]
15. Sánchez, R.; Franco, J.M.; Delgado, M.A.; Valencia, C.; Gallegos, C. Thermal and mechanical characterization of cellulosic derivatives-based oleogels potentially applicable as bio-lubricating greases: Influence of ethyl cellulose molecular weight. *Carbohydr. Polym.* **2011**, *83*, 151–158. [CrossRef]
16. Sánchez, R.; Stringari, G.B.; Franco, J.M.; Delgado, M.A.; Valencia, C.; Gallegos, C. Use of chitin, chitosan and acylated derivatives as thickener agents of vegetable oils for bio lubricant applications. *Carbohydr. Polym.* **2011**, *85*, 705–714. [CrossRef]
17. Alfonso, J.E.M.; Yañez, R.; Valencia, C.; Franco, J.M.; Díaz, M.J. Optimization of the Methylation Conditions of Kraft Cellulose Pulp for Its Use As a Thickener Agent in Biodegradable Lubricating Greases. *Ind. Eng. Chem. Res.* **2009**, *48*, 6765–6771. [CrossRef]

18. Núñez, N.; Alfonso, J.E.M.; Valencia, C.; Sánchez, M.C.; Franco, J.M. Rheology of new green lubricating grease formulations containing cellulose pulp and its methylated derivative as thickener agents. *Ind. Crops Prod.* **2012**, *37*, 500–507. [CrossRef]
19. Sánchez, R. Rheological and mechanical properties of oleogels based on castor oil and cellulosic derivatives potentially applicable as bio-lubricating greases: Influence of cellulosic derivatives concentration ratio. *J. Ind. Eng. Chem.* **2011**, *17*, 705–711. [CrossRef]
20. Acar, N.; Franco, J.M.; Kuhn, E. On the shear-induced structural degradation of lubricating greases and associated activation energy: An experimental rheological study. *Tribol. Int.* **2020**, *144*, 106105. [CrossRef]
21. Kuhn, E. Friction and wear of a grease lubricated contact—An energetic approach. In *Tribology: Fundamentals and Advancements*; Gegner, J., Ed.; InTech: London, UK, 2013; ISBN 978-953-51-1135-1.
22. Fleischer, G.; Gröger, H.; Thum, H. *Verschleiß und Zuverlässigkeit*; VEB Verlag Technik: Berlin, Germany, 1980.
23. Fleischer, G. Zum Energetischen Niveau von Reibpaarungen. In *Schmierungstechnik 16*; VEB Verlag Technik: Berlin, Germany, 1985.
24. Sequard-base, J.; Lenauer, C.; Lazarev, V.; Gavrilov, K.; Doikin, A.; Vorlaufer, G. A Modified Energy-Based Model for Describing Wear Processes Applied to an Internal Combustion Engine. *Int. J. Comp. Methods Exp. Meas.* **2015**, *3*, 150–164. [CrossRef]
25. Brinkschulte, L.; Mattes, J.; Geimer, M. An approach to wear simulation of hydrostatic drives to improve the availability of mobile machines. In Proceedings of the 11th International Fluid Power Conference, Aachen, Germany, 19–21 March 2018.
26. Bartel, D.; Bobach, L.; Illner, T.; Deters, L. Simulating transient wear characteristics of journal bearings subjected to mixed friction. *J. Eng. Tribol.* **2012**, *226*, 1095–1108. [CrossRef]
27. Lang, J.; Knoll, G.; Schönen, R.; Jaitner, D.; Schiffgens, H.J.; Schlüter, S. *Simulation of a High-Pressure Fuel Pump under Thermo-Elastohydrodynamic Conditions*; Springer Fachmedien: Wiesbaden, Germany, 2018. [CrossRef]
28. Foko, F.; Heimes, J.; Magyar, B.; Sauer, B. Reibenergiebasierte verschleisssimulation für radialwellendichtringe. In Proceedings of the Gft-Conference, Göttingen, Germany, 23–25 September 2019.
29. Kučera, M.; Chotčborský, R. Analysis of the process of abrasive wear under experimental conditions. *Sci. Agric. Bohem.* **2013**, *44*, 102–106. [CrossRef]
30. Kučera, M.; Pršan, J.; Kostoláni, P. A systemic approach to testing the tribological properties of selected materials of agricultural machines. *J. Cent. Eur. Agric.* **2014**, *15*, 146–159. [CrossRef]
31. Kuhn, E. Tribological stress of lubricating greases in the light of system entropy. *Lubricants* **2016**, *4*, 37. [CrossRef]
32. Kuhn, E. Correlation between system entropy and structural changes in lubricating grease. *Lubricants* **2015**, *3*, 332–345. [CrossRef]
33. Kragelski, I.P.; Dobicin, M.N.; Kombalov, V.S. *Reibung und Verschleiß*; Technik: Verl, Germany, 1982.
34. Kuhn, E. *Zur Tribologie der Schmierfette: Eine Energetische Betrachtungsweise des Reibungs-und Verschleißprozesses*; Expert Verl: Renningen, Germany, 2017.
35. Borrero-López, A.M.; Valencia, C.; Franco, J.M. Rheology of lignin-based chemical oleogels prepared using diisocyanate crosslinkers: Effect of the diisocyanate and curing kinetics. *Eur. Polym. J.* **2017**, *89*, 311–323. [CrossRef]
36. Triviño, E.C.; Valencia, C.; Delgado, M.A.; Franco, J.M. Modification of alkali lignin with poly (ethylene glycol) diglycidyl ether to be used as a thickener in bio-lubricant formulations. *Polymers* **2018**, *10*, 670. [CrossRef]
37. Cousseau, T.; Graça, B.; Campos, A.; Seabra, J. Experimental measuring procedure for the friction torque in rolling bearings. *Lubr. Sci.* **2010**, *22*, 133–147. [CrossRef]
38. Cousseau, T.; Graça, B.; Campos, A.; Seabra, J. Friction torque in grease lubricated thrust ball bearings. *Tribol. Int.* **2011**, *44*, 523–531. [CrossRef]
39. Gonçalves, D.; Cousseau, T.; Gama, A.; Campos, A.V.; Seabra, J.H.O. Friction torque in thrust roller bearings lubricated with greases, their base oils and bleed-oils. *Tribol. Int.* **2016**. [CrossRef]
40. Gonçalves, D.; Pinho, S.; Graça, B.; Campos, A.V.; Seabra, J.H.O. Friction torque in thrust ball bearings lubricated with polymer greases of different thickener content. *Tribol. Int.* **2016**, *96*, 87–96. [CrossRef]
41. Available online: www.tricocorp.com/product/direct-reading-ferrograph/ (accessed on 31 May 2018).
42. SKF. Evolution online and G morales-espejel. using a friction model as an engineering tool. *Evol. SKF* **2006**, *2*, 27–30.

43. SKF. *SKF General Catalogue*; SKF: Schweinfurt, Germany, 2003.
44. Available online: http://www.plus-sci.co.kr/image/ana/predict-dli/pdf/ferrography_overview.pdf (accessed on 20 December 2019).
45. Available online: https://pdfs.semanticscholar.org/17d4/b8224be1a7df01929af300874e6f5017f18c.pdf (accessed on 20 December 2019).
46. Available online: https://wearcheck.com/virtual_directories/Literature/Techdoc/WCA001.htm (accessed on 20 December 2019).

On the Shear-Induced Structural Degradation of Lubricating Greases and Associated Activation Energy: An Experimental Rheological Study

Nazli Acar [a,b], José M. Franco[b,c], Erik Kuhn[a]

[a] Laboratory of Machine Elements and Tribology, Department of Mechanical Engineering and Production Management, Faculty of Engineering Technology and Computer Science, Hamburg University of Applied Sciences (HAW-Hamburg), Berliner Tor 21, 20099, Hamburg, Germany

[b] Department of Chemical Engineering, University of Huelva, 21071, Huelva, Spain

[c] Pro2TecS-Chemical Product and Process Technology Research Centre, Complex Fluid Engineering Laboratory, University of Huelva, 21071, Huelva, Spain

Published in: ***Tribology International***

Publishing company: Elsevier

Editors: Michel Fillon, Hong Liang, Weimin Liu

Volume 144, pp 106105

Year: April 2020

DOI: 10.1016/j.triboint.2019.106105

ISSN: 0301-679X

Impact Factor (2020): 4.872

CiteScore (2020): 8.0

JCR Category	Rank
Engineering, Mechanical	17/133

Annexe - Published Articles

Debido a restricciones relativas a derechos de autor, el artículo “On the shear-induced structural degradation of lubricating greases and associated activation energy: An experimental rheological study” que forma parte del apartado “Annexe-Published Articles”, ha sido retirado de la tesis. En sustitución del artículo ofrecemos la siguiente información: referencia bibliográfica, enlace a la revista y resumen.

Acar, N.; Franco, J.M.; Kuhn, E. On the shear-induced structural degradation of lubricating greases and associated activation energy: An experimental rheological study. Tribology International, 2020, 144, 106105, https://doi.org/10.1016/j.triboint.2019.106105

Enlace al texto completo: https://doi.org/10.1016/j.triboint.2019.106105

RESUMEN:
The stability of the thickener microstructure in lubricating greases influences their ability to reduce friction and protect the lubricated surfaces in a tribological system. Shear-induced degradation of the thickener network in lubricating greases that occurs as a result of reduced particle interactions can be considered a process associated with exceeding a critical energy level, i.e. the activation energy. The aim of this experimental study was to investigate the relationship between the activation energy, which represents the amount of energy required to produce shear-induced structural degradation, and the extent of the structural degradation that occurs under different shearing conditions. To this end, rotational transient flow tests were carried out in a rheometer at varying temperatures (25–70 °C) and a constant shear rate to quantify the activation energy of six model greases. The model greases differed in the nature and concentration of the thickener used, and the activation energy was calculated by fitting the rheological energy density to the Arrhenius equation. The activation energy was found to depend on the nature and concentration of the thickener in the greases; higher thickener concentrations resulted in lower activation energies. In addition, oscillation amplitude sweep tests were performed to obtain information about the early stages of shear-induced structural degradation. Lower activation energies were found to result in an earlier onset of shear-induced structural degradation. Finally, correlations between the activation energy and structural degradation of the model greases under different shear situations were presented and discussed. This enhanced understanding of the shear-induced degradation will facilitate the improvement of the service life of lubricating greases.